

**INTER-PLANT WATER-ENERGY NETWORK SYNTHESIS CONSIDERING
SEASONAL VARIATIONS**

A Thesis

by

MANAR YOUSEF MOHAMMAD OQBI

Submitted to the Office of Graduate and Professional Studies of
Texas A&M University
in partial fulfillment of the requirements for the degree of

MASTER OF SCIENCE

Chair of Committee,
Committee Members,
Head of Department,

Patrick Linke
Ahmed Abdel-Wahab
Hamid Parsaei
Nazmul Karim

August 2019

Major Subject: Chemical Engineering

Copyright 2019 Manar Yousef Mohammad Oqbi

ABSTRACT

Water and energy are required for almost all industrial processes to convert raw materials into value-added products. Natural water and energy resources are experiencing depletion stress mainly due to increasing industrial activities and population growth. Integrated networks are employed in industrial cities as a solution to capture waste water and energy and reutilize them to reduce freshwater and energy production and consumption. Due to increasingly strict environmental regulations, integration networks became essential. Water and energy integration networks play a crucial role in significantly reducing water and carbon footprints.

Seasonal variations directly affect the performance of water-energy networks. So far, previous works adopted multi-period planning for designing integration networks capable of handling seasonality issue. Multi-period planning may result in complex optimization models. Also, the developed models are sometimes difficult to be implemented due to spatial constraints on pipelines layout. This work mainly investigates the impact of seasonality on network components. Accordingly, a novel approach for designing interplant water-energy integration networks considering seasonal variations is developed in this work.

Seasonality analysis was performed for each network element. Several tools were employed including software packages, empirical correlations, and charts. Analysis results were evaluated to assess the significance of the observed variations. Assessment results indicate that seasonal variations of water/energy supply and demand are insignificant considering the overall system. As a result, some solutions were proposed to design a tolerant water-energy network considering seasonality.

The proposed approach subsumes maximizing network units' capacities and utility system based on peak conditions. Water-energy network connectivity is determined based on average demand/supply. Maximum capacity freshwater-to-sink connections are enforced to compensate for any seasonal changes in water demands. To balance this out, maximum capacity discharge connections are made available to all water sources. Any water source-to-sink pipeline is designed based on maximum potential flowrate. Also, water network is designed based on worst case scenario considering treatment units' minimum removal ratios to ensure compatibility of treatment unit-to-sink connections over different seasons. A formulated mathematical model was expanded to include the proposed approach. Finally, a case study was solved using a stochastic programming tool to illustrate the applicability of the developed model.

DEDICATION

To my parents

ACKNOWLEDGEMENTS

First and foremost, I would like to thank God Almighty for the uncountable and unlimited blessings of strength, patience, knowledge, healthiness, and the opportunity to work on this research and complete it successfully. Without these blessings, this research would not have seen the light.

I would like to express my gratitude to my committee chair, Prof. Patrick Linke for his continuous support, encouragement, patience, and gaudiness. I really appreciate his devoted time and efforts to complete this research study satisfactorily. Many thanks go to my committee members, Prof. Ahmed Abdel-Wahab, and Prof. Hamid Parsaei for their support, and pieces of advice.

I am grateful to the best life-coaches, my parents, I owe it all to their unconditional and endless love, care, and prayers. A very special gratitude goes to my siblings who provide me with moral and emotional support. Many thanks go to all my family members and friends who have shown me support during my master's study. Also, I would like to thank my friends in the research group namely, Dr. Dhabia Al-mohannadi, Jamileh Fouladi, Raid Hassiba, and Sumit Bishnu. Many appreciations for your supportive and encouraging attitude.

Last but not least, I would like to expand my gratitude to all faculty and staff members at Texas A&M University at Qatar. It was a great opportunity to learn from their experiences. A very special thanks go to the office of graduate studies at Qatar and the United States.

Thank you all for your encouragement!

CONTRIBUTORS AND FUNDING SOURCES

This research study was supervised by Prof. Patrick Linke, and Prof. Ahmed Abdel Wahab of the Department of chemical engineering, and Prof. Hamid Parsaei of the Department of mechanical engineering.

This publication was made possible by NPRP grants no. NPRP 4- 1191-2-468 and 7-724-2-269 from the Qatar National Research Fund (a member of Qatar Foundation).

The case study of this research was solved by Sumit Bishnu who developed a stochastic programming tool for solving water-energy optimization problems.

All other work conducted for this research study was completed by the student independently.

NOMENCLATURE

Indices

<i>p</i>	Process/Plant
<i>i</i>	Water source
<i>j</i>	Water sink
<i>i'</i>	Energy source
<i>j'</i>	Energy sink
<i>r</i>	Decentral treatment unit
<i>s</i>	Central treatment unit
<i>t</i>	Central treatment unit type
<i>l</i>	Freshwater type
<i>c</i>	Contaminant
<i>m</i>	Decentral desalination unit
<i>n</i>	Central desalination unit
<i>k</i>	Central desalination unit type
<i>AC</i>	Air cooled heat exchanger
<i>CT</i>	Cooling tower
<i>OCSW</i>	Once-through cooling seawater
<i>WHP</i>	Waste heat to power
<i>E</i>	Evaporation from open treatment unit
<i>Des</i>	Desalination

Sets

P	Set of plants/processes in industrial city
SU_p	Set of water sources in plant p
SN_p	Set of water sinks in plant p
R	Set of decentral treatment units
S	Set of central treatment units
T	Set of central treatment unit types
L	Set of freshwater types
C	Set of contaminants/pollutants
M	Set of decentral desalination units
N	Set of central desalination units
K	Set of central desalination unit types
SU'_p	Set of energy sources in plant p
SN'_p	Set of energy sinks in plant p

Parameters

C_l^{FR}	Cost of freshwater of type l (\$/kg)
C^E	Cost of electricity from external utility (\$/kWyr)
C^{SW}	Cost of seawater (\$/kg)
C^{WW}	Cost of wastewater discharge (\$/kg)
C^{BRINE}	Cost of brine discharge (\$/kg)
C_{rp}^{CC}	Capital cost of decentral treatment unit r in plant p (\$/kg)

C_{st}^{CC}	Capital cost of central treatment unit s of type t (\$/kg)
C_{rp}^{OC}	Operating cost of decentral treatment unit r in plant p (\$/kg)
C_{st}^{OC}	Operating cost of central treatment unit s of type t (\$/kg)
C_{mp}^{CC}	Capital cost of decentral desalination unit m in plant p (\$/kg)
C_{nk}^{CC}	Capital cost of central desalination unit n of type k (\$/kg)
C_{mp}^{OC}	Operating cost of decentral desalination unit m in plant p (\$/kg)
C_{nk}^{OC}	Operating cost of central desalination unit n of type k (\$/kg)
C_{AC}^{CC}	Capital cost of air cooled heat exchanger (\$/kWyr)
C_{CT}^{CC}	Capital cost of cooling tower (\$/kWyr)
C_{WHP}^{CC}	Capital cost of waste heat to power unit (\$/kW)
C_{WHP}^{OC}	Operating cost of waste heat to power unit (\$/kWh)
C_{ip}^{pipes}	Cost of pipelines carrying maximum wastewater discharge from water source i , plant p (\$/yr)
$C_{mp,jp}^{pipes}$	Cost of pipelines carrying maximum required freshwater from decentral desalination unit m , plant p to sink j , plant p (\$/yr)
$C_{nk,jp}^{pipes}$	Cost of pipelines carrying maximum required freshwater from central desalination unit n , type k to sink j , plant p (\$/yr)
$C_{l,jp}^{pipes}$	Cost of pipelines carrying maximum required freshwater type l from external utility to sink j , plant p (\$/yr)
$Z_{c,j,p}^{min}$	Minimum permissible pollutant c composition in sink j , plant p (ppm)
$Z_{c,j,p}^{max}$	Maximum permissible pollutant c composition in sink j , plant p (ppm)

G_{jp}	Water flowrate required in sink j , plant p (kg/h)
W_{ip}	Water flowrate available in source i , plant p (kg/h)
$L_{ip,jp}$	Length of pipe from source i , plant p to sink j plant p (m)
$L_{ip,rp}$	Length of pipe from source i , plant p to decentral treatment r plant p (m)
$L_{ip,st}$	Length of pipe from source i , plant p to central treatment s of type t (m)
$L_{rp,jp}$	Length of pipe from decentral treatment r plant p to sink j , plant p (m)
$L_{st,jp}$	Length of pipe from central treatment s of type t to sink j , plant p (m)
L_{rp}	Length of pipe carrying unused wastewater from decentral treatment r , plant p to mainstream waste (m)
L_{st}	Length of pipe carrying unused wastewater from central treatment s , type t to mainstream waste (m)
Q_p^{min}	Minimum cooling requirement of plant p (MW)
PW_p^{max}	Maximum power generated by waste heat to power unit, plant p (kW)
PW_p^{avg}	Average power generated by waste heat to power unit, plant p (kW)
$\chi_{c,ip}^{Source}$	Pollutant c composition in source i , plant p (ppm)
$\chi_{c,l}^{FRESH}$	Pollutant c composition in external freshwater of type l (ppm)
χ_c^{Max}	Maximum permissible discharge concentration of pollutant c in wastewater discharge (ppm)
R_{rp}	Water recovery ratio in decentral treatment unit r , plant p
R_{st}	Water recovery ratio in central treatment unit s , type t
R_{mp}	Water recovery ratio in decentral desalination unit m , plant p
R_{nk}	Water recovery ratio in central desalination unit n , type k

$RR_{c,rp}^{min}$	Minimum removal ratio of pollutant c in decentral treatment unit r , plant p
$RR_{c,st}^{min}$	Minimum removal ratio of pollutant c in central treatment unit s , type t
$RR_{c,mp}^{min}$	Minimum removal ratio of pollutant c in decentral desalination unit m , plant p
$RR_{c,nk}^{min}$	Minimum removal ratio of pollutant c in central desalination unit n , type k
E_{rp}^{max}	Maximum water evaporation ratio from decentral treatment unit r , plant p
E_{rp}^{avg}	Average water evaporation ratio from decentral treatment unit r , plant p
E_{st}^{max}	Maximum water evaporation ratio from central treatment unit s , type t
E_{st}^{avg}	Average water evaporation ratio from central treatment unit s , type t
$P_{AC}^{PW,avg}$	Air cooler average power demand parameter (kW/MW)
$P_{CT}^{PW,avg}$	Cooling tower average power demand parameter (kW/MW)
$P_{CT}^{MU,avg}$	Cooling tower average makeup water demand parameter (m ³ /h MW)
P_{OCsw}^{PW}	Once-through cooling seawater power demand parameter (kWh/m ³)
P_{OCsw}^{SW}	Once-through cooling seawater water use parameter (m ³ /h MW)
$P_{Des}^{PW,avg}$	Desalination unit average power demand parameter (kWh/m ³)
$P_{T,rp}^{PW,avg}$	Decentral treatment unit r , plant p average power demand parameter (kWh/m ³)
$P_{T,st}^{PW,avg}$	Central treatment unit s , type t average power demand parameter (kWh/m ³)
$P_{ip,rp}^{avg,max}$	Average-to-maximum parameter for wastewater flowrate from water source i , plant p to decentral treatment unit r , plant p
$P_{ip,st}^{avg,max}$	Average-to-maximum parameter for wastewater flowrate from water source i , plant p to central treatment unit s , type t

$P_{mp}^{avg,max}$	Average-to-maximum parameter for seawater flowrate to decentral desalination unit m , plant p
$P_{nk}^{avg,max}$	Average-to-maximum parameter for seawater flowrate to central desalination unit n , type k
$P_{WHP,p}^{avg,max}$	Average-to-maximum power parameter for WHP unit, plant p
$P_{ip}^{avg,max}$	Average-to-maximum parameter for water supply from source i , plant p
$P_{jp}^{avg,max}$	Average-to-maximum parameter for water demand in sink j , plant p
a	Coefficient associated with piping cost calculations
b	Power coefficient associated with piping cost calculations
H_y	Operating hours per year (hr/yr)
K_F	Treatment cost annualizing factor (yr^{-1})
γ	Pipelines cost annualizing factor (yr^{-1})
α	Power coefficient associated with capital cost calculations for treatment units
δ	Power coefficient associated with capital cost calculations for desalination units

Variables

C^{Fresh}	Total freshwater cost (\$/yr)
$C^{Treatment}$	Total central and decentral treatment cost (\$/yr)
C^{Pipes}	Total piping costs (\$/yr)
C^{Waste}	Total wastewater and brine discharge cost (\$/yr)
$C^{Desalination}$	Total central and decentral desalination cost (\$/yr)
C^{WHP}	Total cost for converting waste heat to power (\$/yr)

$C^{Cooling\ sys}$	Total cooling systems cost (\$/yr)
$C^{Seawater}$	Total cost of seawater (\$/yr)
$C_{rp}^{PW,avg}$	Cost of decentral treatment unit power demand (\$/yr)
$C_{st}^{PW,avg}$	Cost of central treatment unit power demand (\$/yr)
$C_{mp}^{PW,avg}$	Cost of decentral desalination unit power demand (\$/yr)
$C_{nk}^{PW,avg}$	Cost of central desalination unit power demand (\$/yr)
CC_p^{AC}	Capital cost of air cooler in plant p (\$/yr)
OC_p^{AC}	Operating cost of air cooler in plant p (\$/yr)
CC_p^{CT}	Capital cost of cooling tower in plant p (\$/yr)
OC_p^{CT}	Operating cost of cooling tower in plant p (\$/yr)
$C_{CT,p}^{PW}$	Cost of cooling tower power demand (\$/yr)
$C_{CT,p}^{MU}$	Cost of cooling tower makeup water demand (\$/yr)
OC_p^{OCSW}	Operating cost of once-through cooling seawater in plant p (\$/yr)
C_{OCSW}^{PW}	Cost of once-through cooling seawater power demand (\$/yr)
C_{OCSW}^{SW}	Cost of seawater required for once-through cooling seawater (\$/yr)
$Q_p^{D,AC,avg}$	Average heat dissipated by air coolers in plant p (MW)
$Q_p^{D,CT,avg}$	Average heat dissipated by cooling towers in plant p (MW)
$Q_p^{D,OCSW,avg}$	Average heat dissipated by once-through cooling seawater in plant p (MW)
$Q_p^{WHP,avg}$	Average heat converted to power by WHP unit in plant p (MW)
$F_{l,jp}^{avg}$	Average freshwater flowrate of type l to sink j , plant p (kg/h)
T_{rp}^{avg}	Average wastewater flowrate to decentral treatment unit r , plant p (kg/hr)

T_{rp}^{max}	Maximum wastewater flowrate to decentral treatment unit r , plant p (kg/hr)
T_{st}^{avg}	Average wastewater flowrate to central treatment unit s , type t (kg/hr)
T_{st}^{max}	Maximum wastewater flowrate to central treatment unit s , type t (kg/hr)
$T_{rp}^{T,avg}$	Average treated water flowrate from decentral treatment unit r , plant p (kg/hr)
$T_{st}^{T,avg}$	Average treated water flowrate from central treatment unit s , type t (kg/hr)
$T_{mp}^{Des,avg}$	Average seawater flowrate to decentral desalination unit m , plant p (kg/hr)
$T_{mp}^{Des,max}$	Maximum seawater flowrate to decentral desalination unit m , plant p (kg/hr)
$T_{nk}^{Des,avg}$	Average seawater flowrate to central desalination unit n , type k (kg/hr)
$T_{nk}^{Des,max}$	Maximum seawater flowrate to central desalination unit n , type k (kg/hr)
$F_p^{OCSW,avg}$	Average required seawater for once-through cooling seawater, plant p (kg/hr)
$WW^{total,avg}$	Average wastewater discharged to the environment (kg/hr)
$B^{total,avg}$	Average brine discharged to the environment (kg/hr)
$F_{ip,jp}^{max}$	Maximum water flowrate from source i , plant p to sink j , plant p (kg/hr)
W_{ip}^{avg}	Average available water supply from source i , plant p (kg/hr)
G_{jp}^{avg}	Average required water flowrate into sink j , plant p (kg/hr)
$M_{ip,jp}^{avg}$	Average water flowrate from source i , plant p to sink j , plant p (kg/hr)
F_{ip}^{max}	Maximum water flowrate from source i , plant p (kg/hr)
F_{jp}^{max}	Maximum required water flowrate into sink j , plant p (kg/hr)
$F_{ip,rp}^{max}$	Maximum water supply from source i , plant p to decentral treatment unit r , plant p (kg/hr)

$F_{ip,st}^{max}$	Maximum water supply from source i , plant p to central treatment unit s , type p (kg/hr)
$F_{rp,jp}^{max}$	Maximum water supply from decentral treatment unit r , plant p to sink j , plant p (kg/hr)
$F_{st,jp}^{max}$	Maximum water supply from central treatment unit s , type p to sink j , plant p (kg/hr)
F_{rp}^{max}	Maximum treated water flowrate from decentral treatment unit r , plant p (kg/hr)
F_{st}^{max}	Maximum treated water flowrate from central treatment unit s , type p (kg/hr)
$F_{mp,jp}^{max}$	Maximum desalinated water flowrate from decentral desalination unit m , plant p to sink j , plant p (kg/hr)
$F_{nk,jp}^{max}$	Maximum desalinated water flowrate from central desalination unit n , type k to sink j , plant p (kg/hr)
$F_{l,jp}^{max}$	Maximum freshwater flowrate of type l , from external utility to sink j , plant p (kg/hr)
$T_{ip,rp}^{avg}$	Average inlet water flowrate from source i , plant p to decentral treatment unit r , plant p (kg/hr)
$T_{ip,st}^{avg}$	Average inlet water flowrate from source i , plant p to central treatment unit s , type p (kg/hr)
$T_{rp,jp}^{avg}$	Average treated water flowrate from decentral treatment unit r , plant p to sink j , plant p (kg/hr)
$T_{st,jp}^{avg}$	Average treated water flowrate from central treatment unit s , type t to sink j , plant p (kg/hr)

$T_{mp,jp}^{Des,avg}$	Average desalinated water flowrate from decentral treatment unit m , plant p to sink j , plant p (kg/hr)
$T_{nk.jp}^{Des,avg}$	Average desalinated water flowrate from central desalination unit n , type k to sink j , plant p (kg/hr)
$T_{rp,E}^{avg}$	Average evaporation rate from decentral treatment unit r , plant p (kg/hr)
$T_{st,E}^{avg}$	Average evaporation rate from central treatment unit n , type k (kg/hr)
$T_{ip,rp}^{max}$	Water flowrate from source i , plant p to decentral treatment unit r , plant p corresponding to maximum outlet pollutant concentration (kg/hr)
$T_{ip,st}^{max}$	Water flowrate from source i , plant p to central treatment unit n , type k corresponding to maximum outlet pollutant concentration (kg/hr)
D_{ip}^{avg}	Average water discharge flowrate from source i , plant p (kg/hr)
$D_{rp}^{T,avg}$	Average discharged treated water from decentral treatment unit r , plant p (kg/hr)
$D_{st}^{T,avg}$	Average discharged treated water from central treatment unit s , type t (kg/hr)
$D_{rp}^{U,avg}$	Average discharged untreated water from decentral treatment unit r , plant p (kg/hr)
$D_{st}^{U,avg}$	Average discharged untreated water from central treatment unit s , type t (kg/hr)
$D_{mp}^{Des,avg}$	Average brine discharges flowrate from decentral desalination unit m , plant p (kg/hr)
$D_{nk}^{Des,avg}$	Average brine discharges flowrate from central desalination unit n , type k (kg/hr)
$DI_{ip,jp}$	Diameter of pipe connecting source i , plant p to sink j plant p (m)
$DI_{ip,rp}$	Diameter of pipe connecting source i , plant p to decentral treatment r plant p (m)

$DI_{ip,st}$	Diameter of pipe connecting source i , plant p to central treatment s of type t (m)
$DI_{rp,jp}$	Diameter of pipe connecting decentral treatment r plant p to sink j , plant p (m)
$DI_{st,jp}$	Diameter of pipe connecting central treatment s of type t to sink j , plant p (m)
DI_{rp}	Diameter of pipe carrying unused wastewater from decentral treatment r , plant p to mainstream waste (m)
DI_{st}	Diameter of pipe carrying unused wastewater from central treatment s , type t to mainstream waste (m)
$z_{c,jp}^{in}$	Pollutant c composition in sink j , plant p (ppm)
$x_{c,rp}^{in,max}$	Maximum inlet concentration of pollutant c into decentral treatment r , plant p (ppm)
$x_{c,st}^{in,max}$	Maximum inlet concentration of pollutant c into central treatment s , type t (ppm)
$x_{c,rp}^{T,max}$	Maximum outlet concentration of contaminant c in the treated water stream produced by decentral treatment r , in plant p (ppm)
$x_{c,st}^{T,max}$	Maximum outlet concentration of contaminant c in the treated water stream produced by centralized treatment s , of type t (ppm)
$x_{c,mp}^{in}$	Inlet concentration of pollutant c into decentral desalination unit m , plant p (ppm)
$x_{c,nk}^{in}$	Inlet concentration of pollutant c into central desalination unit n , type k (ppm)
$x_{c,mp}^{T,max}$	Maximum outlet concentration of contaminant c in the desalinated water stream produced by decentral desalination m , in plant p (ppm)
$x_{c,nk}^{T,max}$	Maximum outlet concentration of contaminant c in the desalinated water stream produced by central desalination n , type k (ppm)

$x_c^{WW,max}$	Maximum concentration of pollutant c in wastewater discharges (ppm)
$x_c^{Brine,max}$	Maximum concentration of pollutant c in brine discharges (ppm)
$x_{c,rp}^{U,max}$	Maximum outlet concentration of pollutant c in brine of decentral treatment unit r , plant p (ppm)
$x_{c,st}^{U,max}$	Maximum outlet concentration of pollutant c in brine of central treatment unit s , type t (ppm)
$x_{c,mp}^{U,max}$	Maximum outlet concentration of pollutant c in brine of decentral desalination unit m , plant p (ppm)
$x_{c,nk}^{U,max}$	Maximum outlet concentration of pollutant c in brine of central desalination unit n , type k (ppm)
$PW_{i'p}^{avg}$	Average available power from energy source i' , plant p (kW)
$PW_{j'p}^{avg}$	Average power demand for energy sink j' , plant p (kW)
$PW_{i',rp}^{T,avg}$	Average power from energy source i' , plant p used for decentral treatment unit r , plant p (kW)
$PW_{i',st}^{T,avg}$	Average power from energy source i' , plant p used for central treatment unit s , type t (kW)
$PW_{i',mp}^{Des,avg}$	Average power from energy source i' , plant p used for decentral desalination unit m , plant p (kW)
$PW_{i',nk}^{Des,avg}$	Average power from energy source i' , plant p used for central desalination unit n , type k (kW)

$PW_{ip,j'p}^{CT,avg}$	Average power from energy source i' , plant p used for cooling tower CT in plant p (kW)
$PW_{ip,j'p}^{OCSW,avg}$	Average power from energy source i' , plant p used for once-through cooling seawater $OCSW$ in plant p (kW)
$PW_{ip,j'p}^{AC,avg}$	Average power from energy source i' , plant p used for air cooler AC in plant p (kW)
$PW_{rp}^{T,avg}$	Average power demand for decentral treatment unit r , plant p (kW)
$PW_{st}^{T,avg}$	Average power demand for central treatment unit s , type t (kW)
$PW_{mp}^{Des,avg}$	Average power demand for decentral desalination unit m , plant p (kW)
$PW_{nk}^{Des,avg}$	Average power demand for central desalination unit n , type k (kW)
$PW_{j'p}^{CT,avg}$	Average power demand for cooling tower CT , plant p (kW)
$PW_{j'p}^{OCSW,avg}$	Average power demand for once-through cooling seawater $OCSW$, plant p (kW)
$PW_{j'p}^{AC,avg}$	Average power demand for air cooler AC , plant p (kW)
$PW_{i'p}^{Export,avg}$	Average exports of power produced from energy source i' , plant p (kW)
$PW^{utility,avg}$	Average power produced via utility system (kW)
A	Binary variable associated with air cooler capital cost
B	Binary variable associated with cooling tower capital cost
C	Binary variable associated with air cooler operating cost
D	Binary variable associated with cooling tower operating cost
E	Binary variable associated with once-through cooling seawater cost

TABLE OF CONTENTS

	Page
ABSTRACT	ii
DEDICATION	iv
ACKNOWLEDGEMENTS.....	v
CONTRIBUTORS AND FUNDING SOURCES.....	vi
NOMENCLATURE.....	vii
TABLE OF CONTENTS.....	xx
LIST OF FIGURES.....	xxiii
LIST OF TABLES	xxvii
CHAPTER I INTRODUCTION AND LITERATURE REVIEW	1
Introduction.....	1
Motivation.....	4
Literature review.....	6
CHAPTER II PROBLEM DESCRIPTION AND METHODOLOGY	19
Objectives	19
Problem statement.....	19
Synthesis approach and superstructure representation	20
Methodology	21
Step 1: Data Acquisition	23
Step 2: Problem analysis.....	23
Step 3: Problem assessment	23

Step 4: Formulating the mathematical model	24
Step 5: Water-energy network synthesis.....	24
CHAPTER III PROBLEM ANALYSIS	25
Seasonal variations of cooling systems.....	25
Air Coolers.....	25
Cooling towers	28
Once-through cooling seawater	43
Seasonal variations of desalination units	47
Seasonal variations of waste heat-to-power unit (WHP).....	50
Seasonal variations of irrigation water demand.....	55
Seasonal variations of treatment units	61
Dissolved air flotation (DAF)	65
Membrane bioreactors (MBR).....	70
Nano-filtration membranes (NF)	75
Wastewater reverse osmosis membranes (RO).....	77
CHAPTER IV PROBLEM ASSESSMENT	80
Process assumptions.....	80
Cooling systems seasonality assessment	82
Air coolers.....	82
Cooling towers	83
Reverse osmosis seasonality assessment	87
Waste heat to power seasonality assessment	88
Irrigation water demand seasonality assessment	90
Treatment unit seasonality assessment	91
Evaporation from open treatment units.....	91
Dissolved air flotation (DAF)	92
Membrane bioreactor (MBR)	94
Nano-filtration membrane (NF).....	95
Wastewater reverse osmosis membrane (RO)	96
CHAPTER V DESIGN APPROACH AND MATHEMATICAL MODELING	99
Seasonality-based classification matrices of water-energy network components	99
Water-energy network proposed design approach.....	102
Water-energy network design adjustments.....	103
Mathematical formulation.....	105
Objective function.....	106

Cost Equations	106
Water Balances and inequality constraints	114
Energy balances and inequality constraints	121
 CHAPTER VI ILLUSTRATIVE CASE STUDY.....	 127
Results and Discussion	134
Base case: Without integration network	135
Scenario 1: Without considering seasonality	135
Scenario 2: Considering seasonality	139
Scenario 3: Considering seasonality and allowing freshwater exports.....	142
 CHAPTER VII CONCLUSION AND FUTURE WORK	 147
Conclusion	147
Future work.....	147
 REFERENCES.....	 149

LIST OF FIGURES

	Page
Figure 1: Visualization of the four seasons considering meteorological method.....	4
Figure 2: Water-energy network superstructure representation with full connectivity	22
Figure 3: Sequential steps towards optimal design of water-energy network considering seasonality.....	22
Figure 4: Illustration of air-cooled heat exchanger as a power sink	26
Figure 5: Seasonal air-cooled heat exchanger power demand per megawatt of heat removed	28
Figure 6: Illustration of cooling tower water/power sources and sinks	29
Figure 7: Seasonal cooling tower evaporation rates per megawatt of heat removed.....	37
Figure 8: Seasonal cooling tower blowdown rates per megawatt of heat removed.....	39
Figure 9: Cooling tower drift losses per megawatt of heat removed.....	40
Figure 10: Seasonal cooling tower makeup water demand per megawatt of heat removed.....	41
Figure 11: Contribution of different cooling tower makeup water demand components.....	42
Figure 12: Seasonal cooling tower power demand per megawatt of heat removed	43
Figure 13: Illustration for once-through cooling seawater	43
Figure 14: Once-through cooling seawater demand per megawatt of heat removed	46
Figure 15: Once-through cooling seawater power demand per megawatt of heat removed	47
Figure 16: Reverse osmosis system configuration.....	48
Figure 17: Seasonal RO power demand per cubic meter of produced desalinated water.....	49
Figure 18: Effect of seasonal feed water temperature on RO removal ratio	50
Figure 19: Illustration of waste heat to power unit	51
Figure 20: Seasonal power generated via WHP unit utilizing cooling tower in (a) ammonia, (b) methanol, and (c) GTL plants	53

Figure 21: Seasonal power generated via WHP unit utilizing air cooler in (a) ammonia, (b) methanol, and (c) GTL plants	53
Figure 22: Seasonal power generated via WHP unit utilizing once-through cooling seawater in (a) ammonia, (b) methanol, and (c) GTL plants	54
Figure 23: Illustration for irrigation water losses and requirements.....	59
Figure 24: Seasonal water demand per unit area for alfalfa irrigation	60
Figure 25: Seasonal water demand per unit area for date palms irrigation	60
Figure 26: Seasonal net evaporation rates from open treatment units per unit area	65
Figure 27: Schematic diagram for dissolved air flotation unit (DAF).....	66
Figure 28: Seasonal power demand of air compressor per cubic meter of air.....	67
Figure 29: Seasonal power demand for recycle pump per cubic meter of recycled effluent.....	68
Figure 30: DAF overall seasonal power demand per cubic meter of treated water.....	69
Figure 31: Seasonal removal ratio of dissolved air flotation unit (DAF)	70
Figure 32: Schematic diagram for aerobic immersed MBR configuration.....	71
Figure 33: Seasonal pumping power demand through MBR immersed UF membrane.....	72
Figure 34: Seasonal air blower power demand per cubic meter of air	73
Figure 35: MBR overall seasonal power demand per cubic meter of treated water.....	74
Figure 36: Seasonal COD removal ratio of immersed MBR treatment unit.....	75
Figure 37: Schematic diagram for Nano-filtration membrane unit	76
Figure 38: Seasonal power demand for NF membranes per cubic meter of treated water.....	76
Figure 39: Seasonal removal ratio of Nano-filtration membrane unit.....	77
Figure 40: Schematic diagram for wastewater reverse osmosis membrane unit	78
Figure 41: Seasonal power demands for wastewater treatment by RO membrane	79
Figure 42: Seasonal removal ratio for treating wastewater via RO membranes.....	79

Figure 43: Air cooler power profile for (a) ammonia, (b) methanol, and (c) GTL plants	82
Figure 44: Percent of the maximum seasonal increase in air cooler power demand to plant basic power load for ammonia, methanol, and GTL plants	83
Figure 45: Cooling tower power profile for (a) ammonia, (b) methanol, and (c) GTL plants	84
Figure 46: Percent of the maximum seasonal increase in cooling tower power demand to plant basic power load for ammonia, methanol, and GTL plants	84
Figure 47: Cooling tower blowdown profile for (a) ammonia, (b) methanol, and (c) GTL plants	85
Figure 48: Cooling tower makeup water demand profile for (a) ammonia, (b) methanol, and (c) GTL plants	86
Figure 49: Percent of the maximum increase in cooling tower makeup water demand to total water demand for ammonia, methanol, and GTL plants	87
Figure 50: RO power demand profile based on seasonal water requirements for (a) ammonia, (b) methanol, and (c) GTL plants	88
Figure 51: Seasonal alfalfa irrigation water demand profile in (a) ammonia, (b) methanol, and (c) GTL plants	90
Figure 52: Seasonal water evaporation from open treatment units in (a) ammonia, (b) methanol, and (c) GTL plants	92
Figure 53: Percent of the increase in evaporation from open treatment units to total wastewater available in winter and summer for ammonia, methanol, and GTL plants.....	92
Figure 54: Seasonal DAF power demand profile in (a) ammonia, (b) methanol, and (c) GTL plants.....	93
Figure 55: Seasonal MBR power demand profile in (a) ammonia, (b) methanol, and (c) GTL plants.....	94
Figure 56: Seasonal NF power demand profile in (a) ammonia, (b) methanol, and (c) GTL plants.....	95
Figure 57: Seasonal power demand profile for wastewater RO membrane unit in (a) ammonia, (b) methanol, and (c) GTL plants	97
Figure 58: Visualization for seasonality aspects of the water-energy network	99

Figure 59: Characterization matrix for water network elements	100
Figure 60: Characterization matrix for energy network elements	102
Figure 61: Flowchart of simulated annealing algorithm.....	134
Figure 62: Water-energy network representation - scenario 1.....	139
Figure 63: Water-energy network representation - scenario 2.....	141
Figure 64: Elements' contribution to TAC increase of scenario 2	142
Figure 65: Water-energy network representation - scenario 3.....	144
Figure 66: Simulated annealing convergence for scenario 1	145

LIST OF TABLES

	Page
Table 1: Recirculating water and seasonal required air flowrates	36
Table 2: Percentages of cooling tower evaporation rates to recirculating water	37
Table 3: Percentages of cooling tower evaporation rates to recirculating water	37
Table 4: Percentages of cooling tower blowdown rates to recirculating water	39
Table 5: Percentages of cooling tower blowdown rates to makeup water.....	39
Table 6: Percentages of cooling tower seasonal blowdown rates to recirculating water.....	41
Table 7: Average seasonal seawater properties in Qatar	45
Table 8: Percentages of increase in power generation using WHP unit and different cooling systems	55
Table 9: Crop tolerance to water deficit based on yield response value.....	56
Table 10: Qatar distance measurements	57
Table 11: Qatar climatological data in 2017.....	57
Table 12: Monthly rainfall data in Qatar	58
Table 13: Soil characteristics in Qatar	58
Table 14: Alfalfa and date palms crop data	59
Table 15: Seasonal evaporation rates from open treatment units per unit area	63
Table 16: Seasonal net evaporation rates from open treatment units	64
Table 17: Basic power load and minimum cooling requirement of each process	81
Table 18: Process water supply and demand	81
Table 19: Water demand for offices	81
Table 20: Percent of increase in cooling tower blowdown rates to process total water supply ...	85

Table 21: Percent of the increase in RO power demand with respect to plant basic power load.....	88
Table 22: Percent of the maximum seasonal increase in the WHP unit power generation using cooling towers to plant basic power load.....	89
Table 23: Percent of the maximum seasonal increase in the WHP unit power generation using once-through cooling seawater to plant basic power load	89
Table 24: Percent of the maximum seasonal increase in the WHP unit power generation using air coolers to plant basic power load.....	89
Table 25: Planting land area	90
Table 26: Percent of the increase in irrigation water demand to process total water demand.....	91
Table 27: Percent of the seasonal increase in DAF power demand to plant basic power load	93
Table 28: Percent of the maximum seasonal increase in MBR power demand to plant basic power load	95
Table 29: Percentages of the maximum seasonal increase in NF power demand to plant basic power load	96
Table 30: Percent of the maximum increase in wastewater RO power demand to plant basic power load	97
Table 31: Regression coefficients for condensing steam turbine with $W_{\max} > 2$ MW.....	125
Table 32: Flowrates and multiple contaminant water source data.....	129
Table 33: Flowrates and multiple contaminant water sink data	130
Table 34: Interceptors minimum removal ratios for all contaminants.....	130
Table 35: Cost parameters for water-energy network elements	131
Table 36: Water/Power demand parameters for cooling systems and interceptors	132
Table 37: Average-to-maximum parameters for water/power sources and sinks.....	132
Table 38: Piping cost coefficients.....	133
Table 39: Interceptors capital cost coefficients	133

Table 40: Operating hours and annualizing factors	133
Table 41: Environmental regulations on discharged pollutants concentration.....	133
Table 42: Source-to-sink or discharge water allocation – Scenario 1	136
Table 43: Source-to-treatment unit water allocation – Scenario 1	136
Table 44: Treated water-to-sink or discharge water allocation – Scenario 1	137
Table 45: Allocation of power generated via WHP unit-scenario 1	138
Table 46: Allocation of power generated via WHP unit - Scenario 2	140
Table 47: Allocation of power generated via WHP unit - Scenario 3	143
Table 48: Scenario 3 results considering ten runs	146
Table 49: Standard deviation, average, and percent SD for scenario 1 results.....	146

CHAPTER I

INTRODUCTION AND LITERATURE REVIEW

Introduction

Freshwater is utilized for different purposes such as domestic and industrial uses, livestock, irrigation, and cooling purposes in different industries such as power generation plants. Freshwater demand is increasing while freshwater supplies are decreasing over the world due to climate changes, population increase, energy generation, and land use alterations. For example, increasing temperature leads to increased consumption of freshwater by people, animals, and plants to survive. Therefore, the competition for these resources increases and results in depletion of freshwater resources. Overexploiting freshwater resources will increase the salinity of water aquifers, and lower water levels. If current water consumption levels continue, future generations may suffer from water shortage and even droughts.

It is important to maintain and develop the quality of life, and prosperity of the economy by meeting present demands of freshwater without compromising the ability of future generations to meet their demands. To ensure sustainable development, governmental plans and policies should consider the constraints on water supply, and formulate plans to maintain freshwater sustainability. To sustainably balance water supply and demand, plans should consider increasing water supplies, and decreasing water demands. This can be achieved by decreasing water losses and utilizing water efficiently. Currently, governments are targeting the reduction of water footprint which is defined as the extent of water use in relation to consumption of people [1]. Equally important, energy is necessary for almost all life aspects.

Energy is needed for most applications such as domestic, and industrial uses, and even for manufacturing the components needed for renewable energy production. The main source of energy nowadays is fossil fuels including coal, oil, and natural gas. Intensive energy consumption originating from continuous population growth, and industrial development will eventually lead to depletion of available fossil fuel resources. Knowing that these resources are limited, governments should find alternatives to replace fossil fuels or draw clear plans and policies to decrease energy losses, and efficiently use the available resources. There is no doubt that fossil fuels provide precious services, but it is problematic due to the limited available sources and the associated environmental impacts. Burning fossil fuels releases significant emissions of carbon dioxide which is the main contributor to global warming. Increasing earth's temperature will melt more icebergs, and increase sea levels, which will cause disturbances for settlement and agriculture in some areas. Accordingly, energy resources should be managed to maintain sustainable development. Also, energy management helps in minimizing the extensive environmental side effects from chemical processes as energy is one of the main building blocks for any chemical process.

The main objective of chemical processes is to convert raw materials into useful products. This conversion requires the involvement of freshwater and energy for different purposes. Accordingly, significant amounts of wastewater, and carbon dioxide emissions are produced. Each process requires various sub-components i.e. for cooling/heating, separation, and conversion. The same product can be produced by utilizing different routes, but these routes vary significantly in terms of water, and energy demands and cost. Industries are one of the main consumers of freshwater, and energy. To achieve sustainable development, industrial freshwater, and energy consumption should be controlled by minimizing their usage and reuse water; as well as waste

energy. One way is to design water and energy integration networks that help to optimize the use of these resources by utilizing process integration techniques.

In the scope of chemical engineering, El-Halwagi [2] defined process integration as a holistic process design approach that accentuates the unity of the process by exploiting the interfaces between different sub-components. Focusing on the wholeness of the process is the main advantage of process design over analytical approaches which optimize and improve process units individually. Process integration techniques are employed for designing new plants or retrofitting existing plants. These techniques are implemented for designing water and energy integration networks. The designed networks help in addressing industry-related challenges such as reducing energy usage, freshwater consumption, wastewater generation, and carbon dioxide emissions. Also, they help increase plant's profits as the cost of energy and freshwater generation is decreased. Designed water and energy integration networks may be directly affected by seasonal climatic variations.

Typically, a year is divided into four seasons. These seasons have different climatic conditions and ecological changes. Seasonal characteristics are originating from the relative axial position of the earth to the ecliptic plane, and earth's orbit around the sun. There are three methods for determining the beginning of the season, namely; the meteorological method, the astronomical method, and the phenological method. The meteorological method is the simplest and it depends on dividing the year into four equal seasons, and each season includes three months. According to the astronomical method, the beginning of the season is determined based on the location of sunshine on the earth's surface. Meteorological and astronomical methods depend on the calendar to determine the beginning of the seasons, while the phenological method is based on behavioral changes in living creatures such as animals' migration and plants' changing colors [3]. In this

study, the meteorological method is used to define the seasons. Figure 1 provides a visualization of the four seasons following the later method. Seasonal variations including air temperature, humidity, and rainfall may have a direct impact on utility systems, cooling systems, desalination plants, treatment units, evaporation rates, and irrigation water demands.

This work will explore seasonality impacts on interplant water-energy integration networks. Also, it will propose a novel mathematical programming model for designing efficient water-energy integration networks considering seasonal variations.

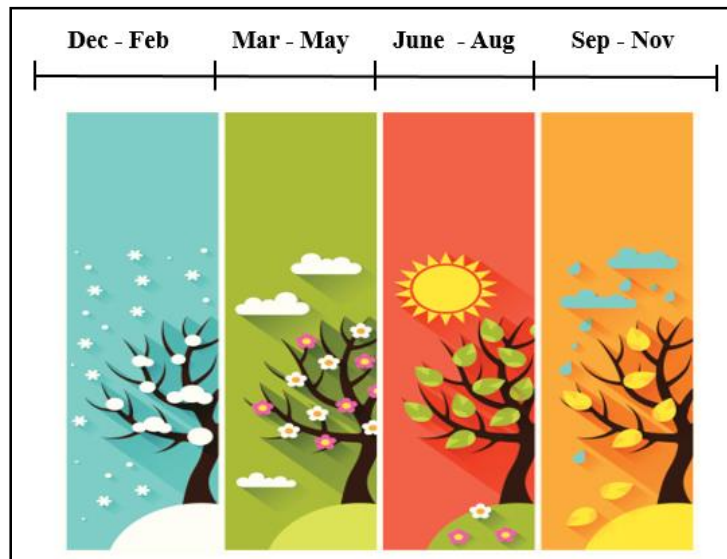


Figure 1: Visualization of the four seasons considering meteorological method [4]

Motivation

Water and energy play significant roles in the development of different sectors. Mainly, water and energy are utilized for residential, industrial, and auxiliary purposes. Natural resources for freshwater and energy are limited and are threatened by the danger of depletion due to excessive

consumption of these resources which is coincident with the rapid growth in global population. Accordingly, many countries are targeting the conservation of water and energy resources. Industrial activities are one of the main contributors to water and energy consumption. To reduce water and energy consumption by industries while maintaining the continuousness of the processes, different water and energy integration networks have been designed. Industrial plants including integration networks should be capable of operating at different operating conditions.

Seasonal variations need to be considered to ensure the stability of water-energy integration networks over the year. Seasonal variability originating from different weather conditions over the year has a direct effect on the components of the integration networks such as cooling systems, treatment units, desalination units, and utility systems. It is required to analyze and assess the significance of the water-energy network seasonal variations and develop a systematic approach to find the optimal design that can handle seasonal variations by implementing different solutions for the seasonality problem. Several works have focused on developing flexible integration networks that are feasible, and energy efficient over different time periods. More specifically, previous works have paid attention to multi-period planning of water and energy integration networks independently, and other works have highlighted the water-energy nexus away from integration networks and multi-period planning. Multi-period planning may result in very complex mathematical optimization models which are difficult to be solved. In addition, the formulated models may face difficulties during implementation due to geographical constraints on piping system layout which may impede water reuse between units.

This work will explore seasonality effects on different components of the water-energy integration networks considering the water-energy nexus and evaluate the seasonal variations significance. Additionally, this work will propose a novel approach for designing integration

networks that can handle the seasonal variations to stabilize the network and hence, stabilizing the whole system.

Literature review

This section provides a summary of previous works done in the field of mass and energy integration. It looks into different techniques and methods which have been employed to design integration networks. Several methods aimed to reduce the generation of wastewater, to minimize the exhaustion of water and energy resources and to enhance the reuse of wastewater and lost energy. Also, other works targeted sustainable development through avoiding overexploiting and depletion of available water, and energy resources. Furthermore, this section provides insights into various works that have been done earlier considering multi-period planning, and seasonal variations.

To ensure sustainability of available water and energy resources, efficient management techniques should be adopted to avoid depleting current resources and to secure future generations' accessibility to these resources. Process integration involving mass and energy integration techniques are widely employed to manage water, and energy resources. The term "process integration" has been generated by first developing the thermal pinch analysis for minimizing energy consumption through waste heat recovery. Thermal pinch analysis is a tool that thermodynamically calculates feasible energy targets or minimum required energy for a process through optimization of heat recovery, process conditions, and energy supply methods. In 1971, Hohmann stated in his Ph.D. that minimum requirements of hot and cold utilities for a process can be calculated without knowing the heat exchanger network (HEN).

A few years later, Linnhoff et al. [5] explained the thermal pinch analysis technique in details. In 1979, this work was built upon by Flower and Linnhoff [6] who developed an

approximation method for performing thermodynamic analysis in process network synthesis to overcome the problem of producing and interpreting the analysis. Then, Linnhoff and Hindmarsh [7] introduced a simple method for designing heat exchanger networks in 1983. This method is capable of identifying the best design which recovers the highest degree of energy, has good controllability, and ensures intrinsic safety. Developing heat exchanger integration networks was possible after utilizing thermal pinch analysis to determine energy targets. Several published works have employed thermal pinch analysis technique. For example, Hall and Linnhoff [8] implemented the pinch analysis technique to develop grand composite curve and to target furnace systems using a non-iterative method.

Heuristics, thermodynamics, and mathematical programming are the three main concepts used for process integration. Heuristics depend on experience and intuitions in the engineering field. Nowadays, process integration depends more on thermodynamics and mathematical programming. Thermodynamics generate creative ideas, and mathematical programming formulates these ideas into models that can be employed to solve complex problems [9]. Employing mathematical programming to improve process integration through heat integration, process synthesis and optimization have been of interest for researchers. Many researchers considered formulating and extending the pinch analysis as a linear programming algorithm (LP) for targeting the minimum utility requirements and as mixed-integer linear programming (MILP). In 1983, Papoulias and Grossmann [10] [11] [12] found the minimum utility, and minimum number of matches simultaneously. The developed mixed-integer linear program model was used to generate heat exchanger networks with minimum utility and investment costs.

Later, some researchers focused more on multi-period planning for heat exchanger synthesis. This involves (MILP) transshipment model with changing pinch point and utility

requirement at each period to cope with changing flowrates, inlet and outlet temperatures such as the work done by Floudus and Grossmann [13]. The model aimed to find minimum utility requirements at each period, with the fewest number of units. In 1986, Saboo et al. [14] developed an interactive software called RESHEX for heat exchanger networks (HEN) synthesis and analysis. One year later, Floudus and Grossmann [15] improved their earlier work to include sizing of the heat exchangers, assigning bypasses around the heat exchangers, and generating the final heat exchanger networks automatically as the previous work required a trade-offs manual generation of the final networks. Later, formulating non-linear programming models was considered by some researches to capture other aspects of the problem under investigation. In 1990, Yee and Grossman [16] formulated a non-linear model that considers trade-offs between the cost of area and utilities to synthesis heat exchanger networks with fixed temperatures, and flowrates. After that, Yee et al. [17] modified the same model into a mixed integer nonlinear program to account for variable temperatures and flowrates.

So far, the steady state behavior of heat exchanger network (HEN) synthesis has been discussed, therefore researchers started to consider the HEN dynamic behavior. For example, in 1990, Colberg et al. [18] formulated a non-linear program to calculate general and practical resilience targets for synthesizing heat exchanger networks. This work found that the general resilience target which has no size and complexity limitations of the designed HEN using any nominal stream data is not practical. It is difficult to design a HEN that covers all possible physical operating conditions, and it will result in a very large, complex, and costly HEN. On the other hand, the practical resilience target which considers synthesizing a practical HEN with extra few units, and stream splits is more useful. The critical uncertainty in supply temperature and flowrates can be identified by calculating the practical resilience target. This identification is followed by

designing a HEN with minimum area for both nominal stream data; as well as critical uncertainty point, and the structures for both cases can be merged to get a resilient HEN.

A method which combines the strengths of pinch analysis and exergy analysis to improve the process by determining required modifications was developed by Feng and Zhu in 1997 [19]. During the same time, Klemes et al. [20] created a new graphical approach and design tools to reduce energy consumption, pollution in the form of carbon dioxide emissions and increase the savings in capital and operating costs. The developed methodology is based on total site integration (TSI) which evolved from pinch analysis technique and used for multiple processes that share a common central utility system. Researchers paid attention to energy targeting by utilizing and developing different techniques.

Attention has been paid to multi-period and seasonal planning in the heat integration area. Several published works have considered introducing time to the energy integration problem considering the whole planning horizon, or periodical cycles (i.e. seasons) to increase the flexibility of developed solutions. In 1993, Papalexandri and Pistikopoulos [21] proposed a mixed integer nonlinear programming (MINLP) model to design/retrofit heat exchanger networks with the flexibility to operate feasibly over various possible operating conditions. Before utilizing this MINLP model, the critical operating conditions for the existing network need to be identified using flexibility analysis. The objective of that model was to minimize the total cost and to increase the flexibility of the heat exchanger network over three time periods $F(T)$, $T(T)$, and $U(T)$. A retrofitted heat exchanger network structure is established by solving the developed MINLP model. Later, in 1994, Papalexandri and Pistikopoulos [22] expanded the previous work to include multi-period mass exchanger network synthesis using MINLP. The model is used to generate mass and heat exchanger networks that are capable of handling possible variations in flowrates,

compositions, and inlet temperatures of process streams. The overall objective was to synthesize flexible mass and heat exchanger networks with minimum total annual cost (TAC) by balancing capital costs to operating costs. To illustrate the developed model, three case studies were considered; two examples were for heat and mass integration separately, and the third one is for simultaneous integration of mass and heat. The modeling system “GAMS” was used to solve the synthesis problems, and in some cases, flexibility analysis was used to ensure the flexibility of the MEN over the whole uncertainty range of rich stream flowrates.

Then, in 2001, a three-step approach based on heuristics and dynamic programming (DP) for short-term (i.e. days/weeks) multi-period planning of utility systems was employed by Kim and Han [23]. The main idea was to decompose the main MINLP problem into sub-problems which include a NLP sub-problems, and dynamic programming (DP) problem which enhances the search for accurate and reliable solutions in a relatively short computation time. The objective function was to minimize total cost over the planning horizon. The total cost composes of operating cost which depends on fuel cost, electricity cost, and water cost, switching cost which occurs due to start-up or shutdown of the equipment, and the transition cost which is related to the repeated drastic changes in equipment’s operation. In 2015, Bungener et al. [24] proposed a methodology for breaking down a year into n-periods to identify minimum and peak energy demands and supplies. Following the identification step, the total site analysis is applied to the industrial cluster that involves several production units. The optimal indices that define the beginning and end of each period are chosen by EMOO (evolutionary multi-objective optimization) algorithm. The n-periods are determined based on production profiles for each unit in the industrial cluster, which allows the consideration of zero-production days in some units.

In 2017, Isafiade et al. [25] integrated renewables in the synthesis of HEN over different seasons of the operational year considering environmental and economic impacts using a MINLP model. Hot utilities included three levels of steam (HP, MP, and LP), while cold utilities included (cold air, and cooling water). These utilities can be produced using renewable energy sources (i.e. solar, wind, and biomass) and non-renewable energy sources (i.e. natural gas, and coal). It also took into account the availability of different renewables over different seasons. The objective function was all about minimizing total annual cost and environmental impacts. In this work, seasonal variations are due to changes in flowrates, and temperatures of the hot, and cold streams over the operational year and they were adjusted by considering the use of different utilities, and alternative connections at different periods.

Additionally, a method for total site (TS) energy targeting considering short-term (days), and long-term (seasons) variations in energy demand and supply was developed in 2018 by Liew et al. [26]. Variations may occur due to variability in operating different units within the industrial cluster (i.e. some units may not operate over the year). The developed analysis can be applied for energy systems with continuous, or batch processes, renewables, urban energy consumptions, and energy storage. The utility requirement for each time slice is found by graphical methods such as the grand composite curve (GCC), total site profile (TSP), and site composite curve (SCC) or by using numerical methods such as total site problem table algorithm (TS-PTA), and multiple utility problem table algorithm (MU-PTA). Then, the short-term and long-term (i.e. seasonal) utility requirements are determined by the total site energy targeting approach along with total site heat cascade (TS-HSC).

In 1980, a very early work in mass integration field was done by Takama et al. [27]. The authors developed a mathematical programming approach to design water utilization system. The

approach targeted minimizing freshwater and wastewater by optimizing water allocation in the system which involve consuming water units and treatment units. This pioneering work tackled two problems simultaneously which are the water and wastewater allocation in process units and treatment units. Graphical methods are crucial due to their culpability of incorporating many design factors compared with mathematical programming. As an analogy to heat integration thermal pinch analysis, El-Halwagi and Manousiouthakis have proposed targeting graphical method for mass exchanger network (MEN) synthesis in 1989. The idea depends mainly on plotting cumulative mass flowrates and composition for rich and lean streams. Later, the authors developed a systematic approach to enable the automatic synthesis of mass exchange networks for one component. The approach mainly consists of a linear programming transshipment formulation to determine minimum utility cost, and locations of pinch points, followed by a MILP transshipment model to provide the minimum required number of exchangers in the network [28].

In 1994, Wang and Smith proposed a method for water minimization by constructing water limiting profile using process water streams; as well as maximum and minimum pollutant concentration [29]. By doing so, the minimum freshwater requirement is determined by constructing freshwater line and match it against the process limiting composite curve. Minimum water demand profile touches process composite curve at the pinch point which sets the target for maximum water reuse. Water network design is analogous to heat integration pinch design method. Drawbacks of this method include the limitation on the number of pollutants to only one. Also, the difficulty of modeling several process water streams entering and leaving the same unit at different concentrations. In addition, this method does not take into account the geographical constrains on long pipelines which may hinder water reuse between process units.

Dhole et al. benefited from the previous method and proposed a more general approach for wastewater minimization called “water pinch” in 1996 [30]. Simply, the method depends on constructing two water profiles using water-based process streams including water demand and water supply composite curves. The potential water reuse is indicated by the shaded area between the water supply and demand profiles. This method helps in determining the minimum freshwater use and minimum wastewater generation. Furthermore, it provides a good tool for engineers to implement some design modifications to the processes including mixing streams.

A simple design procedure was proposed by Olesen and Polley in 1997 [31]. The method can be used for addressing minimization of freshwater problem with single contaminant. The minimum freshwater demand is obtained by using water pinch while the network design is determined by inspection. Accordingly, this method can handle up to five processes only. In the same year, Doyle and Smith developed an iterative procedure to address the problem of water/wastewater allocation considering multiple contaminants [32]. One year later, Galan and Grossmann developed a mathematical programming model for designing optimal distributed wastewater network considering multiple pollutants [33]. The formulated nonconvex nonlinear model was solved by successive search method of relaxed linear model beside the original nonlinear model. The solution method was proposed to overcome the issue of local minima and difficulties in convergence. Also, the authors considered extending the earlier formulated model to involve selection of treatment unit among different options and handling membrane treatment units.

In 2003, Zheng, Feng, and Cao addressed water and energy minimization problem in designing water allocation network using combined pinch analysis and mathematical programming [34]. The two step approach depends on finding the favorable optimal water

network design followed by determining the minimum utilities that guarantee global optimality. Then, the heat integration network was designed accordingly. After one year, Savulescu, Kim, and Smith developed a systematic design methodology for maximizing water reuse and managing water and energy systems simultaneously. This work assumed negligible contaminant loads and depended on utilizing pinch analysis technique. The work consists of two parts; the first part did not take into consideration water reuse while the second part considered systems with maximum water reuse [35] [36]. In 2009, Manan, Tea, and Alwi utilized pinch analysis technique in addition to some numerical tools for simultaneous minimization of water and energy in plants [37]. Minimizing water and wastewater targets; designing water network; and finally designing heat recovery network are the three main steps in the proposed approach. Three years later, Zhou et al. proposed a mixed-integer nonlinear programming (MINLP) models for synthesizing interplant water-allocation and heat exchange networks simultaneously. The work consists of two parts. The first part focused on process with fixed flowrate (FF) while the second part considered fixed pollutants load (FC); as well as fixed flowrate processes [38] [39].

In 2014, Alnouri, Linke, and El-Halwagi proposed a nonlinear mathematical programming model for targeting fresh (and waste) by direct recycle applications to design a cost effective water network [40]. This study considers the spatial aspects of water network within the industrial city. Plant location, existing barriers between plants, and allocated corridors for water transport are considered in the proposed representation of the water network. Afterwards, the authors introduced a novel approach to design optimal interplant water network for industrial city taking into consideration pipeline merging and direct water reuse [41]. Merging water pipelines for transmission of water from or to different destinations helps generating a relatively simple and cost efficient water network representation. Two years later, the previously mentioned work was

extended to include wastewater treatment units [42]. This work considered wastewater treatment and direct water recycling via a formulated mixed integer nonlinear mathematical model. The objective function of the proposed model depends on minimizing the total annual cost of the network including total freshwater, wastewater treatment and disposal costs; as well as piping expenditures.

In 2016, Fouladi et al. proposed a systematic approach for designing optimal interplant water network across water-energy nexus [43]. This work depends on extending the mathematical model developed by Alnouri et al. to include cooling options and waste-heat-to-power unit in order to capture water-energy synergies within industrial processes. The authors considered three types of cooling options including air coolers, cooling towers, and once-through cooling seawater. Additionally, centralized and on-site decentralized treatment units and desalination plants were involved in this work. Water-energy linkages were taken into consideration via utilizing process excess waste heat; as well as across cooling and desalination units.

Recently, more attention has been paid to multi-period and seasonal planning of water and energy integration networks. In 2013, Burgara-Montero et al. [44] developed a multi-objective MINLP optimization model for designing distributed treatment systems for industrial discharges into watersheds. The multi-objective function considers the simultaneous minimization of pollutants' concentrations in the final destination and the total annual cost (TAC) of the wastewater treatment units. The location, the wastewater treatment technology, and the industrial effluents to be treated in each period throughout the year are decided by the formulated mathematical model following the environmental regulations of the region. Material flow analysis (MFA) was employed to consider all changes in inputs, outputs, and tributaries of the river at each period of the year, and natural phenomena such as precipitation, evaporation, and filtration are considered

in the formulated model. In 2014, Bishnu et al. [45] formulated two multi-period optimization models for long term planning of direct water reuse networks. The objectives of the two formulated models are to minimize the consumption of freshwater by maximizing direct water reuse and to minimize the total annual cost to get the lowest-cost network design. This work considers the expansion and changing of the industrial city layout over the whole planning horizon.

In 2015, Optimal multi-period planning of agricultural water systems involving water collections, reuse, and distribution strategies was considered by Ramirez et al. [46] using a multi-objective mixed-integer nonlinear programming model. The seasonal variability is due to changes in water supplies and demands throughout the year. The multi-objective function consists of minimizing both the freshwater consumption and the total annual cost (TAC). The TAC includes the fixed costs of water catchment areas, pumping systems, and storages, in addition to the operating costs which involve the cost for freshwater, and operating pumping systems. The multi-objective MINLP model was developed and solved using the ϵ – constrained method. The results obtained from testing the applicability of the MINLP model through a case study showed a significant reduction in freshwater consumption while considering the economic objective of minimizing the TAC.

A recent MINLP model was presented by Bishnu et al. [47] in 2017. The model considered long term multi-period planning of water network in industrial parks taking into account the entire planning horizon. The model considered direct reuse and regeneration of wastewater with the objective of minimizing the total annual cost. Wastewater is either allocated to other sinks directly, sent to treatment units, or discharged into the environment at a threshold pollutant's limits. The proposed model contributed to the reduction of total annual cost and complexity of the water network. Gaudard et al. [48] explored the seasonality aspects for water-energy nexus through the

seasonality (i.e. inter-year dependency) of water stream flows, and electricity prices. The case of run-of-the river (i.e. without incorporating dams into the river) hydropower plant has been investigated using hydrological model, hydropower model, glacier inventories, and climatic scenarios. The study concluded that variable water stream flows have a slight effect on future revenue while changing electricity prices have a significant effect and brings about more uncertainty on future revenues.

Apart from energy and water network, planning horizon and seasonality aspects have been explored in other research works. For instance, Al-Mohannadi et al. [49] proposed a systematic approach for long term multi-period planning for carbon integration and carbon footprint reduction. The formulated mathematical model aims to minimize total cost (TC) of the carbon integration network whilst meeting the net target of carbon dioxide reduction in the industrial park. The effect of climatic seasonality on ecological network structure involving food webs and mutualistic networks was highlighted by Takemoto et al. [50]. Furthermore, food security researches have addressed the seasonality problem as well. Bakker et al. [51] introduced the Food Distributed Extendable Complementarity (Food-DECO) model to capture the dynamics between climatic changes, economic changes, and policy interventions. In addition, the effect of seasonality on some diseases like brucellosis was considered by Lolika et al. [52] to understand the long-term health risks on humans and animals and help to set effective preventive methods and plans for future.

In short, research works initially assumed a steady state plant operation over the year and the entire planning horizon while in practice, plants operation may vary with time due to changing production capacity, expansion of the industrial park (i.e. by introducing more plants), internal factors like changing streams conditions and flowrates, or due to external factors such as climatic

seasonal changes. Accordingly, some researchers altered their attention to introducing the effect of time into their design problems.

Seasonality term was used interchangeably to refer to internal variations within systems (i.e. changing streams conditions, flowrates, production rates...etc.), and seasonal climatic changes. In this context, the seasonality effects refer to these effects caused by the changing climatic conditions of the year four seasons. This work is the first of its kind that analyzes and evaluates the effect of seasonal variations on inter-plant water-energy integration network synthesis.

CHAPTER II

PROBLEM DESCRIPTION AND METHODOLOGY

Objectives

The main aims of this research are:

- To investigate and assess the seasonal variations of water-energy network components within industrial parks.
- To expand the given water-energy network representation from Fouladi et al. to include water evaporation from open treatment units, in addition to water requirements for irrigation in industrial city.
- To propose a new approach with effective strategies to deal with seasonality issue while designing water-energy integration networks.
- To modify and expand the given optimization model to find the superstructure representation of the optimal water-energy network taking into account seasonal changes.
- Finally, to illustrate the applicability of the proposed model by solving a case study.

Problem statement

The represented problem in this research can be simply described as follows. Given a representation for a water-energy network in an industrial park which includes some plants, central and decentral treatment units, central and decentral desalination plants, utility systems, water demand for processes, and offices; as well as minimum cooling and heating requirements to generate the grand composite curves. It is required to utilize a systematic approach to study and evaluate all related seasonal variations including seasonal water demand for cooling towers, and irrigation, seasonal evaporation rates, seasonal power demand for different treatment units, cooling

systems and desalination units; as well as power produced from waste heat within the industrial city. It is also required to develop solutions to deal with seasonal variations while designing water-energy integration networks. A mathematical optimization model will be formulated determine the optimal network design. The objective of this research is to minimize the total annual cost for the water-energy network synthesis while considering seasonal changes.

Synthesis approach and superstructure representation

Earlier work that considers water-energy network synthesis was done by Fouladi et al. The work includes designing a network by considering all possible connections between sources and sinks of water and energy. The initial formulation considers reusing water directly into other sinks, regeneration of wastewater in treatment units which is then used in other sinks or discharged, and directly discharging water into the environment at threshold pollutants limits. Also, the model considers power generation from waste heat that can be either used to satisfy the power demand of different units in the plant or to produce freshwater in desalination plants. Figure 2 shows the superstructure representation proposed by Fouladi et al. for one plant with full connectivity.

Water and energy demand and supply may change over time due to several causes. The reasons behind these variations could be the expansion of the industrial city by adding more processes, increasing the production capacity of current processes, changing on regulations, or the seasonal climatic variations. This indicates that considering time horizon while planning and designing the water-energy network is crucial. As a result, multi-period planning is used to design integration networks. Multi-period planning is used to plan the operation of integration networks over several periods during a specific time horizon. This type of planning includes some decisions that are formulated at the beginning of the time horizon and some period specific decisions. Multi-

period planning is essential in case expansion plans are involved. So far, the seasonal climatic variations affecting the integration networks are handled by multi-period planning as well.

This work aims to investigate and analyze the effect of seasonal variations on water-energy integration networks and the significance of these variations with respect to the overall system. Accordingly, the main sources of seasonal variability in the integration networks will be determined. Based on the seasonality assessment, it will be decided whether multi-period planning is really needed or some design considerations can help to absorb these seasonal variations while maintaining the stability of the network and the process. This research aims to propose a novel method to design integration networks that are capable of dealing with seasonal variations considering different components in the water-energy network. This can be done by expanding the water-energy integration network developed by Fouladi et al. The newly developed superstructure representation considers water demand for irrigation and water losses due to evaporation from open treatment units.

Methodology

The proposed methodology for designing an optimal water-energy network considering seasonal variations consists of five main steps. The first step depends upon collecting all required data from available references including climatological data; as well as process and units related data. Then, seasonality effects on the water-energy network are analyzed using different available tools and software packages. According to the analysis result, observed seasonal variations of different network elements are assessed. Then, proper solutions and mathematical model are developed. Finally, the water-energy network is synthesized. To illustrate the applicability of the formulated MINLP optimization model, a case study is considered. Figure 3 represents the

sequential five steps of the implemented methodology for synthesizing optimal water-energy network.

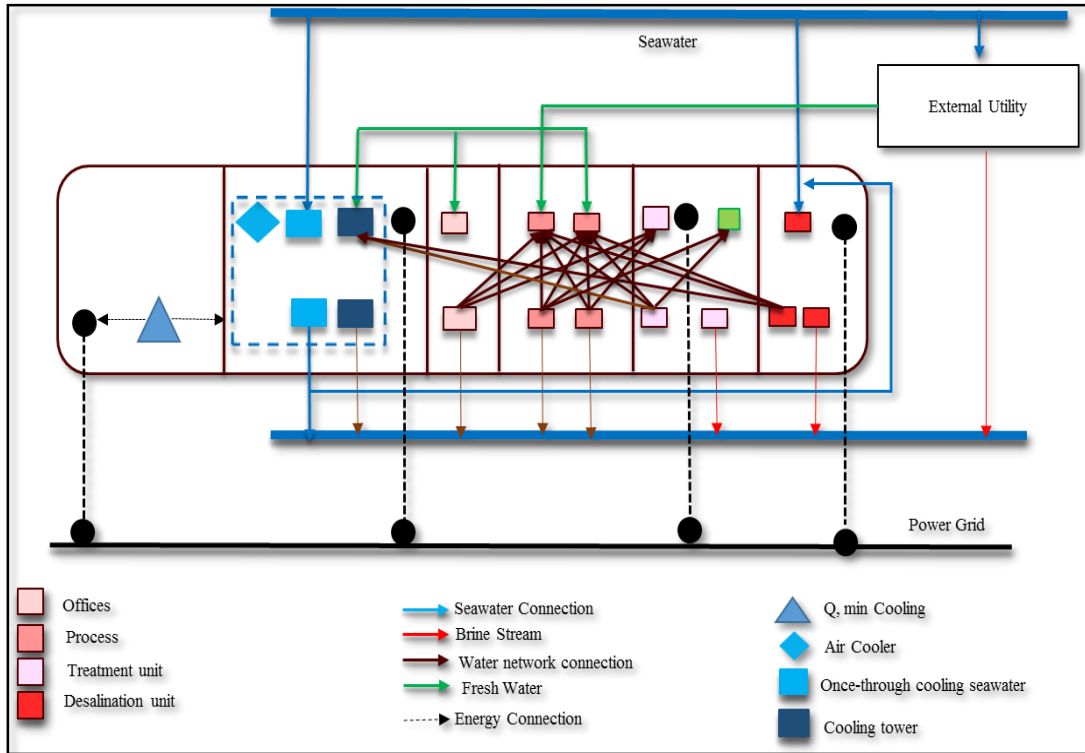


Figure 2: Water-energy network superstructure representation with full connectivity

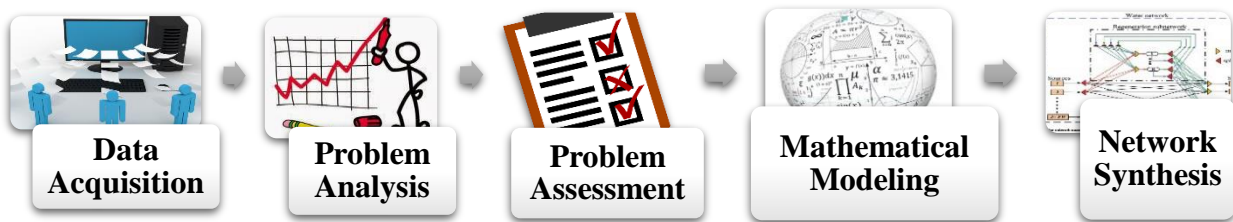


Figure 3: Sequential steps towards optimal design of water-energy network considering seasonality

Step 1: Data Acquisition

The first step towards designing an optimal water-energy network is to obtain all required data and information about all involved elements in the network synthesis. That includes different cooling systems, desalination units, wastewater treatment technologies, and processes. Three types of cooling systems are considered in this work involving; once-through cooling seawater, cooling towers, and air coolers while reverse osmosis (RO) technology is the selected desalination unit. Climatological data is one of the main set of data to be collected as it plays a significant role in assessing the severity of seasonal changes. Environmental constraints, seasonal water/power demands, equipment's design limitations; as well as process data including minimum cooling requirements are acquired. Some parameters are calculated or simulated such as power parameters of cooling systems, desalination units, and treatment units. Additionally, irrigation water demand parameters; as well as seasonal evaporation parameters are estimated.

Step 2: Problem analysis

Analyzing the water-energy network seasonality issue is done through investigation and analysis of different components of the water-energy network. The effect of seasonal variations is evaluated for the three cooling systems, RO unit, irrigation water requirements, evaporation losses, wastewater treatment technologies, and waste heat to power generation. Different software packages are utilized such as HTRI, ROSA, and CropWat. Water/energy demand and supply profiles are generated to analyze the seasonal variability of different network components.

Step 3: Problem assessment

This step is crucial to evaluate the significance of observed seasonal variations for different network elements. Basic water and power demands and supplies are utilized to assess the earlier

maximum spotted seasonal changes. Accordingly, all seasonal variations are evaluated and weighed considering total water/energy demands and supplies of the process.

Step 4: Formulating the mathematical model

A mixed integer nonlinear programming (MINLP) optimization model is modified to handle seasonal variations while designing the water-energy network. The mathematical model consists of mass balances and equality constraints for water flowrates. Also, it includes some inequality constraints for water pollutants concentrations of water sources, sinks, wastewater discharges; as well as treatment units. In terms of the energy model, a set of power equations is used which consists of inequality constraints for the available power from energy sources in addition to sinks required power. The model involves equations that take into account the cost of freshwater, central and decentral treatment units, wastewater discharges, cooling systems, piping system, and waste-heat-to-power unit. The objective function is to minimize the total annual cost that includes all previously mentioned costs (i.e. capital and operating costs).

Step 5: Water-energy network synthesis

Using the previously acquired data, and the proposed mathematical formulation, the water-energy network is synthesized. This unique design ensures smooth and continuous process operation throughout different seasons of the year as it considers potential seasonal variations.

The details of the performed seasonality analysis are described in chapter III. This analysis is followed by an assessment of the seasonality impact on the water-energy network as detailed in chapter IV. Then, proposed assumptions and solutions to design a novel water-energy network capable of handling seasonal variations along with the mathematical formulation are delineated in chapter V. Finally, the applicability of the developed model is illustrated in chapter VI through a case study.

CHAPTER III

PROBLEM ANALYSIS

This chapter highlights all performed investigations to obtain a full understanding of the seasonal variations that may affect the performance of different elements of the water-energy network. This includes the cooling systems; air-coolers, cooling towers, and once-through cooling seawater, desalination units, treatment units; as well as a waste-heat-to-power unit and irrigation water demands. All assumptions used in this analysis are stated clearly in this chapter.

Seasonal variations of cooling systems

The effect of seasonal variations was investigated for three types of cooling systems; air coolers, cooling towers, and once-through cooling seawater. The following sections describe different utilized methods for analyzing the seasonality impacts on cooling systems. This involves theoretical and empirical correlations, relevant assumptions, in addition to the use of different software packages; as well as some relevant charts.

Air Coolers

Air coolers are used to provide required process cooling according to process minimum cooling requirement. Air coolers require power only, so they do not involve any water consumption or generation. Accordingly, air coolers are considered as power sinks. HTRI software was used to design the required air cooler and determine seasonal power demands. It is worth noting that increasing the size of the air cooler (i.e. by increasing the number of bays) will decrease air cooler power demand. Despite that, air cooler size is constrained by the available land area and transportation difficulties from manufacturers to clients.

A sensitivity analysis was performed prior to the air cooler design step to understand the influence of changing different design parameters. This includes inlet/outlet process stream temperatures, inlet pressure, number of tube rows, outer tube diameter, number of bays, components compositions, and physical states. This analysis was performed by maintaining the cooling requirement (i.e. process minimum heat that needs to be removed Q_{min}) fixed while changing the values of the studied parameters.

Sensitivity analysis results showed that all studied parameters affect air cooler power demand. As a result, process streams with different temperatures and pressures would have different power demands. For the same process stream, the main two affecting parameters are the number of tube rows and the number of bays. Figure 4 illustrates the air-cooled heat exchanger.



Figure 4: Illustration of air-cooled heat exchanger as a power sink [53]

Assumptions on using air coolers

- The flow regime in the air cooler is assumed to be counter current.

- The outlet air temperature should not exceed 60 °C to avoid damages to air cooler components.
- Air cooler is designed based on peak conditions (i.e. summer conditions), for example, the number of bays needed for the air cooler is determined based on inlet air temperature in summer season such that cooling requirement is satisfied.
- Due to the limitation on air cooler size, the average power demand per megawatt cooled in summer was assumed to be 48 kW/MW. This value was obtained from literature as the average power demand for air cooler [54].
- The power demand for other seasons is obtained by modifying the summer design to get zero overdesign percent (i.e. some bays are switched off).
- The total combined efficiency of fan and driving motor is 70%.

Seasonal air cooler power demands were obtained using HTRI to design the air cooler.

Figure 5 illustrates normalized air cooler power demands per megawatt of heat removed for each season.

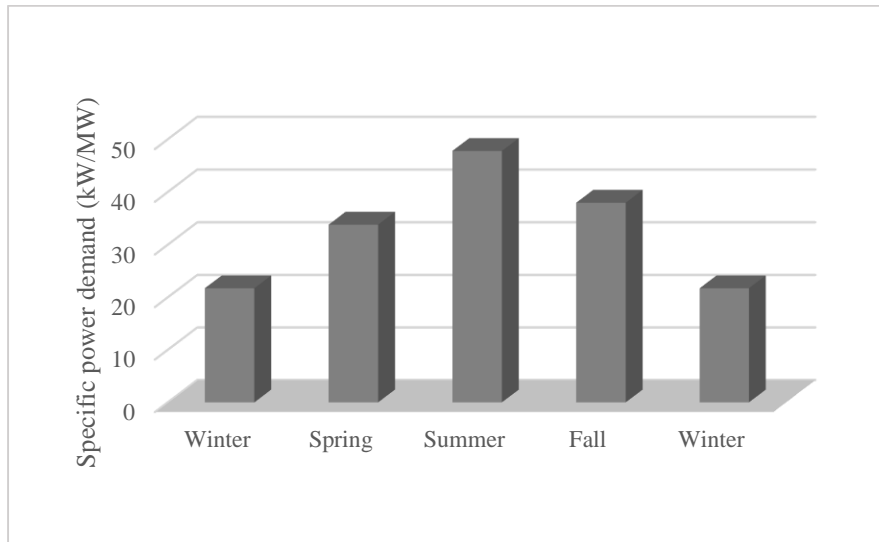


Figure 5: Seasonal air-cooled heat exchanger power demand per megawatt of heat removed

Figure 5 clearly shows that maximum air cooler power demand occurs in summer, while minimum power is required in winter. Comparing maximum and minimum power demand, it is noted that summer power demand increased by 120% relative to winter power requirement.

Cooling towers

Cooling towers are utilized to cool down process streams to satisfy process minimum cooling requirements by rejecting heat through evaporative cooling of water via air. Cooling towers require both power and water. In this context, cooling tower blowdown represents a water source while cooling tower makeup is a water sink. Moreover, cooling towers are power sinks as power is needed to operate cooling tower fans and pumps. The fans are used to move air which cools down the circulating water while pumps are used for water recirculation to cool down process streams. Figure 6 provides a general illustration for a cooling tower with inlet and outlet air and circulating water. Seasonal power demand parameters were obtained using psychrometric charts, mathematical formulas, and some assumptions which are listed below.

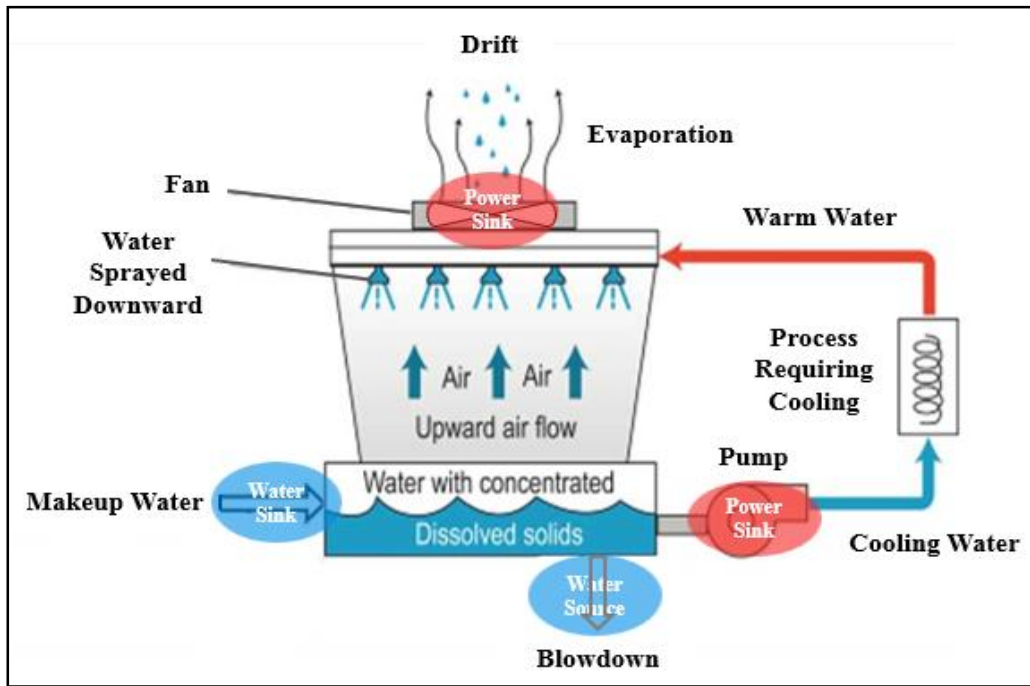


Figure 6: Illustration of cooling tower water/power sources and sinks [55]

Assumptions on using cooling towers

- The outlet cooling water temperature from the cooling tower should be higher than the air wet bulb temperature by at least 2.8 °C which is the minimum guaranteed approach by manufacturers. This value was set to avoid designing an oversized cooling tower which is limited by available land area and transportation constraints.
- The cooling tower is designed based on peak conditions (i.e. summer conditions), for example, the size of the cooling tower is determined to satisfy the cooling requirements during the summer season.

- Splash fills are selected for designing the cooling towers. Despite the fact that splash fills are more expensive than film fills, they are selected as they provide better air-water contact which reduces the power demand.
- Average pumping head requirement using splash fills is 10.5 m.
- Due to the limitation on the available land area, average power demand per megawatt cooled in summer was assumed to be 35 kW/MW. This value was obtained from literature as the average cooling tower power demand [54].
- Other seasons cooling tower power demands are obtained by calculating fans and pumps power requirements using the same cooling tower size and different seasonal climatic conditions.
- The effects of seasonal climatic changes on cooling tower performance are compensated by changing air flowrate using multispeed fan motor as controlling air flow is easier than water flow. Accordingly, fans power demand is different over different seasons.
- Circulating water flowrate is fixed over different seasons as evaporated water is compensated by makeup water from the basin of the cooling tower.
- Inlet and outlet circulating water temperatures into and from the cooling tower are fixed over different seasons which are 33 °C and 26 °C respectively.
- The cycle of concentration was assumed to be 5 as typical range for the COC determined by manufacturers is (4-6).
- Water evaporation from cooling tower basin is eliminated as almost 95% of the water evaporation is due to the evaporative cooling and less than 5% of water evaporation is from basins [56]. In other words, basins are assumed to be fully closed.

- Cooling towers are well designed to prevent any water losses due to leakages.
- Cooling tower design includes drift eliminators which minimize drift losses via fans exhausts to around 0.01% of the recirculating water.
- The efficiency of cooling towers fans and pumps is 70%.

Using the previously mentioned assumptions, psychrometric charts, and some mathematical/empirical formulas, cooling tower seasonal power demands were obtained. The power demand for fans is calculated using the following equation:

$$Power_{fan} = \frac{F_a \Delta P_{air}}{\rho \eta}$$

Where,

F_a Minimum required air flowrate ($\frac{kg}{s}$)

ΔP_{air} Air pressure drop across the fillings (Pa)

ρ Density of air at average temperature of the season ($\frac{kg}{m^3}$)

η Total efficiency of the fan

While, pumps power demand was calculated using the following equation:

$$Power_{pump} = \frac{H F_{cw} g}{\eta}$$

Where,

H Pumping head (m)

F_{cw} Flowrate of cooling water ($\frac{kg}{s}$)

g Gravitational acceleration ($\frac{m}{s^2}$)

η Total efficiency of the pump

Cooling tower total power demand is the summation of fans and pumps power requirements. To calculate the power demand of cooling tower fans, air pressure drop loss coefficient was calculated using the following empirical formulation [57]:

$$K = 3.179688 G_W^{1.083916} G_a^{-1.965418} + 0.639088 G_W^{0.684936} G_a^{0.642767}$$

$$\Delta P_{air} = \frac{K \rho V^2}{2}$$

Where,

K Pressure drop loss coefficient (—)

G_W Water mass velocity ($\frac{kg}{m^2 s}$)

G_a Air mass velocity ($\frac{kg}{m^2 s}$)

ΔP_{air} Pressure drop of air across the filling (Pa)

ρ Density of air at average temperature of the season ($\frac{kg}{m^3}$)

V Air velocity inside the cooling tower ($\frac{m}{s}$)

The air velocity was calculated using air volumetric flowrate (e.g. minimum required air flowrate, and density), and cross-sectional area of the cooling tower as follows:

$$V = \frac{F_a}{\rho A_{c/s}}$$

Where,

$A_{c/s}$ Cooling tower cross sectional area (m^2)

Air and water mass velocities were calculated using the required mass flowrate and cooling tower cross-sectional area as follows:

$$G_a = \frac{F_a}{A_{c/s}}$$

$$G_W = \frac{F_{CW}}{A_{c/s}}$$

Minimum required air flowrate is calculated by performing energy balance around the cooling tower as follows:

$$F_{a,in} h_{a,in} + F_{CW,in} h_{CW,in} = F_{a,out} h_{a,out} + F_{CW,out} h_{CW,out}$$

Where,

$F_{a,in}$ Mass flowrate of inlet air into cooling tower ($\frac{kg}{s}$)

$h_{a,in}$ Enthalpy of inlet air stream into cooling tower ($\frac{kJ}{kg \text{ air}}$)

$F_{a,out}$ Mass flowrate of outlet air from cooling tower ($\frac{kg}{s}$)

$h_{a,out}$ Enthalpy of outlet air stream from cooling tower ($\frac{kJ}{kg \text{ air}}$)

$F_{CW,in}$ Mass flowrate of inlet water into cooling tower ($\frac{kg}{s}$)

$h_{CW,in}$ Enthalpy of inlet water stream into cooling tower ($\frac{kJ}{kg \text{ water}}$)

$F_{CW,out}$ Mass flowrate of outlet water from cooling tower ($\frac{kg}{s}$)

$h_{CW,out}$ Enthalpy of outlet water stream from cooling tower ($\frac{kJ}{kg \text{ water}}$)

Inlet and outlet air enthalpies were obtained using a psychrometric chart, while inlet and outlet water enthalpies were obtained from thermodynamic tables. Using algebra, the fact that inlet and outlet air flowrates are equal ($F_{a,in} = F_{a,out}$), and water mass balance, cooling tower energy balance can be written as follows to calculate the minimum required air flowrate:

$$F_a = \frac{F_{CW,in}(h_{CW,out} - h_{CW,in})}{(h_{a,in} - h_{a,out}) + (W_{out} - W_{in}) h_{CW,out}}$$

The following equation represents water mass balance:

$$F_{CW,out} = F_{CW,in} - (W_{out} - W_{in})F_a$$

Where,

W_{in} Humidity of inlet air into cooling tower ($\frac{kg\ water}{kg\ air}$)

W_{out} Humidity of outlet air from cooling tower ($\frac{kg\ water}{kg\ air}$)

Humidity ratios or air moistures were obtained using psychrometric charts for inlet and outlet air.

Cooling tower working mechanism depends upon cooling recirculating water by direct contact with air inside the tower where some water evaporates as a result of this cooling. As a result, evaporation rates from cooling towers experience some seasonal variations due to changes in air temperatures and humidity ratios. To calculate the amount of evaporated water due to evaporative cooling, outlet warm water flowrate from the cooling tower is calculated using water mass balance. Hence, evaporated cooling water was calculated as follows:

$$F_E = F_{CW,in} - F_{CW,out}$$

Where,

F_E Flowrate of evaporated water from cooling tower ($\frac{kg}{s}$)

Water evaporation from cooling tower increases minerals concentration in the system. Consequently, cooling tower bleeds off some of the highly concentrated circulating water. This process is essential to avoid increasing minerals concentration in the system due to water evaporation during the cooling process. High minerals concentration is undesired in a cooling tower as it causes scale formation throughout the system when the concentration levels exceed saturation points of circulating water [58].

In this analysis, blowdown was calculated using the flowrate of evaporating water, and the cycle of concentration. The cycle of concentration (COC) is a dimensionless number which represents the ratio of minerals concentrations, or water conductivity of system circulating water. Typically, it has the value of (3-7) depending on the manufacturer [59]. In this analysis, COC was assumed to have a value of 5. Cooling tower blowdown was calculated using the following equation:

$$F_B = \frac{F_E}{COC - 1}$$

Where,

F_B Flowrate of blowdown from cooling tower ($\frac{kg}{s}$)

In addition to water evaporation, and blowdown, water escapes from cooling towers in the form of drift losses. Drift losses are fine moisture droplets which escape from cooling tower fan exhaust. Well-designed cooling towers include drift eliminators which can reduce drift losses up to 0.005 percent of the water recirculation rate. Minimizing drift particulates is very important and undergoes regulations which force tightening these losses. In this analysis, drift losses were assumed to represent 0.01% of the water recirculation rate. Accordingly, drift losses from cooling towers were calculated as follows:

$$F_D = 0.01 \times \frac{F_{CW}}{100}$$

Where,

F_D Flowrate of drift losses from cooling tower ($\frac{kg}{s}$)

Makeup water is required to compensate for different water losses from cooling tower including evaporation, blowdown, and drift losses. Makeup water demand is determined by the summation of all water losses from the cooling tower as follows:

$$F_M = F_E + F_B + F_D$$

Where,

F_M Flowrate of required makeup water by cooling tower ($\frac{kg}{s}$)

After elucidating all required calculations, the obtained analysis results are represented and discussed focusing mainly on cooling tower seasonal aspects including; blowdown rates, makeup demand, and power requirement. That is because the blowdown represents a water source, while makeup water demand is a water sink, and power demand indicates a power sink in the water-energy network context. Although evaporation rates do not contribute directly to the network as it is neither a water source nor a water sink, it affects the blowdown rates and makeup demand. Accordingly, the results of evaporation rates seasonality are represented and discussed. Table 1 illustrates the required recirculating water and seasonal air flowrates per megawatt of heat removed.

Table 1: Recirculating water and seasonal required air flowrates

Season	Air flowrate (kg/s MW)	Recirculating water (m ³ /hr MW)
Winter	15.79	123.08
Spring	16.88	
Summer	21.37	
Fall	20.94	

The following results highlight cooling tower seasonality aspects starting with evaporation rates, followed by blowdown rates, makeup water demand, and finally power demand. Figure 7 represents seasonal variations of cooling tower evaporation rates. Table 2 and Table 3 shows the percentages of cooling tower evaporated water to recirculating water, and seasonal makeup water demand respectively.

Evaporation rates

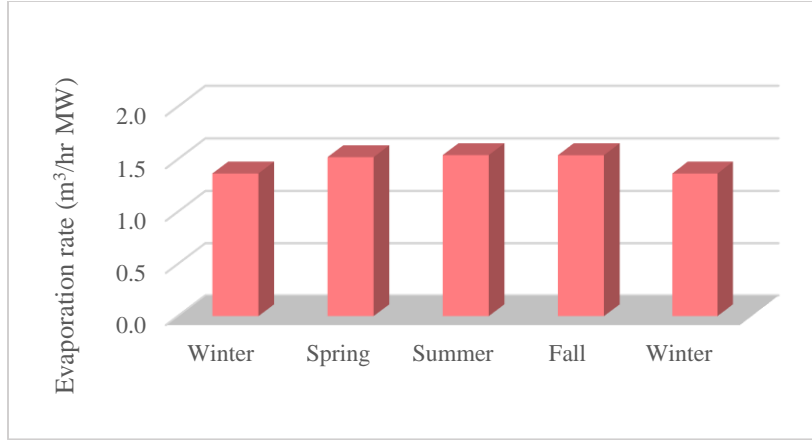


Figure 7: Seasonal cooling tower evaporation rates per megawatt of heat removed

Table 2: Percentages of cooling tower evaporation rates to recirculating water

Season	Water evaporation rates (%)
	With respect to recirculating water
Winter	1.10
Spring	1.23
Summer	1.25
Fall	1.24

Table 3: Percentages of cooling tower evaporation rates to recirculating water

Season	Water evaporation rates (%)
	With respect to Makeup water
Winter	79.427
Spring	79.485
Summer	79.492
Fall	79.491

Seasonal cooling tower evaporation rates graph shows that maximum and minimum evaporation is expected in summer and winter respectively. Evaporation rates differ according to seasonal air temperatures and humidity ratios. Comparing water evaporation rates in summer and winter, results show that evaporation rates in summer increase by 12.82%. In any season, cooling tower evaporating water represents about 79.4% of the makeup water demand. As a result, most of the makeup water consumption is due to evaporative cooling.

Blowdown

Seasonal variations of cooling tower blowdown rates were analyzed. It is worth noting that the seasonality of blowdown rates is due to seasonal changes in evaporation rates. Figure 8 represents the seasonal blowdown rates per megawatt of heat removed.

Analysis results show that maximum and minimum blowdown occurs in summer and winter respectively since blowdown is a direct result of evaporation. Higher evaporation rates increase minerals concentration in circulating water and result in more blowdown in summer compared to winter. Table 4 represents the seasonal percent of cooling tower blowdown rates to recirculating water. During any season, cooling tower blowdown rate is almost 19.8% of makeup water demand as shown in Table 5. The percentage of cooling tower blowdown increased by 12.82% in summer relative to winter rates. The increase in blowdown rates is the same as the increase in evaporation rates as cooling tower blowdown is directly proportional to evaporation rates.

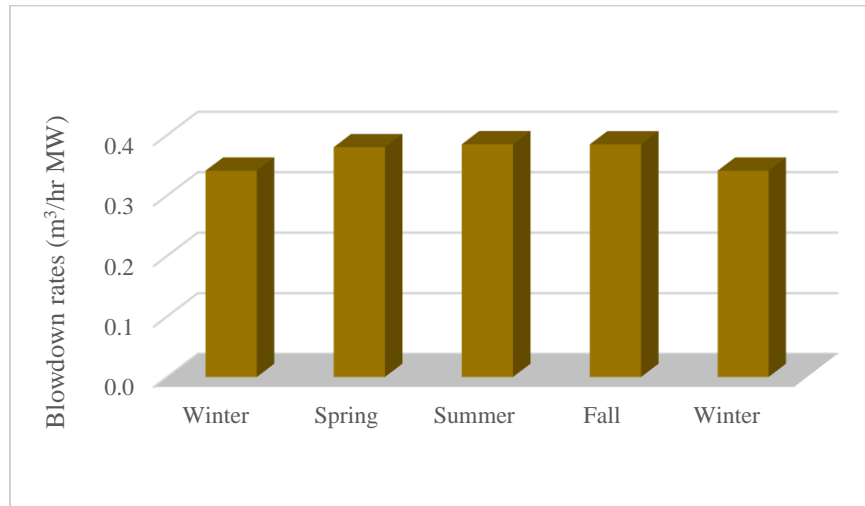


Figure 8: Seasonal cooling tower blowdown rates per megawatt of heat removed

Table 4: Percentages of cooling tower blowdown rates to recirculating water

Season	Blowdown rates (%)
	With respect to recirculating water
Winter	0.277
Spring	0.309
Summer	0.313
Fall	0.312

Table 5: Percentages of cooling tower blowdown rates to makeup water

Season	Blowdown rates (%)
	With respect to Makeup water
Winter	19.857
Spring	19.871
Summer	19.873
Fall	19.873

Drift losses

Drift losses represent a very small fraction of recirculating water. As the later flowrate does not change over the year, drift losses do not experience any seasonality. Although drift losses do not vary over seasons, they affect cooling tower makeup water demand. Figure 9 shows seasonal cooling tower drift losses per megawatt of removed heat. In this analysis, drift losses represent only 0.01% of recirculating water.

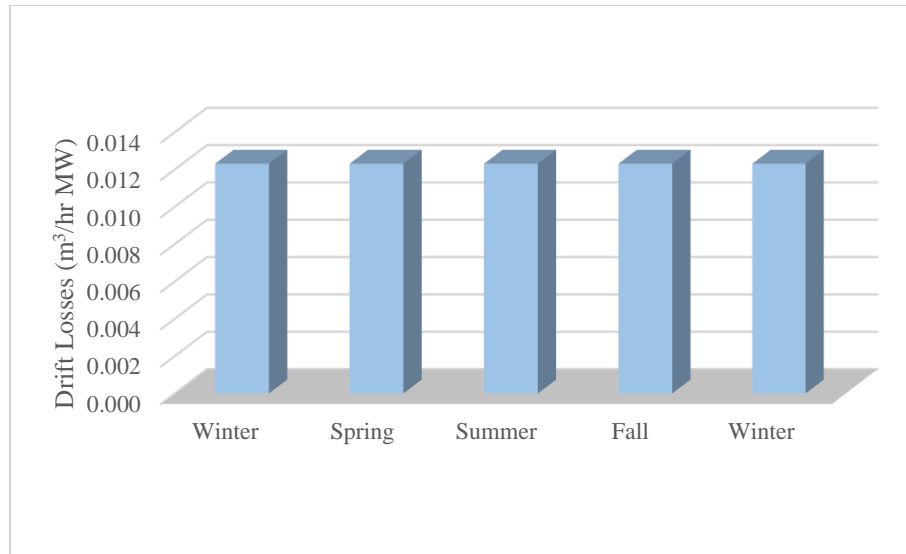


Figure 9: Cooling tower drift losses per megawatt of heat removed

Makeup water demand

Cooling tower makeup water demand depends on evaporation rates, blowdown rates, and drift losses. Previous results show that evaporation and blowdown rates are both vulnerable to seasonal variations; while drift losses do not experience any changes over the year. Seasonal makeup water demands per megawatt of heat removed were calculated and represented in Figure

10. Table 6 represents the percentages of makeup water demand to recirculating water in a cooling tower.

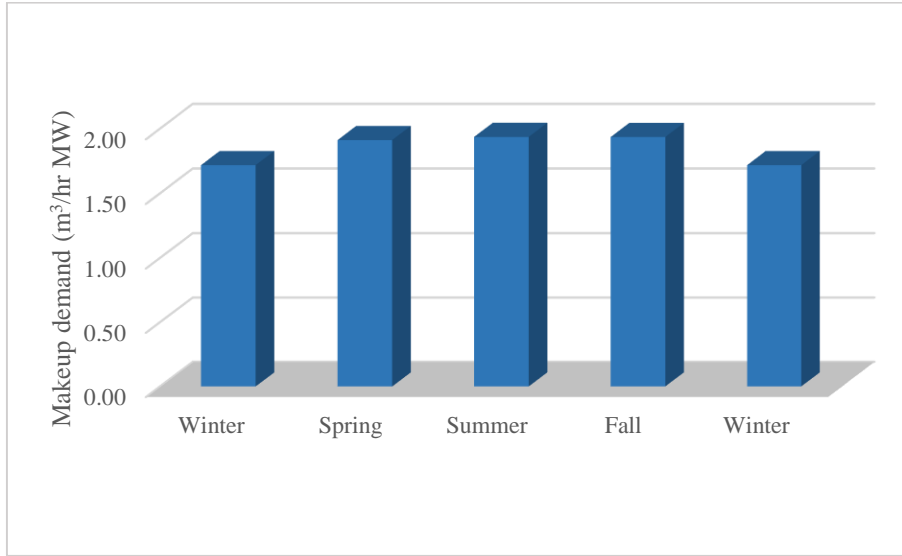


Figure 10: Seasonal cooling tower makeup water demand per megawatt of heat removed

Table 6: Percentages of cooling tower seasonal blowdown rates to recirculating water

Season	Makeup demand with respect to recirculating water (%)
Winter	1.395
Spring	1.553
Summer	1.573
Fall	1.572

Since makeup water demand depends on total water losses from cooling tower, the required makeup water is maximum in summer and minimum in winter following the same trends of evaporation and blowdown rates. According to the analysis results, summer makeup water demand increased by 12.72% relative to winter. Figure 11 demonstrates the percentages of

different makeup water components including; water losses due to evaporation, blowdown; as well as drifting. It clearly shows that the main contributor to the makeup water demand of a cooling tower is the evaporative losses followed by blowdown, and drift losses.

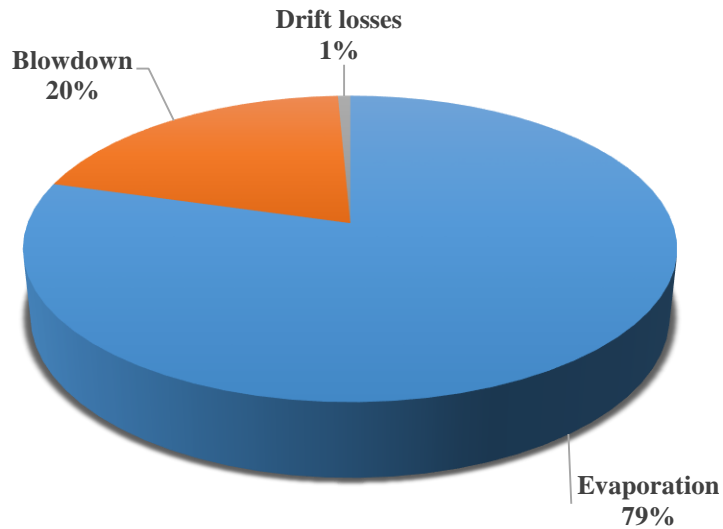


Figure 11: Contribution of different cooling tower makeup water demand components

Power demand

Cooling tower seasonal power demand consists of fans and pumps power requirements. Cooling tower pumps require a fixed power demand while fans have a changing power demand over seasons. That is due to fixing the recirculating water flowrate and changing air flowrates to assure the same heat rejection over the year. Cooling tower seasonal power demand per megawatt of heat removed is shown in Figure 12. It shows that summer cooling tower power demand increases by 146% relative to winter power demand. The increase in cooling tower power

requirement is due to higher air temperatures in summer that increase required air flowrate to reject the same amount of heat, hence fans power demand increases.

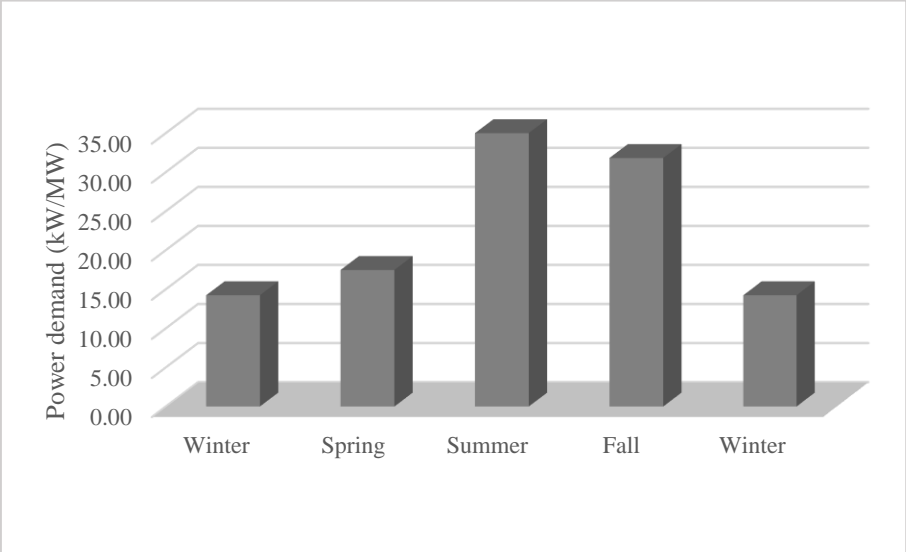


Figure 12: Seasonal cooling tower power demand per megawatt of heat removed

Once-through cooling seawater

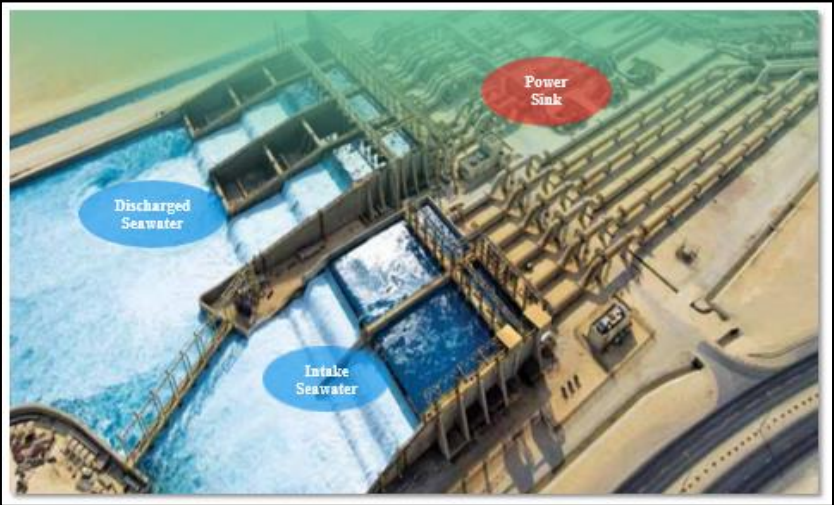


Figure 13: Illustration for once-through cooling seawater [60]

Once-through cooling seawater is a cooling option that depends on using seawater to provide required cooling for the process. Figure 13 clarifies the use of seawater for cooling along with associated water and power sources and sinks. Utilizing seawater for cooling purposes undergoes some environmental constraints which are either based on the maximum temperature difference between inlet and outlet seawater or the maximum outlet temperature of seawater. In Qatar, the maximum allowed temperature difference for seawater is 3 °C. The constraints on seawater use aim to maintain a healthy marine environment and to avoid disturbance to the marine ecosystem. The following assumptions were considered while using seawater for cooling purposes in this study.

Assumptions on using once-through cooling seawater

- The minimum cooling requirement of the process is fixed over the year assuming the process does not undergo any changes over the seasons (i.e. no changes in production capacity or products).
- The maximum difference between inlet and outlet seawater temperature is 3 °C.
- Average seawater temperature and properties are used for each season.
- Pumping head is 8.6 m.
- The efficiency of the pump used for pumping seawater is 70%.

Average seasonal seawater properties based on Qatar seawater temperatures were acquired and shown in Table 7. Then, required seawater flowrates were calculated using the following equation:

$$F_{SW} = \frac{Q^{min}}{Cp_{sw} \Delta T_{sw} \rho_{sw}}$$

Where,

F_{sw} Flow rate of Cooling Seawater ($\frac{m^3}{s}$)

Q^{min} Heat load (J/s)

Cp_{sw} Specific heat capacity ($\frac{J}{kg K}$)

ΔT_{sw} Temperature difference between inlet and outlet seawater (K)

ρ_{sw} Density of cooling seawater ($\frac{kg}{m^3}$)

The pumping power demand was calculated using the following equation:

$$Power_{pump} = \frac{HF_{sw} g \rho_{sw}}{\eta}$$

Where,

H Pumping head (m)

F_{sw} Flow rate of Cooling Seawater ($\frac{m^3}{s}$)

g Gravitational acceleration ($\frac{m}{s^2}$)

ρ_{sw} Density of cooling seawater ($\frac{kg}{m^3}$)

η Total efficiency of the pump

Table 7: Average seasonal seawater properties in Qatar

Season	Average T (°C)	Density (kg/m ³)	Specific capacity (kJ/kg K)
Winter	21.75	1024	4.008
Spring	25.00	1023	4.009
Summer	32.65	1022	4.011
Fall	29.35	1021.5	4.010

Figure 14 and Figure 15 illustrates once-through cooling seawater required flowrate and power demand per megawatt of heat removed respectively. The profiles show that seawater flowrate and power demand are fixed over different seasons. That is due to the fixed seawater flowrate as temperature difference was assumed to be constant according to Qatar environmental constraints. Required seawater flowrate per megawatt of heat removed is $292 \frac{m^3}{MWh}$, and the required power to remove the same amount of heat is $10 \frac{kW}{MW}$ that is equivalent to 0.0342 kilowatt-hours per cubic meter of pumped once-through cooling seawater.

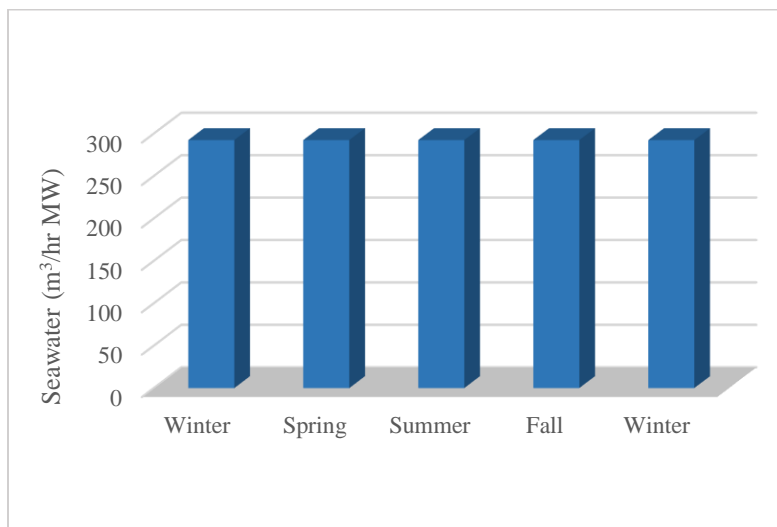


Figure 14: Once-through cooling seawater demand per megawatt of heat removed

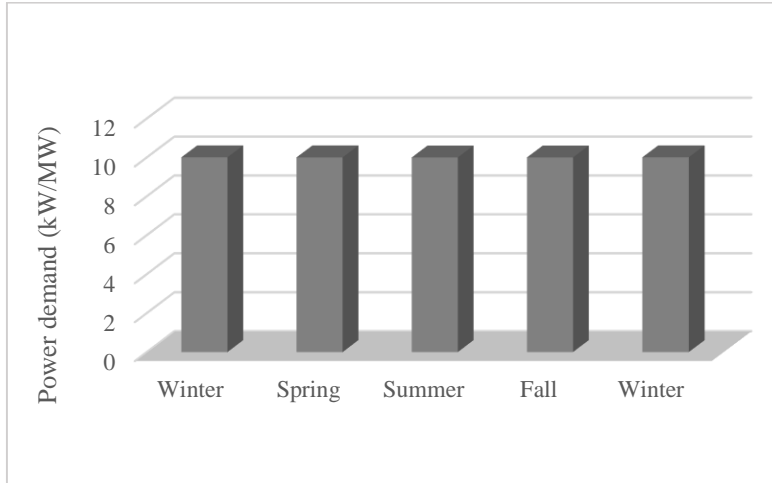


Figure 15: Once-through cooling seawater power demand per megawatt of heat removed

Seasonal variations of desalination units

In this analysis, reverse osmosis was selected as the desalination technology, and ROSA software was used to study the effect of seasonal climatic conditions on the RO unit. The software was developed by DOW chemical company, and the latest version ROSA 9.1 was utilized. The following assumptions were employed in this analysis.

Assumptions on using RO units

- Feed temperature to RO plant is the average seawater temperature in each season represented in Table 7.
- Feed total dissolved solids (TDS) = 35000 ppm.
- Total dissolved solids in treated water should be less than 500 ppm which is the maximum concentration level for potable water set by Environmental protection agency EPA” [61].
- The PH of feed water is 7.6.

- Pumping efficiency is 80%.
- System recovery 40% (conventional recovery for seawater RO)

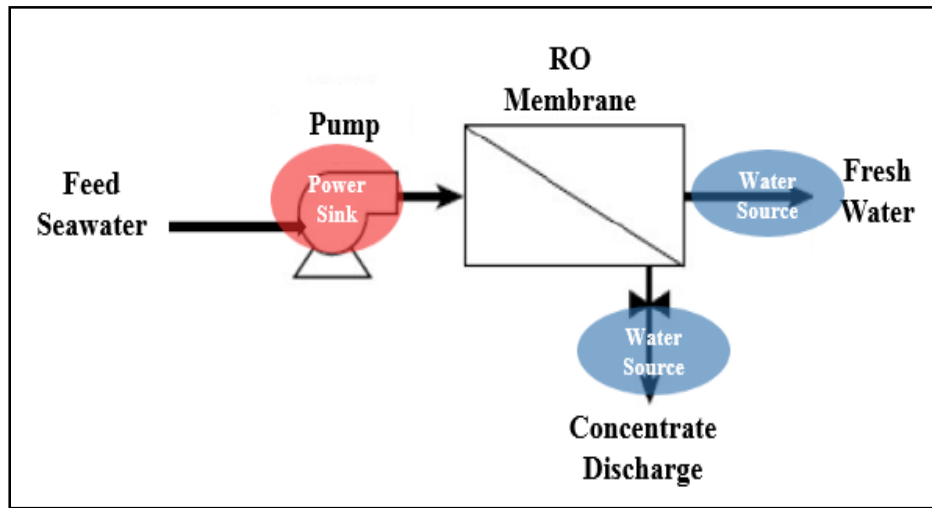


Figure 16: Reverse osmosis system configuration

Some parameters were input into ROSA; while others were calculated by the software. Feed water properties including; seasonal temperature, PH, and total dissolved solids were all specified according to seawater properties in Qatar. In addition, reverse osmosis system configuration including; the number of stages/passes, the efficiency of the pump, and the system recovery were determined before calculating the power demand by ROSA. Figure 16 represents an illustration for the configuration of the reverse osmosis system used in this analysis. The RO seasonal power demands obtained by using ROSA are illustrated in Figure 17.

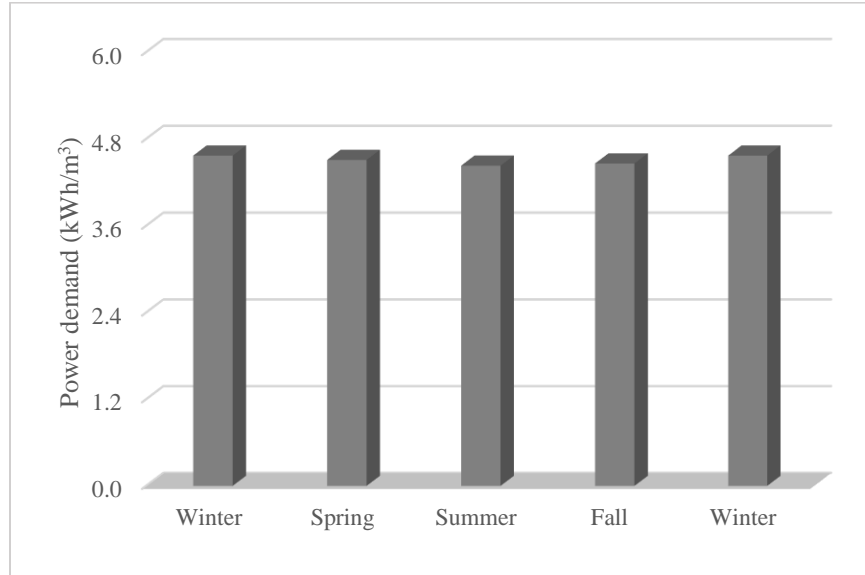


Figure 17: Seasonal RO power demand per cubic meter of produced desalinated water

RO seasonal power demands chart shows that the maximum and minimum power requirements are expected in winter and summer seasons respectively. Differences in power demands are due to different seasonal feed water temperatures. Higher feed water temperature increases the osmotic pressure as they are directly proportional. Accordingly, the feed pressure needs to be increased to prevent the inward flow of treated water across the membrane, and to keep a consistent flowrate through the RO membrane. In other words, more power is needed to compensate for the increasing feed water temperature. On the other hand, increasing feed water temperature lowers the water viscosity which means less force is needed to increase the feed pressure and to maintain the same flowrate. As a result, less power is needed in case of higher feed water temperature. Feed water temperature effect on osmotic pressure is much less than its effect on viscosity. Hence, higher feed water temperature (i.e. in summer) requires less power to

maintain a consistent flowrate through the RO system [62]. The power demand parameter in summer decreases by 3.06% compared to winter power demand parameter.

The effect of seawater temperature on RO removal efficiency was analyzed using ROSA. Results obtained for the same feed flowrate, pH, and recovery ratio indicates that RO removal ratio decreases with increasing wastewater temperature. This means that maximum and minimum RO removal ratios occur in winter, and summer respectively. Figure 18 represents the RO removal ratio over different seasons based on wastewater temperature in Qatar. It shows that as wastewater temperature increases from 21.8 °C in winter to 32.7 °C in summer, the removal ratio decreases by only 0.5% points.

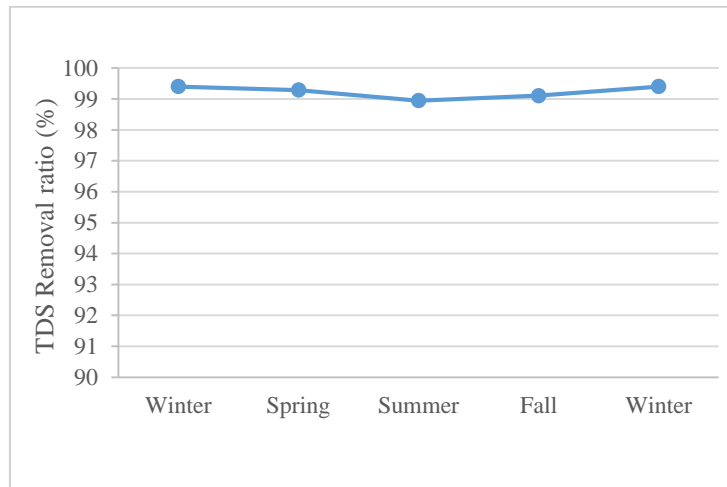


Figure 18: Effect of seasonal feed water temperature on RO removal ratio

Seasonal variations of waste heat-to-power unit (WHP)

Industries are the largest potential for waste heat as more than one-third of the energy used there is lost in the form of waste heat [63]. Using the grand composite curve, the amount of waste heat can be estimated in the form of a minimum cooling requirement (Q^{\min}). Figure 19 provides a

simple schematic diagram for WHP unit. The following equations were used to calculate the maximum theoretical efficiency for generating power using the waste heat from process streams:

For non-isothermal heat sources
$$\eta_{i',p}^{max} = 1 - \frac{T_L [\ln(\frac{T_i}{T_{i+1}})]}{(T_i - T_{i+1})} \quad [64]$$

For isothermal heat sources
$$\eta_{i',p}^{max} = 1 - \frac{T_L}{T_i}$$

Where,

$\eta_{i',p}^{max}$ Maximum theoretical efficiency for power generation

T_L Temperature of cooling medium (K)

T_i Higher temperature of heat source (K)

T_{i+1} Lower temperature of heat source (K)

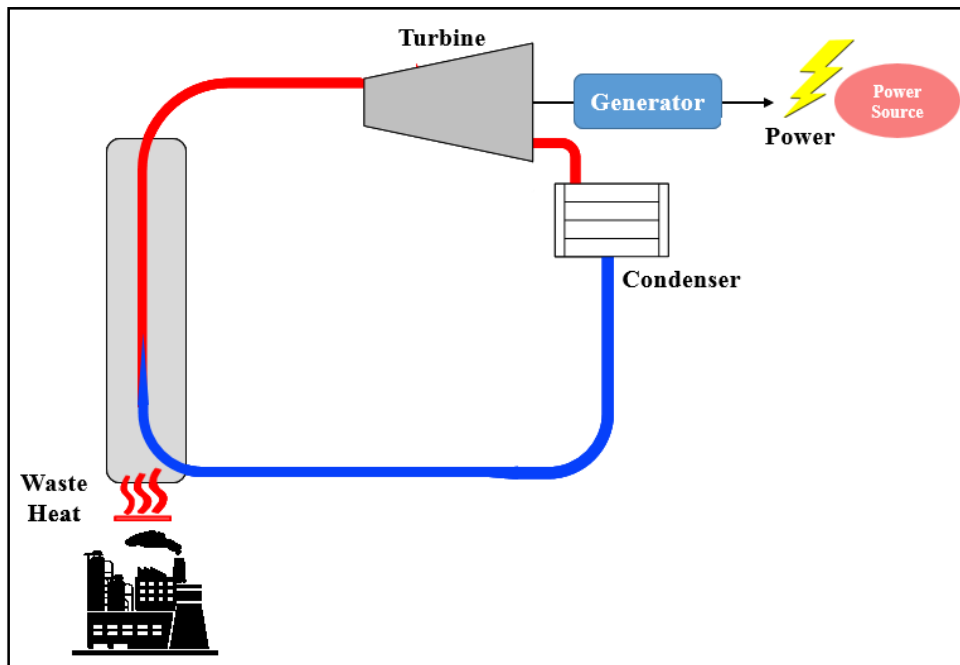


Figure 19: Illustration of waste heat to power unit

The seasonal temperatures of different cooling mediums (i.e. cooling water, air, seawater) utilized to cool down the working fluid were considered. Cooling water temperatures in the cooling tower were calculated based on average wet bulb temperature in each season and the minimum guaranteed approach (2.8°C). Also, average seasonal dry bulb temperatures were used for air in air cooler and seasonal average values for seawater temperatures in the OCSW system. Accordingly, the maximum theoretical power that can be generated is calculated as follows:

$$PW_{i',p}^{max} = \eta_{i',p}^{max} \times Q_{i',p}$$

Where,

$PW_{i',p}^{max}$ Maximum theoretical power that can be generated from waste heat process stream

$Q_{i',p}$ Cooling requirement of the process stream

The total theoretical power that can be generated from all waste heat streams in any plant is the summation of the maximum power that can be generated from each waste heat stream

$$PW_p^{max,total} = \sum_{i' \in SU'_p} PW_{i',p}^{max}$$

Carnot cycle is the most efficient theoretical heat engine. According to the second law of thermodynamics, the heat engine cannot convert all the heat supplied into work, so Carnot efficiency sets the maximum theoretical limiting value on the fraction of heat that can be converted into work. To achieve Carnot efficiency, the process involved in heat engine must be reversible and experience no change in entropy. Hence, Carnot cycle is just an idealization as real engine processes cannot be reversible due to some irreversibility (i.e. energy losses due to friction) and entropy increases for all real physical processes [65].

In this analysis, it was assumed that only 50% of this theoretical power can actually be generated. So, the actual power generated from waste heat was calculated using the following equation:

$$PW_p^{actual,total} = 0.5 \times PW_p^{max,total}$$

Where,

$PW_p^{actual,total}$ Actual power generated from waste heat in plant p

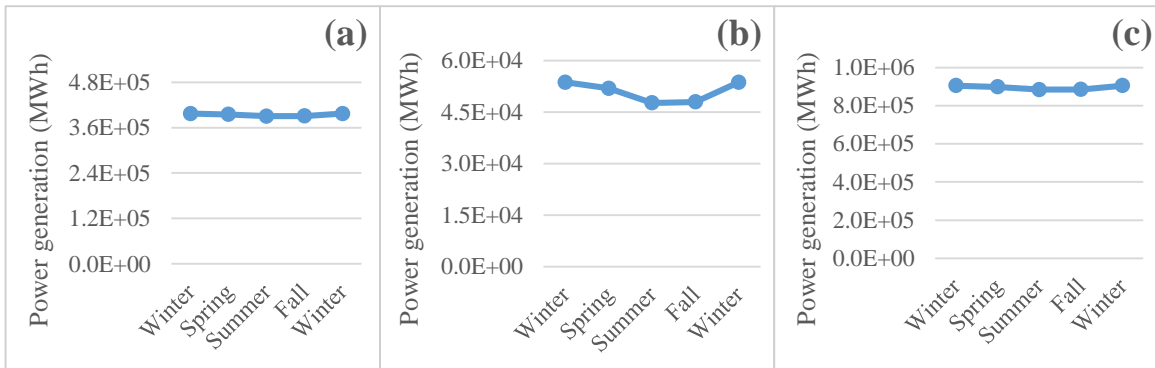


Figure 20: Seasonal power generated via WHP unit utilizing cooling tower in (a) ammonia, (b) methanol, and (c) GTL plants

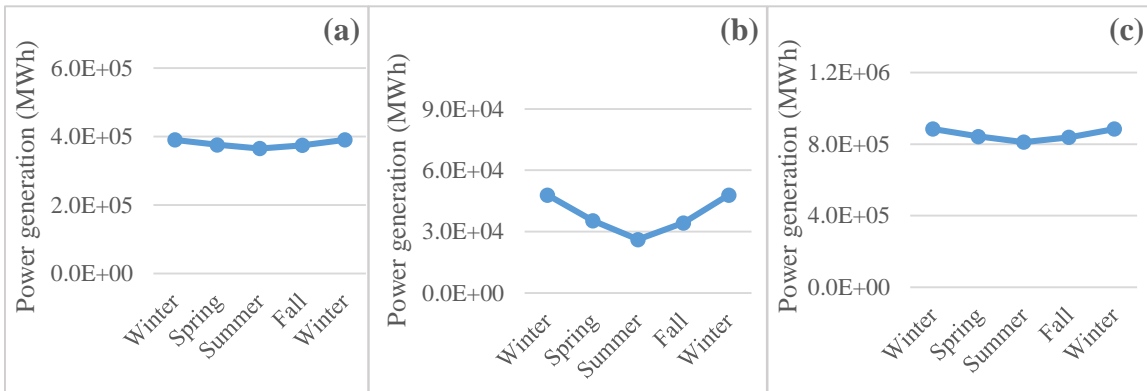


Figure 21: Seasonal power generated via WHP unit utilizing air cooler in (a) ammonia, (b) methanol, and (c) GTL plants

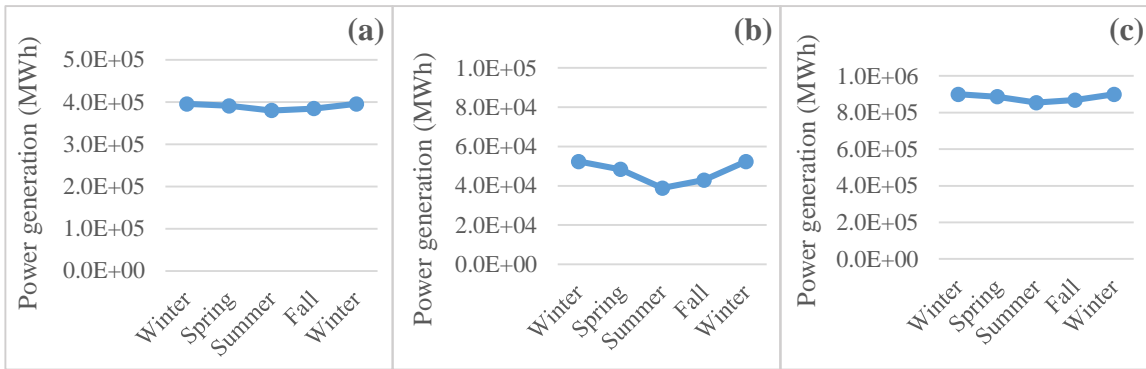


Figure 22: Seasonal power generated via WHP unit utilizing once-through cooling seawater in (a) ammonia, (b) methanol, and (c) GTL plants

Seasonal power generation using waste heat-to-power system is case specific as it depends on the grade of available process waste heat. Accordingly, the analysis of the power generated via the WHP unit was performed for three processes including; ammonia, methanol, and GTL plants. Also, three types of cooling systems (cooling towers, air coolers, and once-through cooling seawater) were utilized to cool the cycle working fluid (i.e. steam). Seasonal power production by WHP unit is shown in Figure 20 for cooling towers, Figure 21 for air coolers, and Figure 22 for once-through cooling seawater.

Results show that the maximum power generated from waste heat in all plants occurs in winter when cooling medium has the minimum temperature amongst other seasons. As a result, the highest WHP unit efficiency is expected in winter as well. On the other hand, the minimum power generation from waste heat in all plants takes place in summer as cooling medium temperature is at its maximum value with least WHP efficiency. The percentages of increase in power generated from waste heat in winter relative to summer using different cooling systems to discharge the remaining waste heat are represented in Table 8. Methanol plant experiences higher

percentages of seasonal variations in power generated from waste heat as the process includes low-grade heat streams which are not suitable for power production in summer due to the higher cooling water temperature. Accordingly, these streams are not utilized for power production and the heat must be discharged using a cooling system.

Table 8: Percentages of increase in power generation using WHP unit and different cooling systems

	Ammonia	Methanol	GTL
Cooling tower	1.79	12.61	2.25
Air Cooler	6.89	83.06	9.07
Once-through cooling seawater	4.14	35	5.38

Seasonal variations of irrigation water demand

Many software packages were developed to calculate the amount of water needed for irrigation purposes. DAILYET, CropWat, CLIMWAT, New-LocClim, SPAW are some of these packages. In this analysis, version 8.0 of CropWat which was developed by the Food and Agriculture Organization of the United Nations (FAO) was used. It is required to input some data related to climate, rainfall, soil, and crops. For example, minimum temperature, maximum temperature, humidity, wind speed, and sunshine hours are the essential monthly climatic data. In addition, some regional information is needed regarding the country of planting such as the altitude, latitude, and the longitude.

Some crop-related information is acquired as well such as crop coefficient (K_c), rooting depth at first and third stages, length of each stage in days, the fraction of critical depletion, the fraction of yield response (K_y), and crop height which is optional. The crop coefficient is the ratio of evapotranspiration from crop or soil surface to the evapotranspiration from a reference surface

(i.e. fully vegetated soil surface by clipped grass) [66]. Critical depletion is represented as the fraction of soil moisture to total available water in the soil where the first drought stress occurs and affects crop production. Critical depletion value usually varies between 0.4 and 0.6 [67]. Yield response fraction K_y is a representation of crop sensitivity to water deficit. The following table explains the three possible values for yield response [68].

Table 9: Crop tolerance to water deficit based on yield response value

Yield response K_y	Crop tolerance to water deficit
$K_y > 1$	Crop is very sensitive to water deficit
$K_y < 1$	Crop is more tolerant to water deficit
$K_y = 1$	Yield reduction is directly proportional to reduced water use

CropWat provides results for evapotranspiration (ETO) - based on provided climate data-, net water requirement, gross water requirement, and crop irrigation schedule. Main crops in Qatar are dates, 88% of required fodder, only 0.7% of required cereals (wheat, rice, maize, and barely); as well as 23% of required vegetables and some fruits. On the other hand, Qatar is importing 100% requirements of edible oil, and 95% of legumes [69]. The sets of data and assumptions used in this analysis are represented below.

Assumptions on using CropWat

- Different crops are planted in the industrial city in Qatar (i.e. tomatoes, alfalfa, etc.), and in this study, seasonality was analyzed for alfalfa and date palms.
- The planting year (i.e. from planting to harvesting) is divided into four stages which are; the initial stage, development stage, mid-season stage, and late-season stage.
- The soil type in Qatar is sandy silt.

- Crop data is obtained from CropWat database.
- Alfalfa planting starts at the same time (i.e. month) for all processes involved in this analysis.

Regional distance measurements are shown in Table 10; while Table 11 shows monthly climatological data used in this analysis [70].

Table 10: Qatar distance measurements

Altitude	15 m
Latitude	25.28 °N
Longitude	51.53 °E

Table 11: Qatar climatological data in 2017

Month	Minimum temperature (°C)	Maximum temperature (°C)	Humidity (%)	Wind (km/day)	Sun (hours)
January	17	24	60	460	7.9
February	16	22	61	510	8.0
March	21	27	56	413	7.7
April	26	34	41	460	9.2
May	31	39	37	467	10.5
June	32	41	34	552	11.3
July	34	42	42	321	10.5
August	34	42	51	328	10.8
September	32	39	53	278	10.2
October	29	36	46	398	9.8
November	25	30	50	379	9.2
December	19	27	62	475	8.1

Monthly rainfall data obtained for Qatar in 2017 are shown in the following table [70].

Table 12: Monthly rainfall data in Qatar

Month	Rain (mm)
January	0.1
February	41.1
March	77.5
April	0.0
May	1.1
June	0.0
July	0.0
August	0.2
September	0.0
October	0.0
November	0.1
December	0.0

Soil characteristics are represented in Table 13 [71]. Also, alfalfa and date palms data were obtained from CropWat database and shown in Table 14.

Table 13: Soil characteristics in Qatar

Total available soil moisture (mm/meter)	180
Maximum rain infiltration rate (mm/day)	225
Maximum rooting depth (cm)	600
Initial soil moisture depletion (%)	50
Initial available soil moisture (mm/meter)	90

Table 14: Alfalfa and date palms crop data

Alfalfa				
Parameter	Initial stage	Development stage	Mid-season	Late season
Crop Coefficient K_c	0.4	-	0.95	0.9
Stage (days)	150	30	150	35
Rooting depth (m)	1.2	1.2	1.2	1.2
Critical depletion fraction	0.55	-	0.55	0.55
Yield response K_y	1	1	1	1
Date Palms				
Parameter	Initial stage	Development stage	Mid-season	Late season
Crop Coefficient K_c	0.9	-	0.95	0.95
Stage (days)	140	30	150	45
Rooting depth (m)	1.5	-	2.5	-
Critical depletion fraction	0.71	-	0.71	0.71
Yield response K_y	0.8	0.8	0.8	0.8

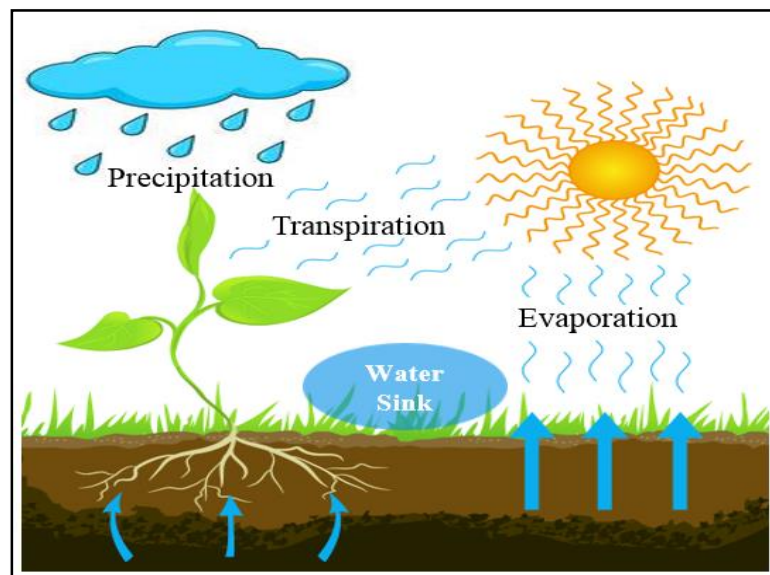


Figure 23: Illustration for irrigation water losses and requirements [72]

It is worth noting that planting date affects the irrigation water demand, and in this analysis, the planting date (i.e. the planting month) was determined based on least total water demand. After performing what-if analysis on the planting month, it was found that starting planting in March in

Qatar would require the least total water demand. Moreover, evaporation from crop and soil is already considered by CropWat (i.e. evapotranspiration), and water needed for irrigation was calculated accordingly. Water cycle for irrigation purposes is demonstrated in Figure 23.

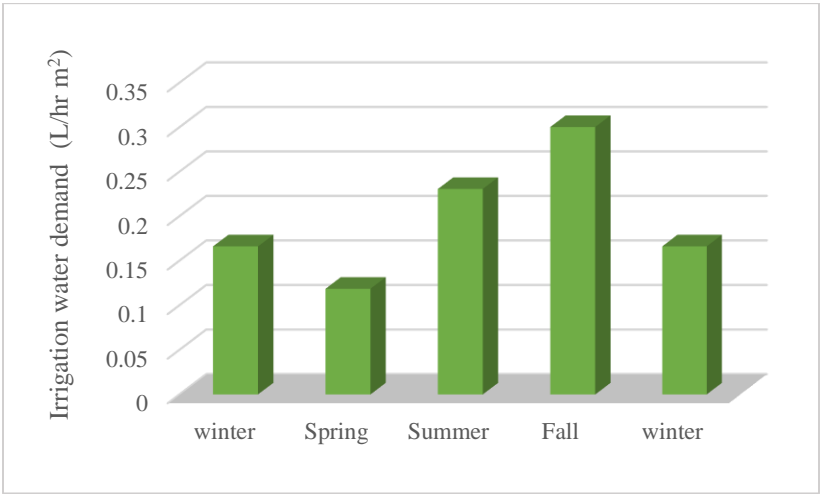


Figure 24: Seasonal water demand per unit area for alfalfa irrigation

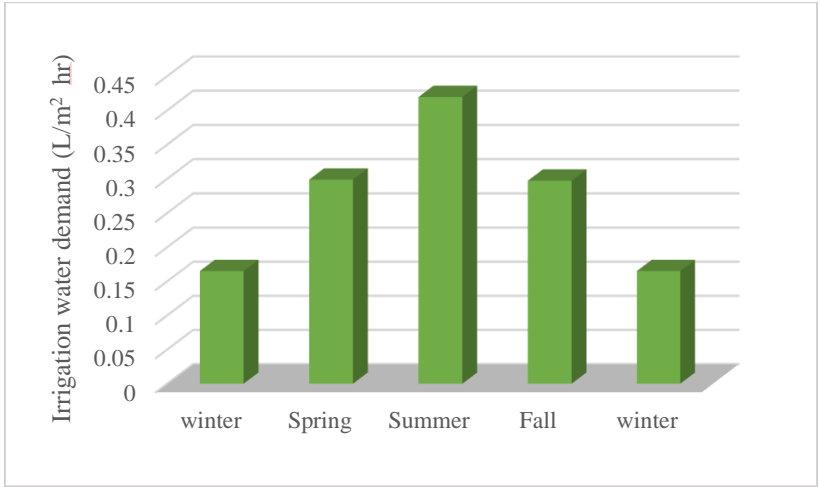


Figure 25: Seasonal water demand per unit area for date palms irrigation

After inserting all data into CropWat, seasonal irrigation water demands were determined. Figure 24 and Figure 25 represent seasonal water demand parameters for irrigating alfalfa and date palms respectively. It is clearly shown that maximum water is required in fall while minimum water demand takes place in spring for alfalfa; while date palms require maximum water in summer and minimum water in winter. It is worth pointing out that irrigation water demand is not only affected by the climatological data, but crop characteristics and water demand play a significant role in determining these values as well. In other words, some crop characteristics such as crop coefficient affect water demand as higher crop coefficient means that more evapotranspiration from the plant and the soil occurs, hence more water is needed for irrigation. The difference between alfalfa water demand in spring and fall is about (0.2 L/hr m²) and the percent of increase is 153%. Similarly, the maximum observed seasonal change in date palms water demand is (0.23 L/hr m²) and the percent of increase is 154%

Seasonal variations of treatment units

Treatment units are used to reduce the amount of discharge water; as well as freshwater consumption by utilizing the wastewater from different sources, treat it and use it in other sinks. Maximum total wastewater sent to the treatment unit is the summation of wastewater from all available water sinks. Wastewater originating from offices and process sources is fixed over the year while cooling tower blowdown experiences some seasonality due to seasonal variations in evaporation rates from cooling towers. As a result, any variations in wastewater is due to changes in cooling tower blowdown rates. In addition, the maximum and minimum wastewater occur in summer and winter respectively.

It is important to determine the maximum wastewater to be treated over the seasons as the treatment unit should be designed based on peak conditions. Moreover, treatment interceptors are

either open or closed. Open treatment units are vulnerable to evaporation. Evaporation from any open surface depends on some factors like water temperature, and air properties such as temperature, humidity, and air velocity above the water surface. Accordingly, evaporation rates change over different seasons and these rates can be calculated using the following equations.

The amount of evaporated water can be calculated as follows:

$$g_h = \Theta A (X_s - X)$$

Where,

g_h Amount of evaporated water per hour ($\frac{kg}{hr}$)

Θ Evaporation coefficient ($\frac{kg}{m^2 hr}$)

A Water surface area (m^2)

X_s Maximum humidity ratio of saturated air at the same temperature as the water surface
 ($\frac{kg H_2O}{kg dry Air}$)

X Humidity ratio air ($\frac{kg H_2O}{kg dry Air}$) (from Psychrometric chart)

Evaporation coefficient is calculated using the following empirical correlation:

$$\Theta = (25 + 19 V)$$

V Velocity of air above the water surface ($\frac{m}{s}$)

The maximum humidity ratio is calculated using the following equation:

$$X_s = \frac{0.62198 \times P_{ws}}{(P_a - P_{ws})}$$

X_s Maximum saturation humidity ratio of air ($\frac{kg H_2O}{kg dry Air}$ or $\frac{lb H_2O}{lb dry Air}$)

P_{ws} Saturation (maximum) pressure of water vapor at specified temperature (Pa, psi)

P_a Atmospheric pressure of moist air (Pa, psi)

Table 15 summarizes the results of seasonal evaporation rates calculations.

Table 15: Seasonal evaporation rates from open treatment units per unit area

Season	Water Temp °C	Air Temp °C	Max Saturation humidity ratio $\text{kg}_{\text{water}}/\text{kg}_{\text{air}}$	Humidity kg/kg	Air velocity m/s	Evaporation coefficient $\text{kg}/\text{m}^2 \text{ hr}$	Evaporation rate per unit area $\text{kg}/\text{m}^2 \text{ hr}$
winter	20.93	25.37	0.016	0.0099	5.44	128.34	0.73
Spring	23.80	35.43	0.019	0.0075	5.17	123.24	1.37
Summer	31.94	42.8	0.030	0.0094	4.63	113.05	2.32
Fall	30.00	36.3	0.027	0.0114	4.07	102.29	1.61

By considering seasonal rainfall rates, the seasonal net evaporation in meters per unit area was calculated as illustrated in Table 16.

Table 16: Seasonal net evaporation rates from open treatment units

Season	Evaporation rate (L/m ² .hr)	Rainfall (L/m ² .hr)	Net evaporation (L/m ² .hr)
winter	0.73	5.50×10^{-2}	0.68
Spring	1.37	5.09×10^{-4}	1.37
Summer	2.32	9.26×10^{-5}	2.32
Fall	1.61	4.63×10^{-5}	1.61

Seasonal evaporation rates are shown in Figure 26 where evaporation rates are represented per unit area. It is clearly shown that maximum and minimum evaporation takes place in summer and winter respectively. The percent of increase in evaporation from winter to summer is 242.55%.

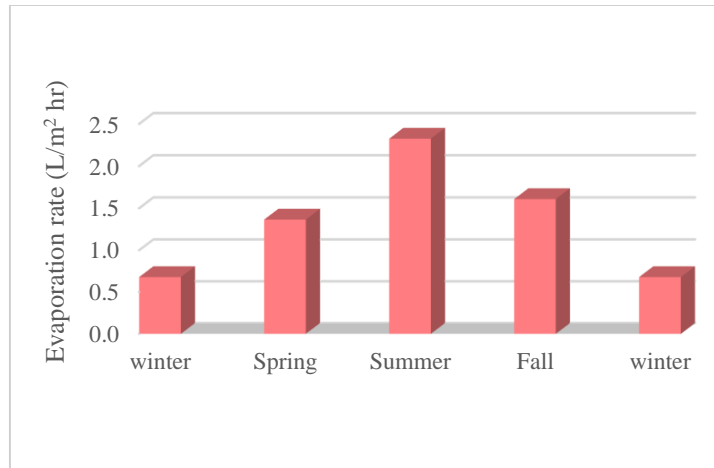


Figure 26: Seasonal net evaporation rates from open treatment units per unit area

Treatment units considered in this analysis are dissolved air flotation (DAF), membrane bioreactors (MBR), Nano-filtration membranes (NF), and reverse osmosis (RO). Power is required for all types of treatment units to operate. This section will highlight the effect of seasonality on power demand of treatment units, and the performance of these interceptors.

Dissolved air flotation (DAF)

Dissolved air flotation is a wastewater treatment unit designed to remove suspended solids, oil and greases (O&G); as well as biochemical oxygen demand (BOD) [73]. Pressurized dissolved air flotation systems include three operational modes; namely, the full flow, split flow and recycle flow. The recycle flow DAF unit is the most commonly used and it consists of flotation tank which receives the influent wastewater, pump for recycling part of the effluent, air compressor, and air drum. The theory of dissolved air flotation process depends on separating suspended solid particles from wastewater by enhancing their buoyancy via air bubbles. Air bubbles are formed by saturating the recycled treated water - which usually represents (20-100) % of the total treated water - with compressed air typically at (4-6) atmosphere in a pressure vessel called air drum [74]

[75]. The air-saturated water stream is depressurized through a pressure reduction valve before it enters the front of the flotation tank. As a result, tiny air bubbles - typically (10-100) micrometer - are formed that bring the suspended solids to the surface to be eventually skimmed.

Typically, DAF tanks involve some chemical additives such as polyelectrolytes. These polymers dissociate in water and forms charged polycations and polyanions. The charged polymers enhance coagulation in DAF unit by neutralizing the charged dispersed suspended solids such as clay and color-producing organic matters, so particles stick together and form larger micro-flocs. The advantages of DAF systems over other sedimentation processes subsumes the better water quality, higher operation rates, less space, and easier setup [76]. This research is mainly concerned about studying the effect of seasonal variations on power demand of dissolved air flotation units including changing air and water temperatures.

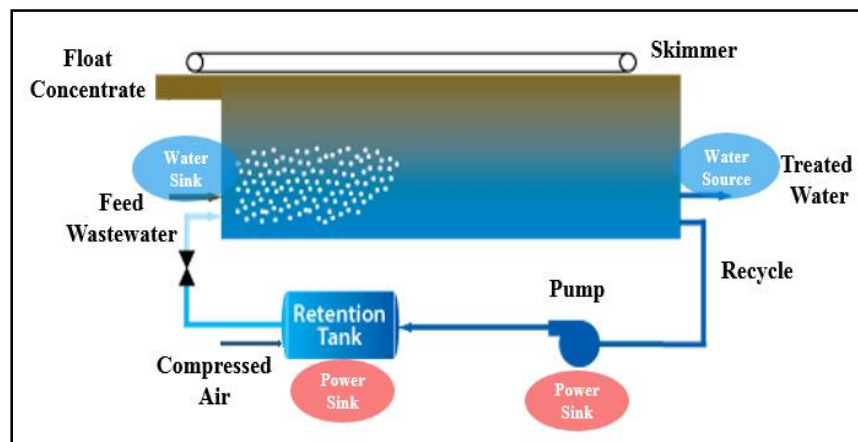


Figure 27: Schematic diagram for dissolved air flotation unit (DAF) [77]

Figure 27 illustrates the DAF unit water and power sources and sinks. It is clearly shown that the unit represents a power sink in the water-energy network as it requires power for pumping

recycled effluent water, and for the air compressor. The effect of seasonal changing air and wastewater temperature on power demand of pump and air compressor was studied using ASPEN, and enthalpy-entropy air mollier diagram respectively. Mollier diagram provides the relation between pressure, temperature, enthalpy, and entropy of air. The compression power demand is determined using enthalpy difference between pressurized air and air at different weather conditions (i.e. temperature, and pressure); as well as compressor's efficiency. Figure 28 demonstrates seasonal power demand required by the DAF unit air compressor per cubic meter of air per hour. Air was assumed to be pressurized at 5 atm in air compressor with 85% efficiency.

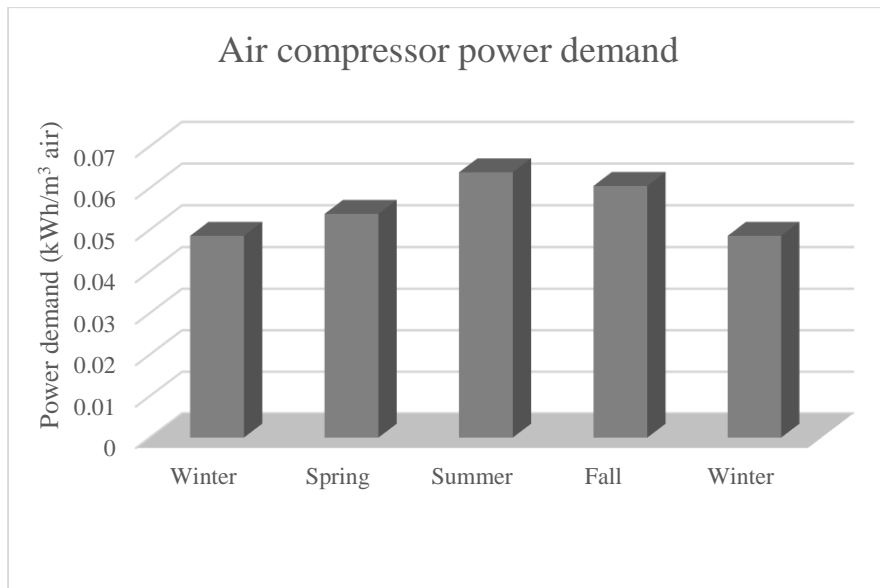


Figure 28: Seasonal power demand of air compressor per cubic meter of air

It is clearly shown that maximum power demand for air compressor occurs in summer, while winter requires the minimum power demand. This is due to the effect of increasing

temperature on expanding air which increases the power demand for air compression. The percent of increase in power demand from winter to summer is 31.33%.

Similarly, the recycle pump power demand was evaluated using ASPEN. The pump effluent pressure was assumed to be 5 atm in this analysis. Figure 29 shows the seasonal power demand per cubic meter per hour of DAF recycled effluent. It is clearly noticed that the effect of wastewater temperature on pumping power demand is insignificant as it only increases slightly in summer relative to winter. The percent of increase is around 0.83% which is mainly due to changes in water density as the temperature changes.

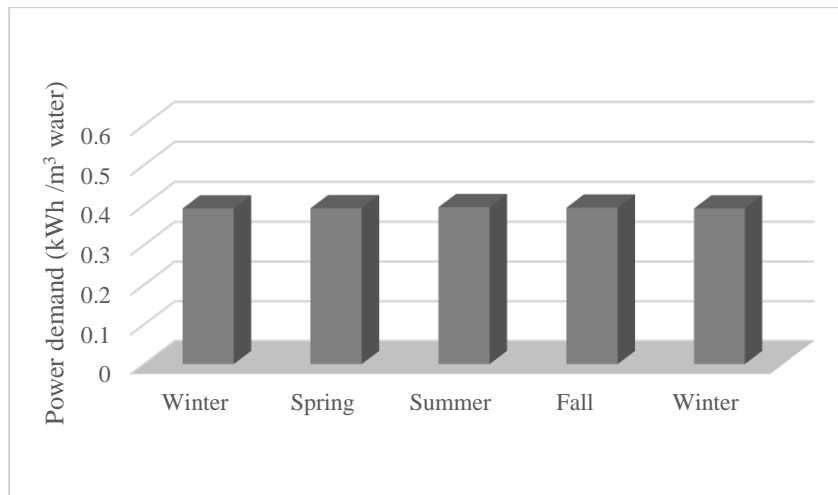


Figure 29: Seasonal power demand for recycle pump per cubic meter of recycled effluent

Seasonal air solubility in water and theoretical air release were considered to generate DAF overall power demand assuming 20% of DAF effluent is recycled. Figure 30 clearly shows that DAF requires maximum power in summer and minimum power in winter. The percent of increase in DAF power demand is about 7.18%.

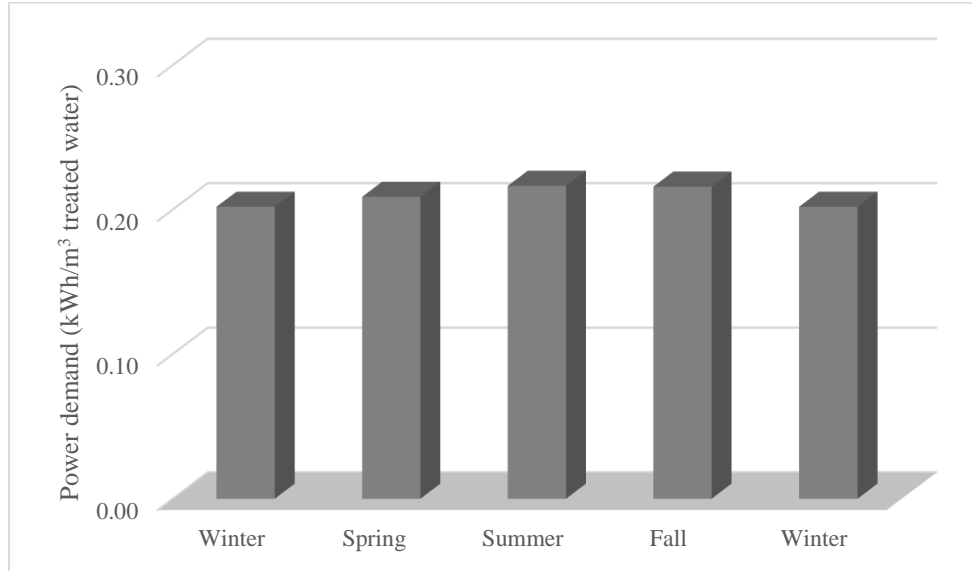


Figure 30: DAF overall seasonal power demand per cubic meter of treated water

Changing wastewater temperature affects the performance of the dissolved air flotation unit. A previous study conducted by Li et al. proved that as the temperature of the wastewater increases, removal efficiency increases and it reaches its maximum value at an optimum temperature [78]. According to this study, the maximum removal ratio achieved using this system was 90% at an optimum temperature of 32 °C. The study found that the removal ratio will remain fixed if the wastewater temperature increased beyond this optimum value (i.e. up to 40 °C). It is worth noting that operating conditions were fixed at optimum values while studying the effect of wastewater temperature on DAF performance. This subsumes wastewater PH, air flowrate, pressure; as well as coagulants and flocculants dosage. Moreover, Liers et al. analyzed the DAF performance and concluded that increasing wastewater temperature from 2 °C to 20 °C gave a difference of 10% in bubble filter efficiency [79].

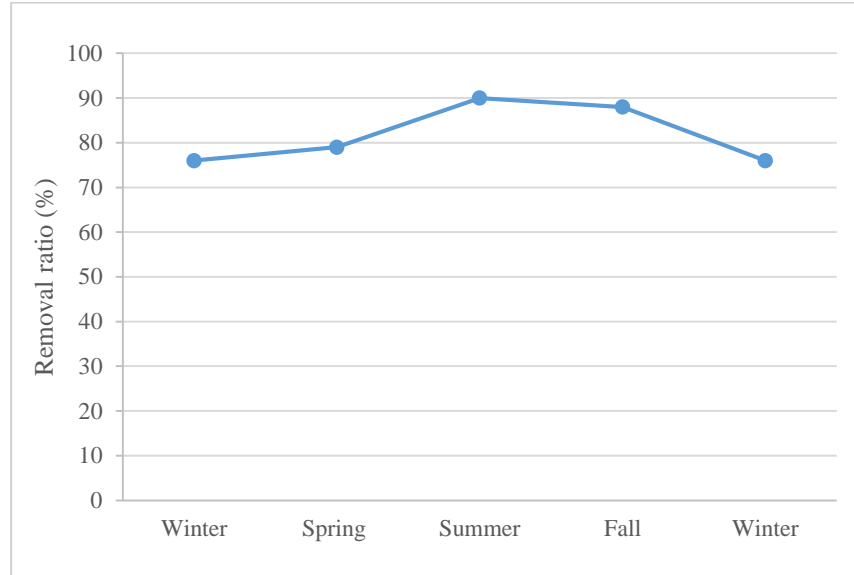


Figure 31: Seasonal removal ratio of dissolved air flotation unit (DAF)

Figure 31 represents seasonal removal ratios of the DAF unit. It shows that maximum removal ratio of DAF unit occurs in summer as increasing wastewater temperature will enhance the flocculation of micro-flocs to form larger visible suspended solids that can be removed by either sedimentation or flotation (i.e. via skimming).

Membrane bioreactors (MBR)

Membrane bioreactor mainly consists of conventional biological treatment method - usually the activated sludge -, and filtration membranes usually low-pressure microfiltration or ultrafiltration. Membrane filtration is employed for critical solid-liquid separation which is performed by secondary and tertiary clarifiers along with tertiary filtration in conventional activated sludge facilities [80].

Membrane bioreactor could be aerobic or anaerobic. Two main configurations of membrane bioreactors exist namely; the 'side-stream MBR', and the 'immersed MBR'.

Nowadays, the immersed MBR configuration is more commercially significant than the side-stream MBR as it is less energy intensive and has less fouling potentials [81]. Membrane bioreactor is usually utilized for municipal and industrial wastewater treatment applications [82]. Immersed membrane bioreactor (iMBR) is illustrated schematically via Figure 32.

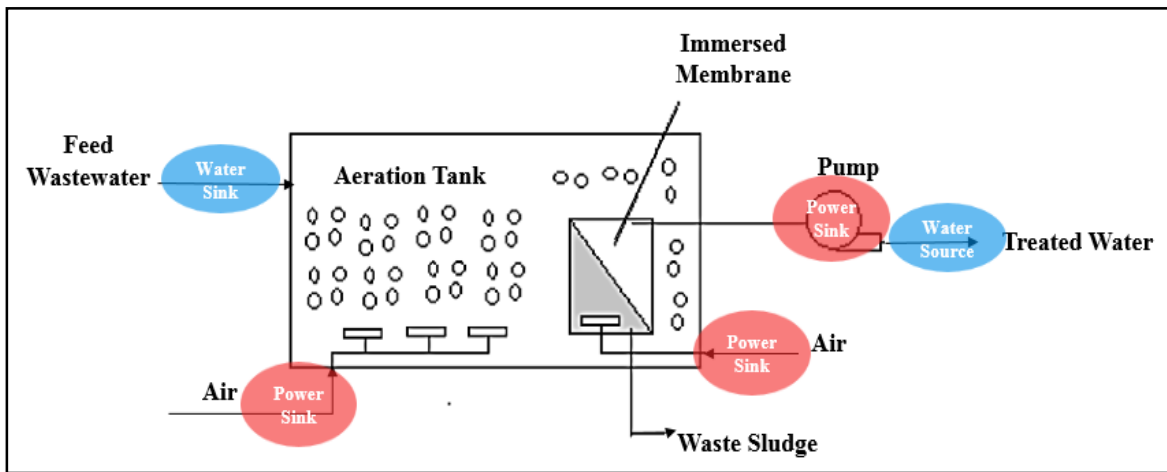


Figure 32: Schematic diagram for aerobic immersed MBR configuration [83]

Membrane bioreactors have some advantages over other conventional treatment units including the small footprint by producing more concentrated sludge that is further treated via activated sludge process. In addition, membrane bioreactors can be operated at high suspended solids concentration and characterized by high-quality effluent. Membrane bioreactor is classified as a batch treatment process, so it is not affected by seasonal evaporation. In this analysis, aerobic MBR was considered as air flowrate through the immersed MBR ameliorates membrane fouling. Also, in the context of this problem, MBR is considered as a power sink as it requires power to withdraw the effluent through the immersed membrane via a suction pump. Moreover, power is

required to blow air through the biological tank as aerobic MBR may utilize ambient air or pure oxygen for feeding the microorganisms and reducing membrane fouling.

The seasonal power demand for pumping MBR effluent through the membrane is represented by Figure 33. It is noticed that increasing wastewater temperature results in higher permeation rate, hence power is reduced to maintain consistent flowrate through the membrane. The percent of decrease in pumping power demand from winter to summer is around 51.9%.

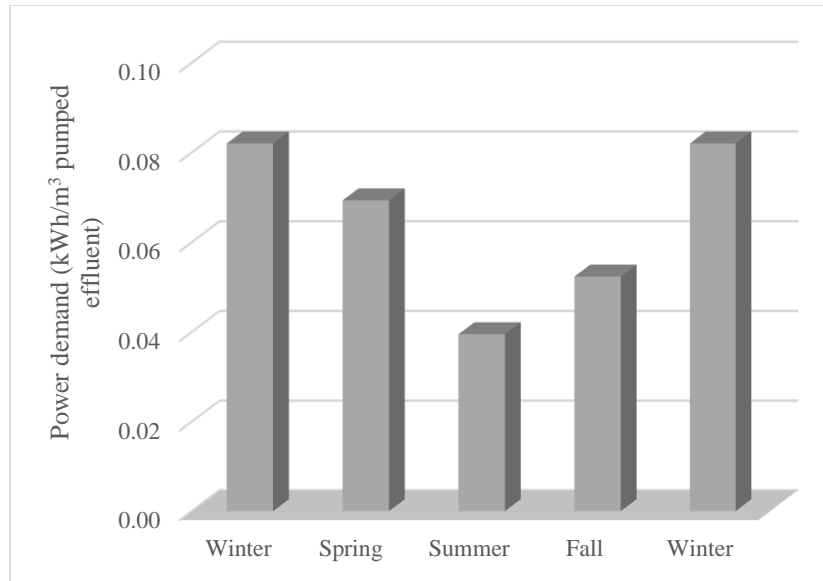


Figure 33: Seasonal pumping power demand through MBR immersed UF membrane

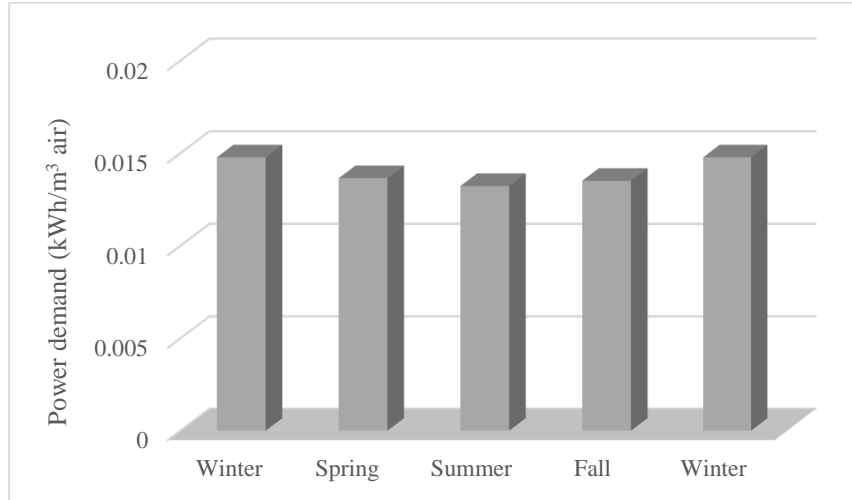


Figure 34: Seasonal air blower power demand per cubic meter of air

Figure 34 represents the seasonal power demand for moving one cubic meter of air per hour via air blower through the biological tank and MBR membrane. As the air temperature increases, air blower power demand decreases as less pressure increase is required to move the air with higher temperature. Therefore, maximum and minimum power demand for MBR air blower occurs in winter and summer respectively. The percent of decrease in power demand from winter to summer is 11.7%. It is worth mentioning that total MBR air demand increases in summer due to increasing microorganisms' activity.

The overall seasonal power demand for MBR treatment unit in kilowatt-hour per cubic meter of water treated is represented by Figure 35. It is noticed that winter is associated with maximum power demand while summer is accompanied by the least power demand. The percent of decrease in power demand from winter to summer is 21.51%.

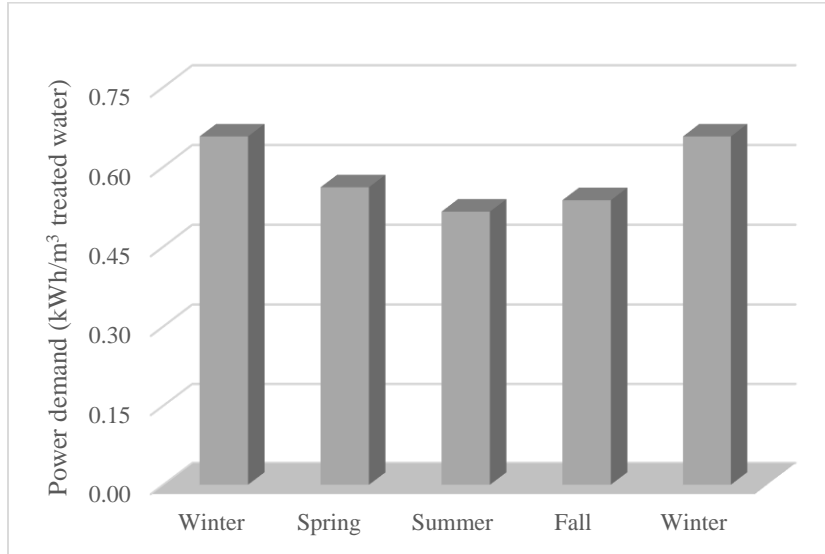


Figure 35: MBR overall seasonal power demand per cubic meter of treated water

Liu et al. explored the effect of wastewater temperature on aerobic MBR removal efficiency using mesophilic bacteria. According to that study, the performance of MBR enhanced as wastewater temperature increased from 19 °C to 29 °C, where it reaches the maximum removal efficiency. Wastewater temperature beyond the optimum value would decrease the removal efficiency. The effect of wastewater temperature on MBR performance is due to the temperature impact on microorganisms' activity. All microorganisms have a living temperature range, and once the temperature is beyond this range, the microbial activity is inhibited and the system performance is deteriorated [84]. Mesophiles typically grow best in moderate temperatures (20-45) °C.

The effect of seasonal wastewater temperature on MBR chemical oxygen demand (COD) removal efficiency is demonstrated in Figure 36. It indicates that the COD removal efficiency of MBR is slightly affected by seasonality.

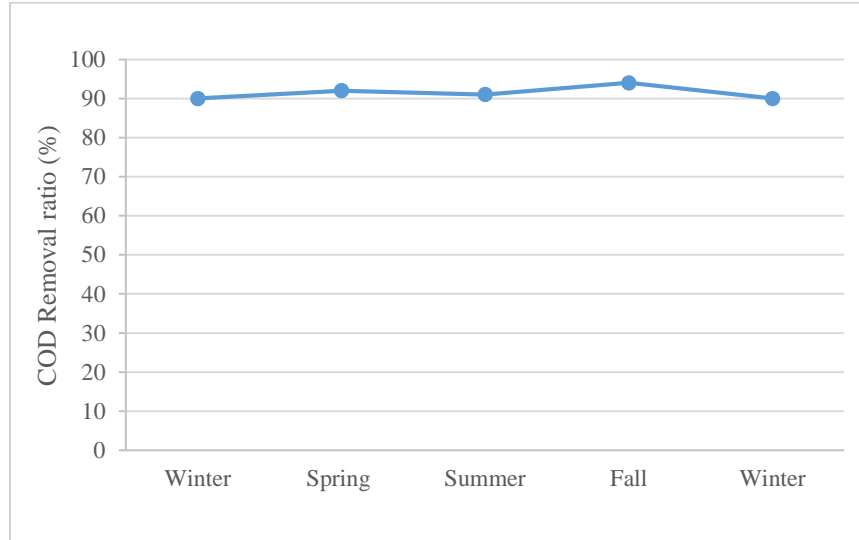


Figure 36: Seasonal COD removal ratio of immersed MBR treatment unit

Nano-filtration membranes (NF)

Nano-filtration membranes are characterized by pore sizes that range from (1-10) nanometers, which are just larger than reverse osmosis pore sizes [85]. Nano-filtration was selected for this study since they are suitable for organic pollutants' removal. Since Nano-filtration is a batch treatment unit, it is invulnerable to evaporation. Figure 37 provides a schematic diagram for Nano-filtration membranes.

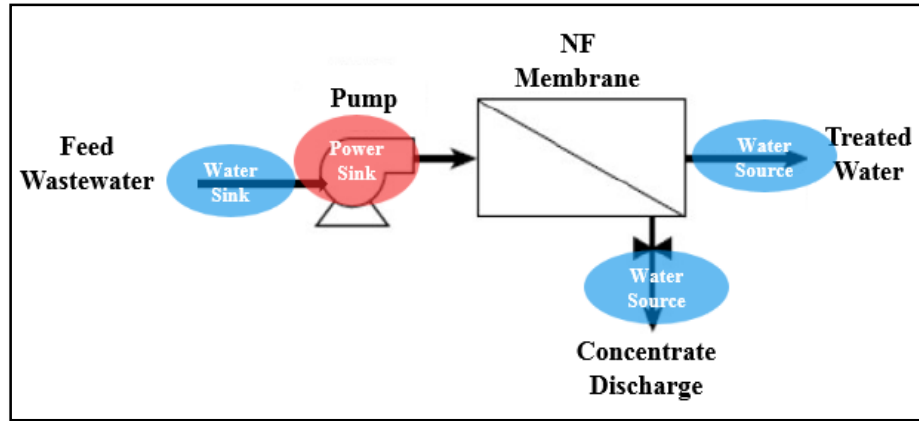


Figure 37: Schematic diagram for Nano-filtration membrane unit

ROSA software was utilized to find the seasonal power demand parameters for Nano-filtration membranes. Seasonal NF power demand parameters were determined and the average power demand for Nano-filtration membranes using ROSA is 0.583 kilowatt-hour per cubic meter of treated water. The following figure demonstrates seasonal power demand parameters for NF membranes.

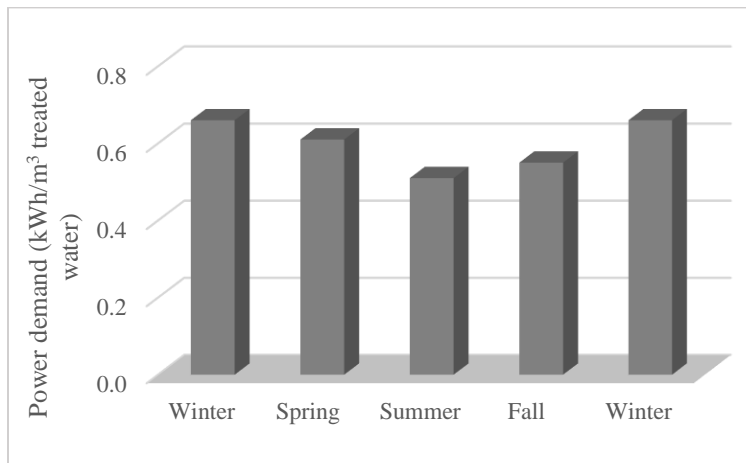


Figure 38: Seasonal power demand for NF membranes per cubic meter of treated water

Figure 38 clearly shows that maximum and minimum power demand parameters for nano-filtration membranes occur in winter and summer respectively. The percent of decrease in nano-filtration power demand from winter to summer is 22.73%.

The effect of wastewater temperature on NF removal efficiency was evaluated using the results of outlet concentration obtained by ROSA. These results indicate that NF removal ratio decreases as the wastewater temperature increases due to the increase in solute transport through membrane pores. Figure 39 shows the seasonal removal efficiency for NF based on wastewater temperature in Qatar. The maximum and minimum removal ratio are observed in winter, and summer respectively. As wastewater temperature increases from 21.8 °C in winter to 32.7 °C in summer, the removal ratio decreases by almost 7% points from 89.8% to 82.6%.

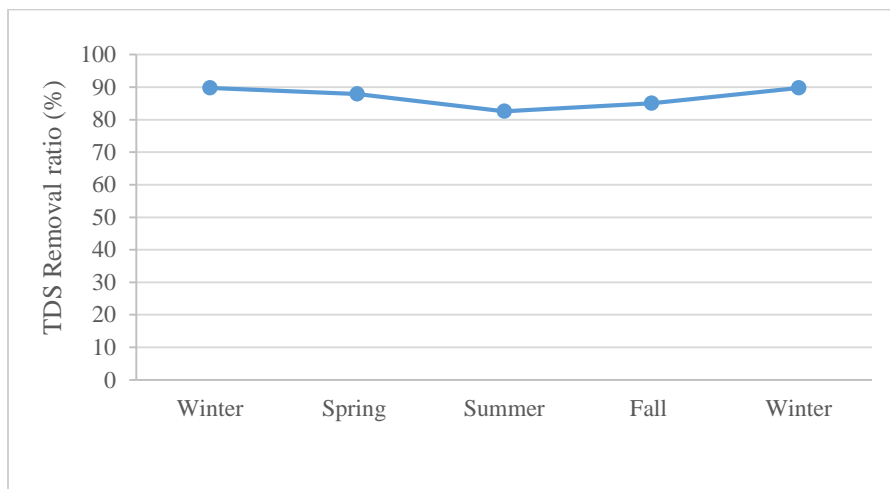


Figure 39: Seasonal removal ratio of Nano-filtration membrane unit

Wastewater reverse osmosis membranes (RO)

Beside desalinating seawater, reverse osmosis membranes can be used for treating wastewater. ROSA software was utilized to analyze the effect on changing wastewater

temperatures on RO membranes power demand and performance. Figure 40 provides a schematic diagram for RO elements used for treating wastewater.

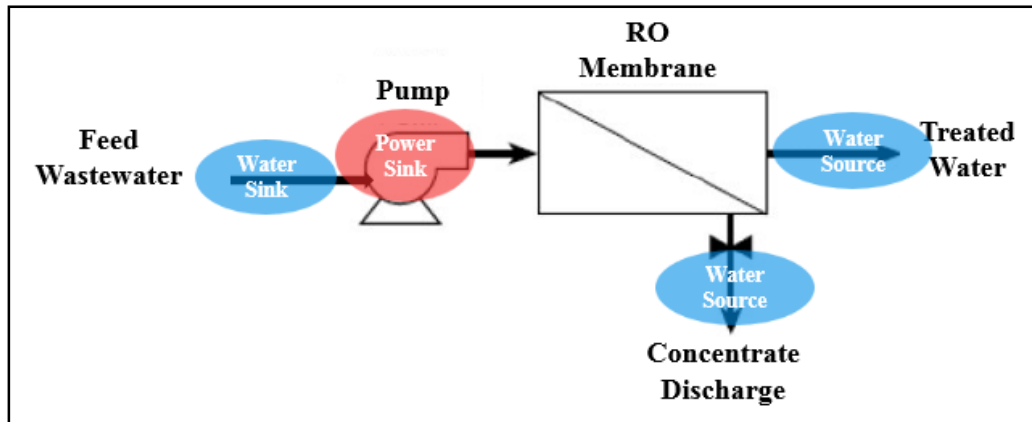


Figure 40: Schematic diagram for wastewater reverse osmosis membrane unit

Similar to RO desalination units, RO elements used for wastewater treatment experience a decrease in power demand with increasing wastewater temperature. RO seasonal power demand is illustrated in Figure 41. RO power requirement decreases from winter to summer by 26.2%. Furthermore, the removal ratio is affected by increasing wastewater temperature. It is noticed that the RO removal ratio decreases from 98.7% in winter to 97.6% in summer due to the increase in solute permeate flux. Seasonal removal ratios of wastewater RO unit are demonstrated in Figure 42.

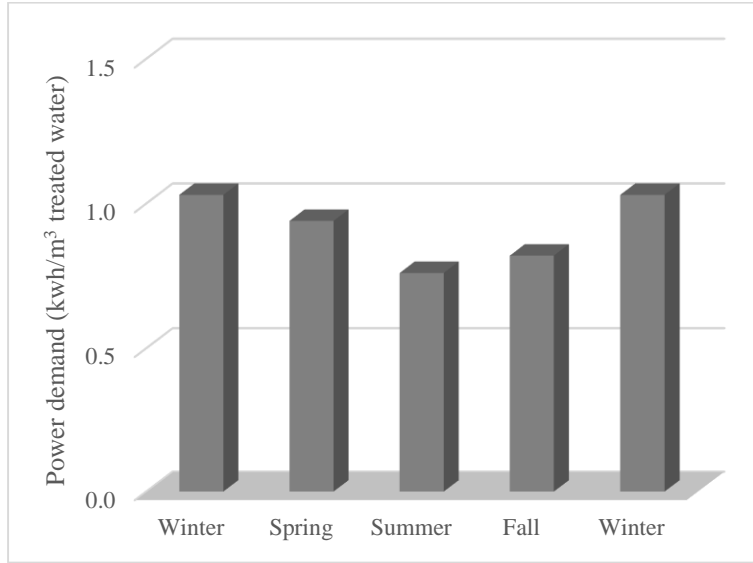


Figure 41: Seasonal power demands for wastewater treatment by RO membrane

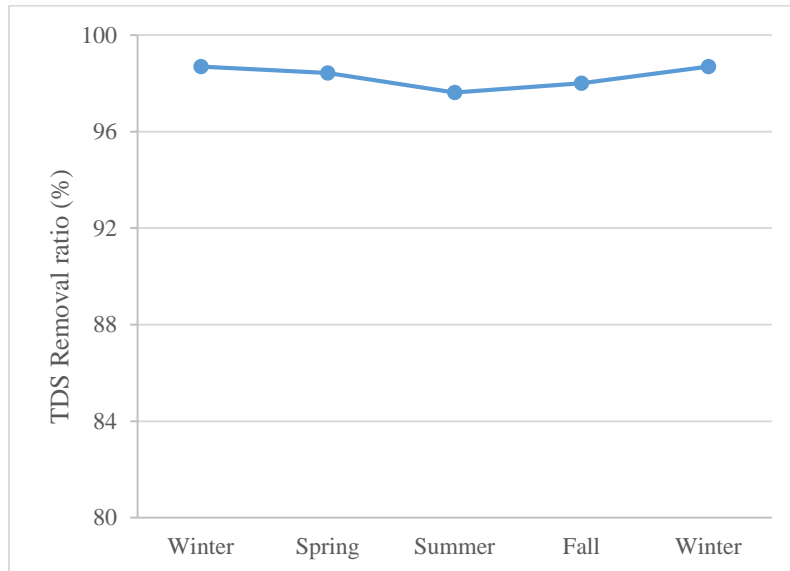


Figure 42: Seasonal removal ratio for treating wastewater via RO membranes

CHAPTER IV

PROBLEM ASSESSMENT

To analyze the impacts of seasonal variations on different components of the water-energy network, three processes were considered in the problem assessment; namely ammonia, methanol, and gas-to-liquids (GTL) plants. Accordingly, proper process-related and network elements-related adjustments were proposed to design a novel water-energy network capable of dealing with seasonal variations.

Process assumptions

- Any process has fixed production capacity over the year, such that the core process does not undergo any seasonal variations.
- Each process is assumed to be fully heat integrated before designing the water-energy network.
- Accordingly, the minimum cooling requirement of the process is fixed over the year as well.
- Also, process water supply and demand from process water sources and sinks; as well as water for offices are fixed over the year.
- In addition, basic power demand for each process (i.e. compressors, pumps, fans) is constant and does not change with different seasons.

Some sets of data were acquired before assessing the seasonal variations of water-energy network components. The following tables show process power demand, and minimum cooling

requirements, in addition to process water demand and supply; as well as offices water demand for each process.

Table 17: Basic power load and minimum cooling requirement of each process

	Basic power load	Minimum cooling requirement
Plant	Power (MW)	Q^{\min} cooling (MW)
Ammonia	111	750
Methanol	162	409
GTL	287	1961

Table 18: Process water supply and demand

Plant	Process supply (sources) (m ³ /day)	Process demand (sinks) (m ³ /day)
Ammonia	599	2571
Methanol	896	1912
GTL	16795	7115

Table 19: Water demand for offices

Plant	Water demand for offices (m ³ /day)
Ammonia	840
Methanol	500
GTL	163

Seasonal variations of different elements in the water-energy network including cooling systems, interceptors; as well as WHP unit were assessed using the acquired sets of data. The evaluation depends mainly on generating water/power demand and supply profiles for all water/energy sources and sinks. Then, the maximum observed seasonal variation is compared to a reference point to evaluate the significance of this change with respect to the whole process. The

reference points include total water demand/supply, basic process power load (i.e. for compression, pumping, etc), and total generated wastewater.

Cooling systems seasonality assessment

Air coolers

To evaluate the significance of detected seasonal variations in air cooler power demand, power demand profiles were generated and the maximum observed increase was compared to the plant basic power load. Air cooler power profiles and the increase in air coolers power demand as a percentage of process basic power demand are demonstrated in Figure 43 and Figure 44.

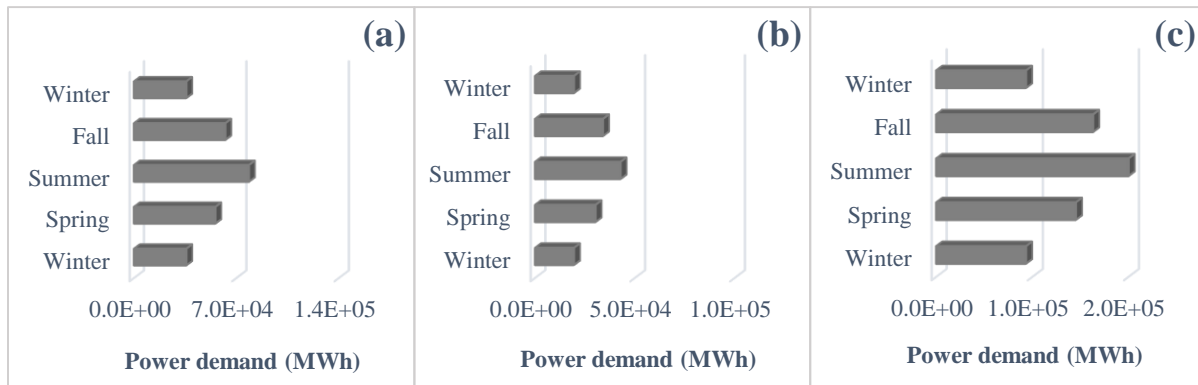


Figure 43: Air cooler power profile for (a) ammonia, (b) methanol, and (c) GTL plants

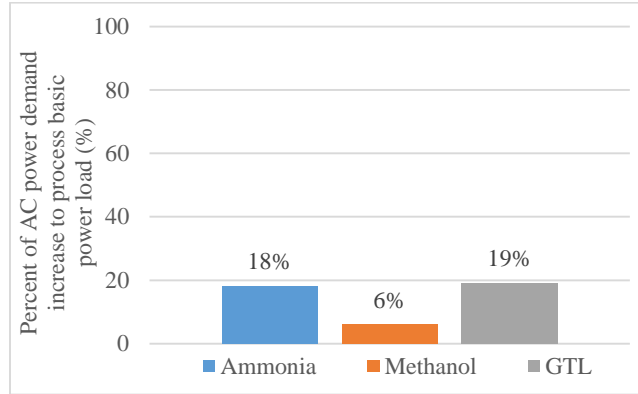


Figure 44: Percent of the maximum seasonal increase in air cooler power demand to plant basic power load for ammonia, methanol, and GTL plants

It is clearly noted that the variations in air cooler seasonal power demand are small relative to the basic power load of the plant. Despite the high percentages of increase in power demand in summer relative to winter, the maximum seasonal change in ammonia, methanol, and GTL plants represents 18%, 6%, and 19% of the basic power load for each plant respectively.

Cooling towers

Power demand

Similar to air coolers, cooling tower power profiles are represented in Figure 45 for all three processes. Also, the increase in cooling tower power requirement from winter to summer was assessed via a comparison established with the basic power load of ammonia, methanol, and GTL plants as demonstrated in Figure 46. This comparison shows that the increase in power demand from winter to summer represents only 14.1%, 5.2%, and 14.2% of the basic power demand in ammonia, methanol, and GTL plants respectively.

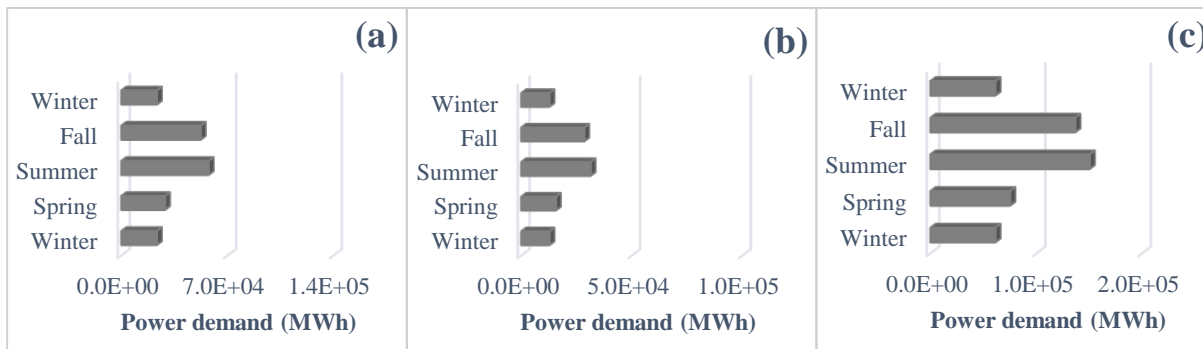


Figure 45: Cooling tower power profile for (a) ammonia, (b) methanol, and (c) GTL plants

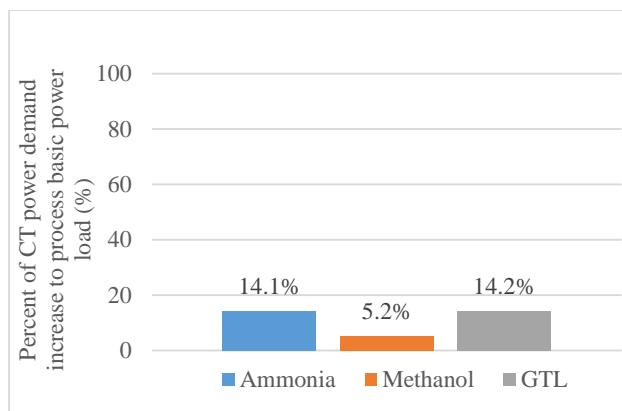


Figure 46: Percent of the maximum seasonal increase in cooling tower power demand to plant basic power load for ammonia, methanol, and GTL plants

Air-cooled heat exchanger and cooling tower power profiles show that GTL plant is associated with higher power demand compared to ammonia and methanol plants as GTL is a cooling intensive process. Also, it is observed that ammonia and GTL have almost the same percentage of seasonal power increase with respect to the basic power load as basic power demand increases with the increased cooling requirement. In other words, processes with substantial cooling requirement are usually large processes with high basic power demand. On the other hand, methanol is always associated with a lower percentage of power increase with respect to basic

power load because it requires less cooling while basic power demand is quite moderate relative to ammonia and methanol plants.

Blowdown

Likewise, cooling tower blowdown profiles are shown in Figure 47. The weight of the blowdown seasonality is estimated by a comparison established between the maximum seasonal increase in blowdown rates and total water supply in each process considering cooling towers. Table 20 indicates that the maximum increase –from winter to summer- in cooling tower blowdown represents less than 1% of the total water supply from each process.

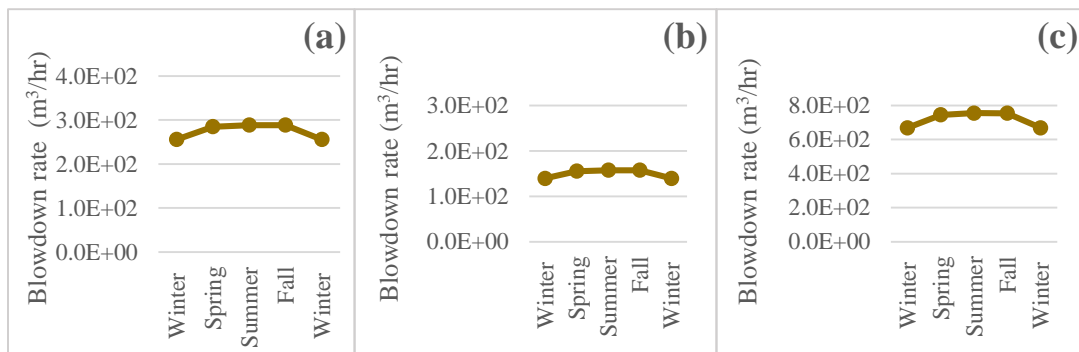


Figure 47: Cooling tower blowdown profile for (a) ammonia, (b) methanol, and (c) GTL plants

Table 20: Percent of increase in cooling tower blowdown rates to process total water supply

Process	Ammonia	Methanol	GTL
Percent of the maximum seasonal increase in cooling tower blowdown rates to process total water supply (%)	0.11	0.09	0.06

Makeup water

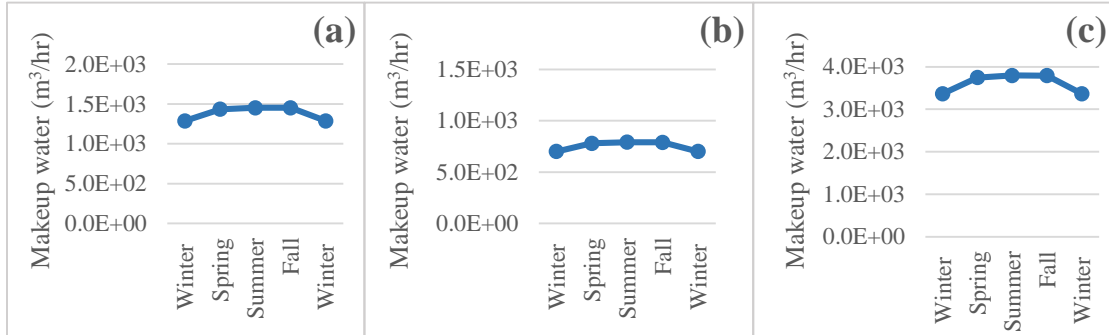


Figure 48: Cooling tower makeup water demand profile for (a) ammonia, (b) methanol, and (c) GTL plants

Cooling tower makeup water profiles are similar to evaporation and blowdown profiles simply because makeup water demand is a result of water evaporation and blowdown. The profiles are clearly shown in Figure 48 for ammonia, methanol, and GTL plants. It is noticed that the GTL process requires higher water makeup rates as it requires more cooling compared to ammonia, and methanol processes. The maximum increase in seasonal makeup water demand from winter to summer was compared to process total water demand considering cooling towers. Figure 49 represents the increase in makeup water demand as a percentage of the process water demand for ammonia, methanol, and GTL plants. For all processes, this increase represents almost 10% of the process total water demand.

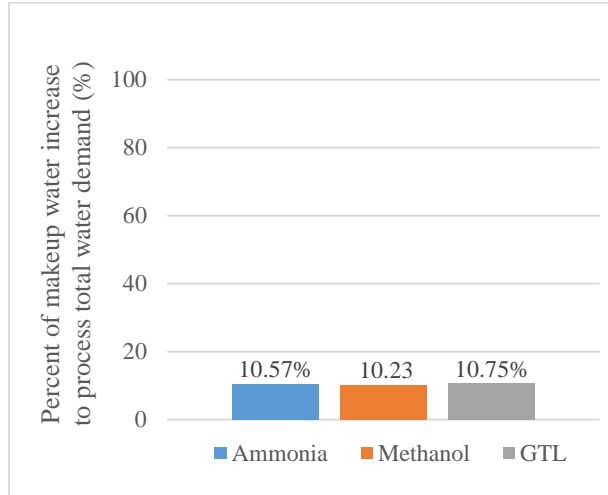


Figure 49: Percent of the maximum increase in cooling tower makeup water demand to total water demand for ammonia, methanol, and GTL plants

Reverse osmosis seasonality assessment

Figure 50 represents RO power profile considering seasonal water requirements based on changing irrigation and cooling tower demands. As a result of the different water requirements, and the different seasonal power demand parameters, the maximum power demand for the RO unit is observed in fall while the minimum power requirement is in winter. The percent of increase in power demand from winter to fall in ammonia, methanol, and GTL plant is 8.80%, 8.81%, and 8.99% respectively. Furthermore, the increase in power demand from winter to fall represents 0.52%, 0.20%, and 0.53% of the basic power demand in ammonia, methanol, and GTL plants respectively as shown in Table 21.

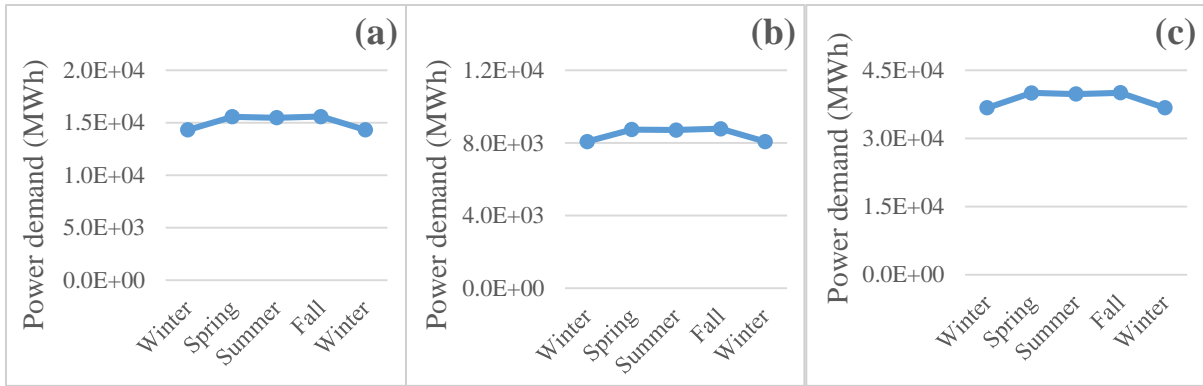


Figure 50: RO power demand profile based on seasonal water requirements for (a) ammonia, (b) methanol, and (c) GTL plants

Table 21: Percent of the increase in RO power demand with respect to plant basic power load

Plant	Ammonia	Methanol	GTL
Percent of the maximum seasonal increase in RO power demand to plant basic power load (%)	0.52	0.20	0.53

Waste heat to power seasonality assessment

A comparison between the required process basic power load and seasonal changes in power generation from waste heat via the WHP unit was established. The comparison using cooling towers, once-through cooling seawater, and air coolers for discharging the remaining heat is shown in Table 22, Table 23, and Table 24 respectively. It is clearly shown that the increase in power production by the WHP unit is insignificant with respect to the total basic power demand in ammonia, methanol, and GTL plants. More variation is expected in power generation by WHP unit when air coolers are used for discharging heat, followed by once-through cooling seawater,

and cooling towers. The variation depends mainly on the seasonal temperature of the cooling medium.

Table 22: Percent of the maximum seasonal increase in the WHP unit power generation using cooling towers to plant basic power load

Plant	Ammonia	Methanol	GTL
Percent of the maximum increase in WHP power production with to plant basic power load (%)	2.88	1.70	3.24

Table 23: Percent of the maximum seasonal increase in the WHP unit power generation using once-through cooling seawater to plant basic power load

Plant	Ammonia	Methanol	GTL
Percent of the maximum increase in WHP power production with to plant basic power load (%)	6.50	3.83	7.32

Table 24: Percent of the maximum seasonal increase in the WHP unit power generation using air coolers to plant basic power load

Plant	Ammonia	Methanol	GTL
Percent of the maximum increase in WHP power production with to plant basic power load (%)	10.39	6.12	11.70

Irrigation water demand seasonality assessment

Assessing seasonal variation of irrigation water requirements involves generating irrigation profiles, and comparing the increase in water demand with total process water demand. The seasonality assessment was performed for alfalfa water demands as it is planted in the industrial city. The available planting land area was estimated using google earth for each process in this analysis, and the areas are shown in Table 25.

Table 25: Planting land area

Plant	Planting area (m ²)
Ammonia	8188
Methanol	28332
GTL	15067

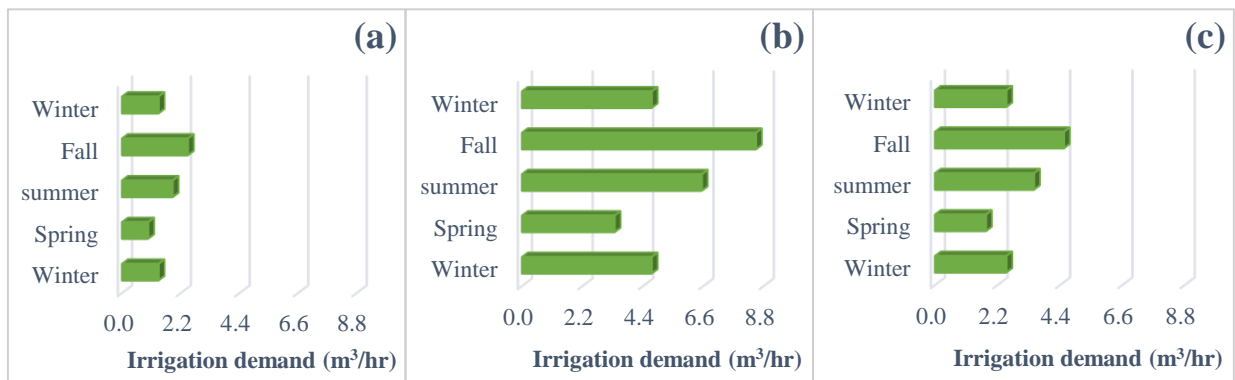


Figure 51: Seasonal alfalfa irrigation water demand profile in (a) ammonia, (b) methanol, and (c) GTL plants

Table 26: Percent of the increase in irrigation water demand to process total water demand

Plant	Ammonia	Methanol	GTL
Percent of the maximum seasonal increase in irrigation water demand to process total water demand (%)	0.0005	0.0022	0.0004

Irrigation water requirement was estimated for each process using seasonal irrigation parameters and estimated planting land areas and the results are demonstrated in Figure 51. Although the percent of increase in alfalfa water demand from spring to fall seems to be high (153%), the increase in irrigation water demand is negligible compared to process total water demand. This is clearly shown in Table 26 where the increase in irrigation water demand represents only a small percentage of the total water demand in ammonia, methanol, and GTL processes.

Treatment unit seasonality assessment

Evaporation from open treatment units

Seasonal evaporation rates from open treatment units were calculated by estimating first the surface area of available units in each process using Google Earth. Seasonal evaporation trends for all processes are shown in Figure 52. The increase in evaporation rates was compared to the total available wastewater in winter and summer in each plant. Figure 53 illustrates the percent of increase in evaporation from open treatment units to total wastewater in winter and summer for ammonia, methanol, and GTL plants. It shows that in all plants the increase in evaporation rates from open treatment units does not exceed 2% of the total available wastewater.

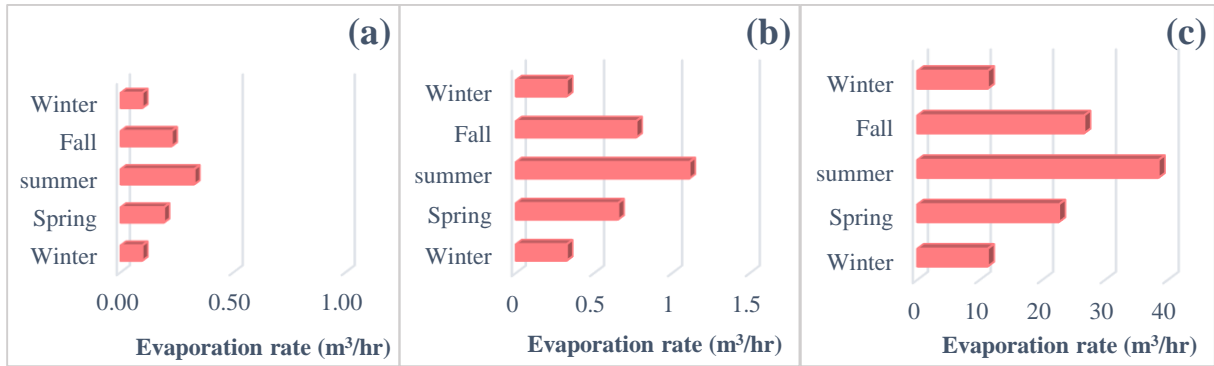


Figure 52: Seasonal water evaporation from open treatment units in (a) ammonia, (b) methanol, and (c) GTL plants

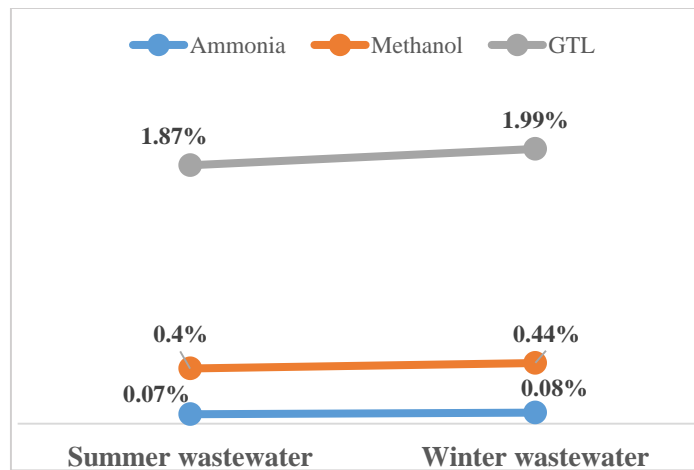


Figure 53: Percent of the increase in evaporation from open treatment units to total wastewater available in winter and summer for ammonia, methanol, and GTL plants

Dissolved air flotation (DAF)

To calculate DAF air compressor power demand, the seasonal theoretical air release was calculated which depends mainly on air solubility in water at atmospheric pressure. Then, the overall power demand profile was generated for the DAF unit including power requirements of the recycling pump and air compressor. Figure 54 represents the DAF unit power profile in ammonia, methanol, and GTL plants respectively. It clearly indicates that maximum and

minimum power is required in summer and winter respectively following the power profile of the DAF air compressor. The percent of increase in DAF power demand is 23%, 21%, and 17% for ammonia, methanol, and GTL processes respectively. This increase has been evaluated by comparison with the basic process power load.

Table 27 indicates that the maximum observed seasonal increase in DAF unit power demand for any process is very negligible compared to the basic plant power load.

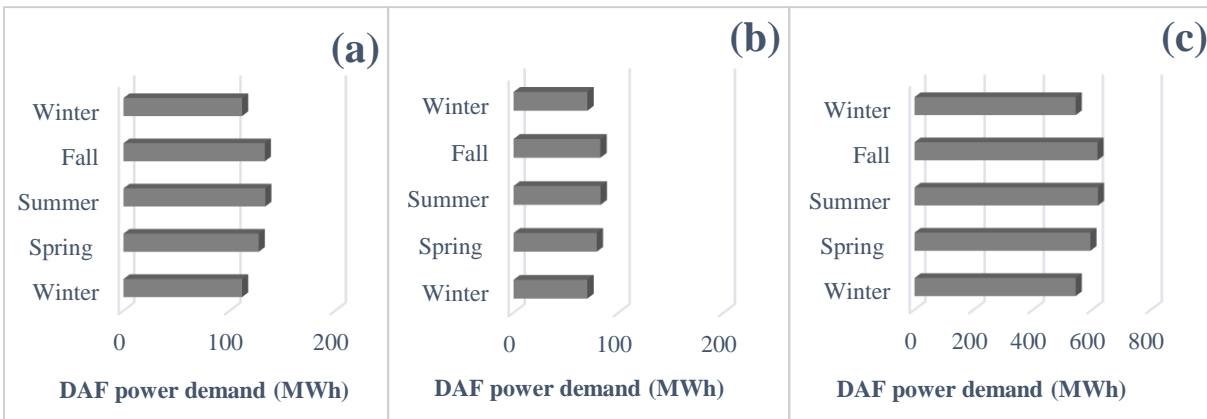


Figure 54: Seasonal DAF power demand profile in (a) ammonia, (b) methanol, and (c) GTL plants

Table 27: Percent of the seasonal increase in DAF power demand to plant basic power load

Plant	Ammonia	Methanol	GTL
Percent of the maximum seasonal increase in DAF unit power demand to plant basic power load (%)	0.0003	0.0003	0.0032

Membrane bioreactor (MBR)

The seasonal increase in MBR power demand is due to changes in air blower and suction pump power demands. Accordingly, required air flowrate is determined to calculate air blower power demand. It is worth mentioning that air is necessary for scouring the immersed membrane to reduce fouling and to feed the microorganisms. MBR overall power demand profile was generated for each process. Figure 55 demonstrates seasonal MBR power demands in ammonia, methanol, and GTL plants.

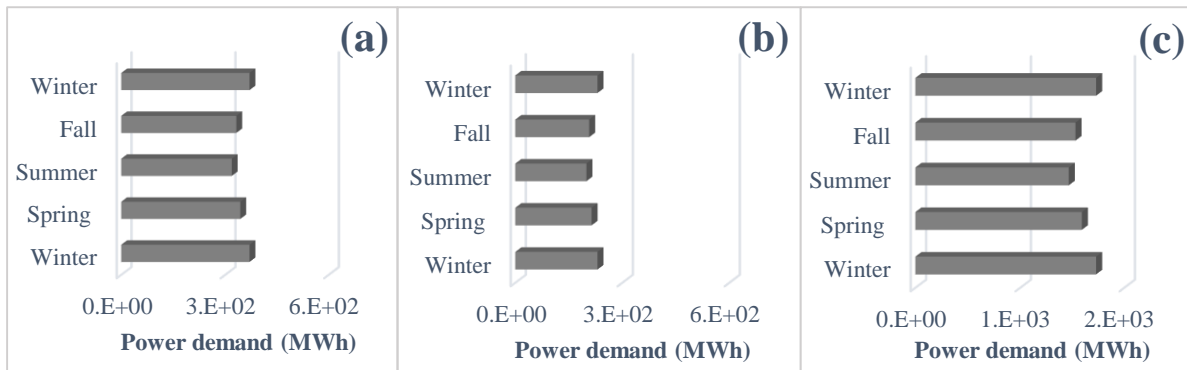


Figure 55: Seasonal MBR power demand profile in (a) ammonia, (b) methanol, and (c) GTL plants

Figure 55 shows that the maximum and minimum power demand for MBR unit occurs in winter and summer respectively for all processes. Furthermore, the GTL plant requires more power in comparison with ammonia, and methanol plants since more wastewater is generated from the GTL process. Table 28 illustrates the increase in MBR power demand as a percentage of the basic plant power load for ammonia, methanol, and GTL plants. It is noticed that the MBR power demand increase is negligible relative to the basic power load for all considered processes.

Table 28: Percent of the maximum seasonal increase in MBR power demand to plant basic power load

Plant	Ammonia	Methanol	GTL
Percent of the maximum seasonal increase in MBR power demand to plant basic power load (%)	0.0006	0.001	0.02

Nano-filtration membrane (NF)

As the amount of wastewater sent to treatment unit changes over different seasons, the total power demand in each season depends on the associated power parameter and the flowrate of treated water generated from the treatment units. The following figures represent the power demand as a result of the total amount of treated water in each season and the seasonal power demand parameter. In this analysis, it was assumed that all generated wastewater has been treated.

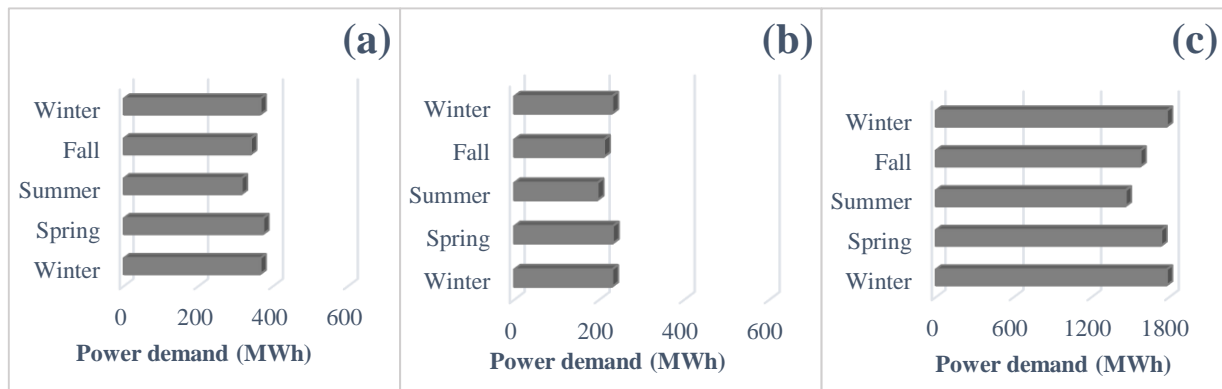


Figure 56: Seasonal NF power demand profile in (a) ammonia, (b) methanol, and (c) GTL plants

The maximum power demand for nano-filtration in ammonia and methanol plants take place in spring whilst summer is associated with the minimum power demand. The maximum

power demand occurs at different seasons compared to maximum power demand parameters because it depends on the amount of treated wastewater which changes over the seasons. The minimum wastewater to be treated is generated in winter while in summer the treatment units receive the maximum wastewater. The percent of increase in power demand during spring is 18.3%, and 18.7% relative to power demand in summer for ammonia, and methanol plants respectively as indicated in Figure 56. The seasonality assessment for nano-filtration membrane in the GTL plant showed that winter and summer seasons are associated with the maximum and minimum power demands respectively. The percentages of the maximum seasonal power increase to the plant basic power requirement are shown in Table 29 for all considered processes.

Table 29: Percentages of the maximum seasonal increase in NF power demand to plant basic power load

Plant	Ammonia	Methanol	GTL
Percent of the maximum seasonal increase in NF power demand to plant basic power load (%)	0.024	0.01	0.051

Wastewater reverse osmosis membrane (RO)

Similar to nano-filtration membranes, the overall power requirement for treating wastewater via RO membranes depends on RO specific power demand parameters and treated wastewater flowrate for each season. Power profiles for the three processes are represented in Figure 57. The minimum power demand for RO treatment unit is observed in summer for all processes while maximum power is required in spring for ammonia plant, and in winter for methanol, and GTL processes. The variation in maximum and minimum power demand

occurrence depends on different RO seasonal power demand per cubic meter of treated water and wastewater flowrate in each season. Percentages of the maximum increase in RO power demand to the basic power load are represented in Table 30. In all processes, the increase in RO treatment unit power demand was less than or equal to 0.1% of the basic process power load.

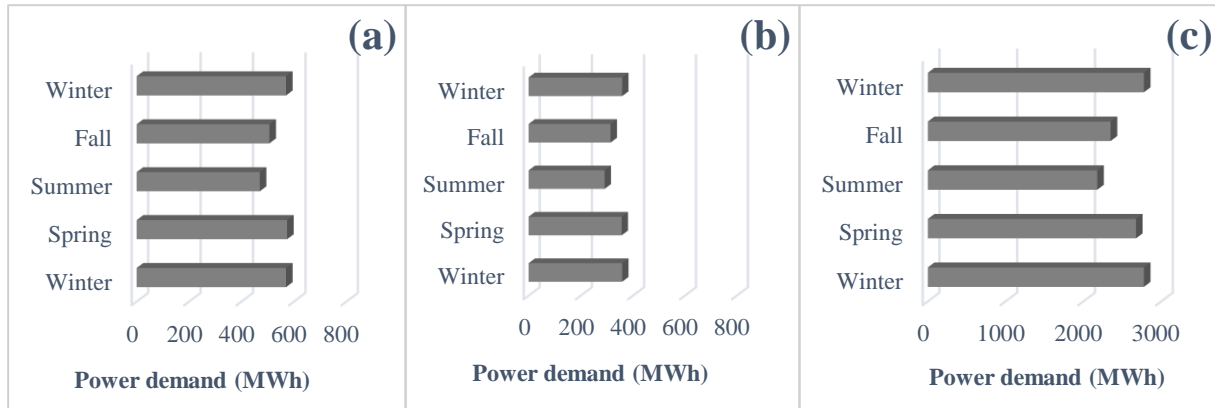


Figure 57: Seasonal power demand profile for wastewater RO membrane unit in (a) ammonia, (b) methanol, and (c) GTL plants

Table 30: Percent of the maximum increase in wastewater RO power demand to plant basic power load

Plant	Ammonia	Methanol	GTL
Percent of the maximum increase in RO power demand to plant basic power load (%)	0.04	0.02	0.10

The results of all performed assessments show that water and energy supply/demand seasonal variations are quite insignificant with respect to the overall process water/energy supply and demand. It was noticed that the ratios of the increase in seasonal power demand relative to

basic process power load are higher for cooling systems (i.e. air coolers, cooling towers) compared to desalination and treatment units. Additionally, irrigation water demand does not experience significant seasonal changes and it is not a critical part of the water-energy network as it only represents a water sink which does not affect the core process. Seasonal variations in the evaporation from open treatment units are minimal and evaporation can be eliminated by using closed treatment units.

CHAPTER V

DESIGN APPROACH AND MATHEMATICAL MODELING

Seasonality-based classification matrices of water-energy network components

After analyzing the impact of seasonal variations on the water-energy network components, and evaluating the significance of these changes, the given water-energy network was modified to absorb spotted seasonal variances. According to the analysis and assessment results, a novel approach was proposed. Hence, a mathematical model was modified to cope with the seasonality issue in industrial parks. Figure 58 shows the water-energy network representation with elements affected by seasonality highlighted.

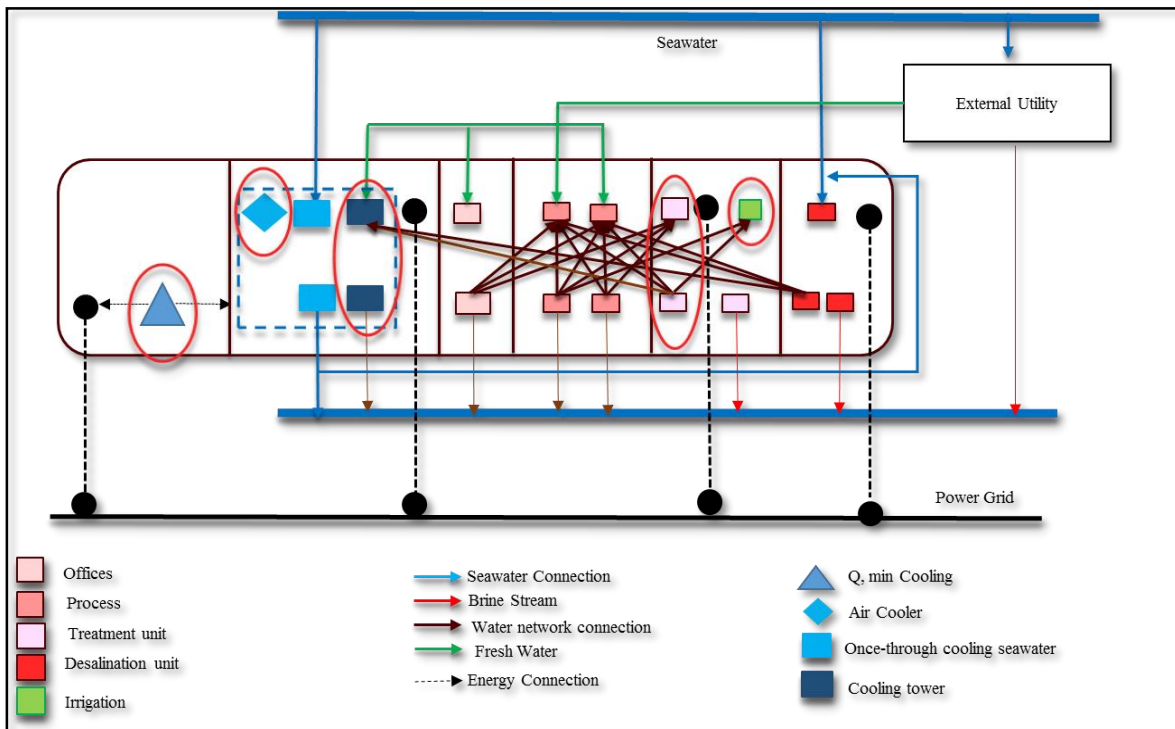


Figure 58: Visualization for seasonality aspects of the water-energy network

Variable water sources subsume cooling tower blowdown, and open treatment units vulnerable to evaporation and changing influent while changing water sinks include cooling tower makeup water demand, treatment units, and irrigation water demand. In terms of energy, variable energy sources include the waste-heat-to-power unit (WHP), while air coolers, cooling towers, and treatment units are classified as variable energy sinks. It is clearly noticed that water-energy network components can be classified into either fixed, or variable sources/sinks. Also, variable components can be categorized into two types; type I, and type II. Type I variable components involve changes due to seasonality while the variations in Type II variable components are scalable based on human-made decisions, so it can be managed accordingly. Figure 59 and Figure 60 represent characterization matrices for water and energy network components.






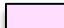


		Water Sink (Demand)			
		-	Fixed	Variable Type I	Variable Type II
Water Source (Supply)	-				
	Fixed		   		
	Variable Type I			 	
	Variable Type II				

Figure 59: Characterization matrix for water network elements

Figure 59 indicates that the treatment interceptor can be either categorized as a fixed source and sink which is the case of closed units with fixed influent over the year. Treatment units are classified as type I variable source/sink in case of evaporation or varying seasonal influent (i.e. due to variation of cooling tower blowdown). Irrigation water demand can be managed by changing planting plans, so they represent type II variable water sinks. Desalination units and are classified as type II variable source and sink as the amount of desalinated water can be scaled according to water demand.

In terms of energy sources, the WHP unit is classified within type II variable sources. That is because power generation via WHP unit can be controlled by producing different power rates – up to maximum possible power generation – and discharging the remaining waste heat. Similar to water sinks, energy sinks can be fixed, or variable with two types. Fixed energy sinks include once-through cooling seawater, while air coolers, cooling towers, and treatment units are classified as type I variable energy sinks. It is worth mentioning that desalination plants are considered as type II variable energy sinks since power demand can be controlled by scaling the RO unit based on water demand.





		Energy Sink (Demand)			
		-	Fixed	Variable Type I	Variable Type II
Energy Source (Supply)	-				
	Fixed				
	Variable Type I				
	Variable Type II				

Figure 60: Characterization matrix for energy network elements

Water-energy network proposed design approach

This section highlights some potential solutions to cope with the seasonality of the water-energy network components. All solutions, assumptions, and adjustments for seasonal variations in the water-energy network are explained in details.

The water network is designed by connecting different sources and sinks based on water supply and demand; as well as pollutants concentrations. Since the observed seasonal changes are insignificant relative to the basic process water/energy supply and demand, it is proposed to design the water network based on average water flowrates. Any extra water demand should be supplied to sink using desalinated water via either storage tanks or desalinated water-sink pipelines. On the other hand, maximum capacity discharge connections should be made available to all water sources to absorb any seasonal increase in the water supply from these sources. In terms of capacity, treatment and desalination units should be designed based on maximum capacity.

Similar to the water network, the energy network is designed based on average power supplies and demands of different available power sources and sinks. Based on the analysis and assessment results, it is proposed to connect all power sinks to the utility system. Accordingly, the utility system should be designed based on the maximum power demand of all sinks over the year. Designing the utility system according to peak demands helps to handle the power network seasonality; as well as maintaining the plant's operability in case of network failure. The following design adjustments elucidate the proposed approach for designing the water-energy network taking into account the seasonal variations.

Water-energy network design adjustments

- The water network is designed based on average flowrates for available sources and sinks.
- The water network is designed based on worst case scenario considering the minimum treatment unit removal ratio to guarantee the operability and reliability of the network throughout all seasons.
- All pipes are designed based on the maximum available flowrate in sources/sinks over different seasons (i.e. peak flowrate).
- All water sinks are connected to desalinated water source based on maximum demand either from an external utility or a desalination plant. This connection is utilized to compensate for seasonal changes in water demand and to ensure continuity of plant operation in case of network failure.
- Desalinated water connections/storage are designed based on maximum sink demand over different seasons.
- Desalination plants should be designed based on peak water demand over the year.

- All water sources are connected to discharge to handle any seasonal variations in the water supply.
- Discharge connections are designed based on maximum available water in each source over different seasons.
- Treatment units are designed based on peak conditions of maximum wastewater to be treated.
- Energy network is designed based on average power demands and supplies over different seasons.
- The utility system is designed based on the maximum power demand over seasons to compensate for seasonal changes in power demands and to ensure the continuity of plant operation in case of network failure.
- Basic plant power load is supplied by the utility system, while power generated from waste heat is used for network power sinks such as cooling systems including air coolers, cooling towers, and once-through cooling seawater, desalination plants, and treatment units.
- Extra power generated via the WHP unit is allowed to be exported to satisfy other process power demands i.e. basic power load.
- All power sinks should be connected to the utility system/external utility, and this connection should be designed based on the maximum power demand by this sink.
- Cooling systems should be designed based on process minimum cooling requirement, to discharge maximum potential waste heat.

As mentioned earlier, sinks should be supplied with desalinated water to compensate for seasonal demand changes. Desalinated water can be either supplied via a piping system or stored

in storage tanks and used as required. A simple economic analysis between sinks desalinated water connections and storage tanks was performed. The results of the analysis show that the cost of typical seasonal water storage tanks is almost five times the cost of piping the same amount of water. Consequently, desalinated water connections for all water sinks was selected and implemented as the solution to handle seasonality of water demands. Also, discharge connections were installed for all water sources based on maximum available flowrate from each source to balance out any change in water supplies.

It is worth mentioning that the water-energy network designed in this study takes into account the probability of network failure and guarantees a standalone and continuous plant operation. This is accomplished by designing the desalinated water and discharge connections based on maximum potential flowrate in each sink and source respectively. Also, by designing the utility system and desalination plants based on maximum process power and water demands. To the best of author's knowledge, this novel design is the first of its kind and it provides more tolerance to seasonal variations.

Mathematical formulation

The main objective of this work is to minimize the total annual cost (TAC) of the water-energy network including; the capital and the operating cost of different elements considering climatic seasonal variations. According to the results of performed analysis and assessment, all the units involved in the network (i.e. interceptors, cooling systems, WHP unit, and desalination unit); as well as the utility system should be designed based on peak conditions. As a result, the capital cost is calculated based on the maximum capacity over the seasons. Also, the pipes should be designed based on maximum flowrates, so it can be feasibly utilized with different seasonal

flowrates. The results of this analysis showed that the water-energy network can be feasibly designed based on average water and energy supplies and demands. Furthermore, water demand seasonal variations can be compensated by using maximum capacity desalinated water and discharge connections. Also, this study showed that the energy network can be designed based on average power demand and supply considering the design of maximum capacity utility system. Accordingly, the operating cost of the network elements is calculated based on average values.

Objective function

Minimize TAC = Min (CAPEX + OPEX) which includes the following terms:

$$TAC = C^{Fresh} + C^{Seawater} + C^{Treatment} + C^{Pipes} + C^{Waste} + C^{Desalination} + C^{Cooling\ systems} + C^{WHP}$$

A mixed-integer nonlinear programming model (MINLP) developed earlier by Alnouri et al. and Fouladi et al. was expanded and modified to design a novel inter-plant water-energy network considering seasonal variations. The following section starts by stating cost equations followed by water and energy balances; as well as equality and inequality constraints.

Cost Equations

The cost of freshwater imported from any external utility is calculated using the following equation which depends on average required freshwater flowrate, freshwater cost parameter, and annual operating hours.

Freshwater cost

$$C^{Fresh} = H_y \sum_{l \in L} \sum_{p \in P} \sum_{j \in SN_p} F_{l,jp}^{avg} C_l^{FR}$$

Central/Decentral wastewater treatment unit cost

The capital cost of central/decentral treatment units was modified to be calculated using the maximum wastewater flowrate to be treated, and the capital cost parameter for each unit while the operating cost depends on average flowrate of wastewater sent to the interceptor, and the operating cost parameter.

$$C^{Treatment} = K_F \left(\sum_{p \in P} \sum_{r \in R} (T_{rp}^{max})^\alpha C_{rp}^{CC} + \sum_{s \in S} \sum_{t \in T} (T_{st}^{max})^\alpha C_{st}^{CC} \right) + H_y \left(\sum_{p \in P} \sum_{r \in R} T_{rp}^{avg} C_{rp}^{OC} + \sum_{s \in S} \sum_{t \in T} T_{st}^{avg} C_{st}^{OC} \right)$$

Where,

$$T_{rp}^{max} = \sum_{p \in P} \sum_{i \in SU_p} P_{ip,rp}^{avg,max} \times T_{ip,rp}^{avg}$$

$$T_{st}^{max} = \sum_{i \in SU_p} P_{ip,st}^{avg,max} \times T_{ip,st}^{avg}$$

The average power demand for decentral/central treatment units is calculated using the following equations:

$$PW_{rp}^{T,avg} = T_{rp}^{T,avg} \times P_{T,rp}^{PW,avg}$$

$$T_{rp}^{T,avg} = \sum_{p \in P} \sum_{j \in SN_p} T_{rp,jp}^{avg} + D_{rp}^{T,avg}$$

$$PW_{rp}^{T,avg,total} = \sum_{p \in P} \sum_{r \in R} PW_{rp}^{T,avg}$$

$$PW_{st}^{T,avg} = T_{st}^{T,avg} \times P_{T,st}^{PW,avg}$$

$$T_{st}^{T,avg} = \sum_{p \in P} \sum_{j \in SN_p} T_{st,jp}^{avg} + D_{st}^{T,avg}$$

$$PW_{st}^{T,avg,total} = \sum_{s \in S} \sum_{t \in T} PW_{st}^{T,avg}$$

The cost of decentral/central treatment unit power demand can be calculated using the following equations:

$$C_{rp}^{PW,avg} = PW_{rp}^{T,avg,total} \times C^E$$

$$C_{st}^{PW,avg} = PW_{st}^{T,avg,total} \times C^E$$

Central/Decentral desalination unit cost

Similarly, the capital cost of central/decentral desalination units was modified to be calculated based on maximum seawater flowrates to the desalination unit; while the operating cost is calculated using average seawater flowrates.

$$C^{Desalination} = K_F \left(\sum_{p \in P} \sum_{m \in M} (T_{mp}^{Des,max})^\delta C_{mp}^{CC} + \sum_{n \in N} \sum_{k \in K} (T_{nk}^{Des,max})^\delta C_{nk}^{CC} \right) \\ + H_y \left(\sum_{p \in P} \sum_{m \in M} T_{mp}^{Des,avg} C_{mp}^{OC} + \sum_{n \in N} \sum_{k \in K} T_{nk}^{Des,avg} C_{nk}^{OC} \right)$$

The maximum flowrate of seawater to desalination is calculated using average-to-maximum parameter and the average required sweater flowrate.

$$T_{mp}^{Des,max} = P_{mp}^{avg,max} \times T_{mp}^{Des,avg}$$

$$T_{nk}^{Des,max} = P_{nk}^{avg,max} \times T_{nk}^{Des,avg}$$

The average power demand for decentral/central desalination unit is calculated using the following equations:

$$PW_{mp}^{Des,avg} = T_{mp}^{T,avg} \times P_{Des}^{PW,avg}$$

$$PW_{nk}^{Des,avg} = T_{nk}^{T,avg} \times P_{Des}^{PW,avg}$$

$$PW_{mp}^{T,avg,total} = \sum_{p \in P} \sum_{m \in M} PW_{mp}^{T,avg}$$

$$PW_{nk}^{T,avg,total} = \sum_{n \in N} \sum_{k \in K} PW_{nk}^{T,avg}$$

The cost of decentral/central desalination unit power demand can be calculated using the following equations:

$$C_{mp}^{PW,avg} = PW_{mp}^{T,avg,total} \times C^E$$

$$C_{nk}^{PW,avg} = PW_{nk}^{T,avg,total} \times C^E$$

Cost of cooling process

The cost associated with cooling systems can be calculated by the summation of capital and operating cost of different possible cooling options including; air coolers, cooling towers, and once-through cooling seawater.

$$C^{cooling\ sys} = A \sum_{p \in P} CC_p^{AC} + B \sum_{p \in P} CC_p^{CT} + C \sum_{p \in P} OC_p^{AC} + D \sum_{p \in P} OC_p^{CT} + E \sum_{p \in P} OC_p^{OC_{SW}}$$

The capital cost of any cooling system is calculated considering the maximum waste heat that needs to be discharged from any process; which represents the minimum cooling requirement.

Cooling systems operating costs are calculated considering average power/water demand.

Air coolers

$$CC_p^{AC} = C_{AC}^{CC} \times Q_p^{min}$$

$$OC_p^{AC} = PW_p^{AC,avg} \times C^E, \text{ where } PW_p^{AC,avg} = Q_p^{D,AC,avg} \times P_{AC}^{PW,avg}$$

$$Q_p^{D,AC,avg} = Q_p^{min} - Q_p^{WHP,avg}$$

Cooling towers

$$CC_p^{CT} = C_{CT}^{CC} \times Q_p^{min}$$

Cooling tower operating cost is the sum of power cost and makeup water cost.

$$OC_p^{CT} = C_{CT,p}^{PW} + C_{CT,p}^{MU}$$

$$C_{CT,p}^{PW} = PW_p^{CT,avg} \times C^E, \text{ where, } PW_p^{CT,avg} = Q_p^{D,CT,avg} \times P_{CT}^{PW,avg}$$

$$Q_p^{D,CT,avg} = Q_p^{min} - Q_p^{WHP,avg}$$

The cost of the cooling tower required makeup water is calculated based on average demand using the following equation in case the freshwater is supplied from an external utility.

$$C_{CT,p}^{MU} = H_y (P_{CT}^{MU,avg} \times Q_p^{D,CT,avg} \times C_l^{FR})$$

It is worth noting that the cost of makeup water is accounted for in the desalination cost equation if the makeup water demand is supplied from decentral/central desalination plants.

Once-through cooling seawater

The cost of once-through cooling seawater (OC^{CS}_p) involves mainly the cost of average power and average seawater demands.

$$OC_p^{OCSW} = C_{OCSW}^{PW} + C_{OCSW}^{SW}$$

$$C_{OCSW}^{PW} = PW_p^{OCSW,avg} \times C^E, \text{ where } PW_p^{OCSW,avg} = F_p^{OCSW,avg} \times P_{OCSW}^{PW}$$

$$C_{OCSW}^{SW} = H_y (C^{SW} \times F_p^{OCSW,avg})$$

$$F_p^{OCSW,avg} = P_{OCSW}^{SW} \times Q_p^{D,OCSW,avg}$$

$$Q_p^{D,OCSW,avg} = Q_p^{min} - Q_p^{WHP,avg}$$

The seawater temperature difference is fixed, however, the dissipated heat through once-through cooling seawater (OCSW) changes as average heat converted to power via WHP unit changes. As a result, required seawater flowrate will change over seasons, hence seasonal power demand is changing too. If heat converted to power was fixed assuming that cooling medium temperature is fixed over the seasons, then dissipated heat via the once-through cooling seawater, seawater flowrate and power demand will all be fixed for OCSW with fixed seawater temperature difference.

Wastewater and brine discharge cost

The cost of wastewater discharges includes charges associated with the disposal of unused wastewater from any source; as well as brine. The disposal of any wastewater should comply with the industrial city policies and regulations. Discharge costs are calculated based on the average flowrate of disposed wastewater and brine in the industrial city.

$$C^{Waste} = H_y (C^{WW} WW^{total,avg} + C^{BRINE} B^{total,avg})$$

Waste heat to power cost

The cost of waste heat to power (WHP) unit is calculated considering both the capital and the operating costs. The capital cost is calculated by the maximum power produced over the year (i.e. in winter); while the operating cost is calculated by the average power generated throughout the year.

$$C^{WHP} = K_F \sum_{p \in P} PW_p^{max} C_{WHP}^{CC} + H_y \sum_{p \in P} PW_p^{avg} C_{WHP}^{OC}$$

$$\text{Where } PW_p^{max} = P_{WHP}^{avg,max} \times PW_p^{avg}$$

Standardized pipelines diameters

The piping cost is calculated based on the cost per meter of length and the length of the piping segment. The cost per meter length depends on the standardized diameter of each piping segment which is obtained using the following equation. Maximum flowrate in each piping segment is utilized to design a piping system that is appropriate for all seasonal flowrates. It is worth noting that maximum flowrates are obtained based on average flowrates and average-to-maximum flowrate parameters.

$$DI = Roundup \left(0.363 \left(\left(\frac{F^{max}}{3600 \rho} \right)^{0.45} \rho^{0.13} \right) \right)$$

Maximum flowrate for any source-to-sink connection is the minimum flowrate out of the two maximum source and sink flowrates which can be determined as follows:

$$F_{ip,jp}^{max} = \text{minimum} (F_{ip}^{max}, F_{jp}^{max})$$

The maximum flowrate from any water source -which is either sent to water sinks in the plant or discharged directly- is obtained by utilizing the average-to-maximum parameter and average water available in that source over different seasons.

$$F_{ip}^{max} = P_{ip}^{avg,max} W_{ip}^{avg}$$

Similarly, maximum water flowrate allowed into any water sink in the plant is determined using the average-to-maximum flowrate parameter and average flowrate required into that sink over different seasons.

$$F_{jp}^{max} = P_{jp}^{avg,max} G_{jp}^{avg}$$

The maximum flowrate from any water source in the plant to decentral/central treatment unit is the maximum available flowrate from that source. The treatment units are designed based on maximum wastewater available from all sources in each/all plants respectively.

$$F_{ip,rp}^{max} = F_{ip}^{max} = P_{ip}^{avg,max} W_{ip}^{avg}$$

$$F_{ip,st}^{max} = F_{ip}^{max} = P_{ip}^{avg,max} W_{ip}^{avg}$$

The maximum flowrate from any decentral/central treatment unit to any water sink is the minimum flowrate amongst the two maximum flowrates of the treatment unit and the sink.

$$F_{rp,jp}^{max} = \text{minimum} (F_{rp}^{max}, F_{jp}^{max})$$

$$F_{st,jp}^{max} = \text{minimum} (F_{st}^{max}, F_{jp}^{max})$$

The maximum flowrate from any decentral/central treatment unit -which can be either used in water sinks or discharged to the environment- is calculated using treated water average-to-maximum flowrate parameter and average treated water flowrate.

$$F_{rp}^{max} = P_{rp}^{avg,max,T} T_{rp}^{T,avg}$$

$$F_{st}^{max} = P_{st}^{avg,max,T} T_{st}^{T,avg}$$

In addition, the maximum flowrate from decentral/central desalination units to any water sink depends on the maximum water required into that sink as the desalination plants are designed based on maximum water demands. In other words, the required water flowrate into any water sink will always be less than the maximum flowrate from desalination units so the piping system is designed based on the sink's maximum water flowrate.

$$F_{mp,jp}^{max} = F_{jp}^{max}$$

$$F_{nk,jp}^{max} = F_{jp}^{max}$$

Likewise, the maximum flowrate of freshwater from any external utility system depends on the maximum water demand into that sink.

$$F_{l,jp}^{max} = F_{jp}^{max}$$

The piping cost can be calculated using the obtained standardized piping diameters and the length of each piping segment. The cost of enforced maximum capacity freshwater and discharge connections is considered.

Piping cost

$$\begin{aligned}
C^{Pipes} = \gamma & \left[\sum_{p,p' \in P} \sum_{i \in SU_p} \sum_{j \in SN_p} a(DI_{ip,jp})^b L_{ip,jp} + \sum_{p \in P} \sum_{r \in R} \sum_{i \in SU_p} a(DI_{ip,rp})^b L_{ip,rp} \right. \\
& + \sum_{p \in P} \sum_{i \in SU_p} \sum_{s \in S} \sum_{t \in T} a(DI_{ip,st})^b L_{ip,st} + \sum_{p \in P} \sum_{r \in R} \sum_{j \in SN_p} a(DI_{rp,jp})^b L_{rp,jp} \\
& + \sum_{p \in P} \sum_{j \in SN_p} \sum_{s \in S} \sum_{t \in T} a(DI_{st,jp})^b L_{st,jp} + \sum_{p \in P} \sum_{r \in R} a(DI_{rp})^b L_{rp} \\
& \left. + \sum_{s \in S} \sum_{t \in T} a(DI_{st})^b L_{st} \right] + C_{ip}^{pipes} + C_{mp,jp}^{pipes} + C_{nk,jp}^{pipes} + C_{l,jp}^{pipes}
\end{aligned}$$

Water Balances and inequality constraints

Water source balance

The average water available from any water source is equal to the summation of source-to-sink average water flowrates, and the source-to-decentral/central treatment units' average water flowrates; as well as the average flowrate of water discharged from this source to the environment.

$$\sum_{p \in P} \sum_{j \in SN_p} M_{ip,jp}^{avg} + \sum_{p \in P} \sum_{r \in R} T_{ip,rp}^{avg} + \sum_{s \in S} \sum_{t \in T} T_{ip,st}^{avg} + D_{ip}^{avg} = W_{ip}^{avg}$$

$$\forall p \in P ; \forall i \in SU_p$$

Water sink balance

The average water available in any water sink is equal to the summation of average water flowrate from any water source, decentral/central treatment units, decentral/central desalination units, and average freshwater from external utility to the sink.

$$\begin{aligned} & \sum_{p \in P} \sum_{i \in SU_p} M_{ip,jp}^{avg} + \sum_{p \in P} \sum_{r \in R} T_{rp,jp}^{avg} + \sum_{s \in S} \sum_{t \in T} T_{st,jp}^{avg} + \sum_{p \in P} \sum_{m \in R} T_{mp,jp}^{Des,avg} + \sum_{n \in N} \sum_{k \in K} T_{nk,jp}^{Des,avg} \\ & + \sum_{l \in L} F_{l,jp}^{avg} = G_{jp}^{avg} \end{aligned}$$

$$\forall p \in P ; \forall j \in SN_p$$

Water sink pollutant equality

The summation of total pollutant flowrate from any water source, treatment units, and desalination units should equal total permissible pollutant concentration into the sink. Maximum outlet pollutant concentration from treatment and desalination units are considered while designing water network based on the worst case scenario of minimum treatment unit removal ratios.

$$\begin{aligned} & \sum_{p,p' \in P} \sum_{i \in SU_p} M_{ip,jp}^{avg} x_{c,ip}^{Source} + \sum_{p \in P} \sum_{r \in R} T_{rp,jp}^{avg} x_{c,rp}^{T,max} + \sum_{s \in S} \sum_{t \in T} T_{st,jp}^{avg} x_{c,st}^{T,max} \\ & + \sum_{p \in P} \sum_{m \in R} T_{mp,jp}^{Des,avg} x_{c,mp}^{Des,max} + \sum_{n \in N} \sum_{k \in K} T_{nk,jp}^{Des,avg} x_{c,nk}^{Des,max} + \sum_{l \in L} F_{l,jp}^{avg} x_{c,l}^{FRESH} \\ & = G_{jp}^{avg} z_{c,jp}^{in} \end{aligned}$$

$$\forall p \in P ; \forall j \in SN ; \forall c \in C_p$$

Water sink pollutant concentration inequality

$$z_{c,jp}^{min} \leq z_{c,jp}^{in} \leq z_{c,jp}^{max}$$

$$\forall p \in P ; \forall j \in SN_p ; \forall c \in C$$

Wastewater decentral treatment balance

Total average inlet wastewater flowrate into any decentral treatment unit is equal to the summation of average treated water used in other water sinks, average discharged treated and

untreated water; as well as the average amount of water evaporated from open decentral treatment units.

$$\sum_{p \in P} \sum_{i \in SU_p} T_{ip,rp}^{avg} = \sum_{p \in P} \sum_{j \in SN_p} T_{rp,jp}^{avg} + D_{rp}^{T,avg} + D_{rp}^{U,avg} + T_{rp,E}^{avg}$$

$$\forall p \in P ; \forall r \in R$$

The average water evaporated from any open treatment unit is calculated using average evaporation parameter and total average inlet wastewater into that decentral treatment unit.

$$T_{rp,E}^{avg} = E_{rp}^{avg} \times T_{ip,rp}^{avg}$$

Wastewater decentral treatment recovery

Total average wastewater discharges from any decentral treatment unit are calculated using the recovery ratio, average evaporation ratio, and total inlet average wastewater to that decentral treatment unit.

$$(1 - R_{rp}) (1 - E_{rp}^{avg}) \sum_{p \in P} \sum_{i \in SU_p} T_{ip,rp}^{avg} = D_{rp}^{U,avg} , \forall p \in P ; \forall r \in R$$

Outlet pollutant concentration from wastewater decentral treatment unit

Maximum outlet pollutant concentration from any decentral treatment unit depends on maximum inlet pollutant concentration and associated minimum removal ratio of the decentral unit.

$$x_{c,rp}^{T,max} = x_{c,rp}^{in,max} (1 - RR_{c,rp}^{min}) \forall p \in P ; \forall r \in R ; \forall c \in C$$

Maximum pollutant concentration in any decentral treatment unit results mainly from the maximum evaporation rate from that decentral unit over the year.

$$x_{c,rp}^{in,max} = \frac{\sum_{p \in P} \sum_{i \in SU_p} T_{ip,rp}^{max} x_{ip,rp}^{source}}{\sum_{p \in P} \sum_{i \in SU_p} T_{ip,rp}^{max} (1 - E_{rp}^{max})}$$

$$T_{ip,rp}^{max} = P_{ip,rp}^{avg,max} \times T_{ip,rp}^{avg}$$

Wastewater central treatment balance

Total average inlet wastewater flowrate into any central treatment unit is equal to the summation of average treated water used in other water sinks, average discharged treated and untreated water; as well as the amount of average water evaporated from open central treatment units.

$$\sum_{p \in P} \sum_{i \in SU_p} T_{ip,st}^{avg} = \sum_{p \in P} \sum_{j \in SN_p} T_{st,jp}^{avg} + D_{st}^{T,avg} + D_{st}^{U,avg} + T_{st,E}^{avg}, \quad \forall s \in S; \forall t \in T$$

$$T_{st,E}^{avg} = E_{st}^{avg} \times T_{ip,st}^{avg}$$

Wastewater central treatment recovery

Total average wastewater discharges from any central treatment unit are calculated using the recovery ratio, average evaporation ratio, and total inlet average wastewater to that central treatment unit.

$$(1 - R_{st})(1 - E_{st}^{avg}) \sum_{p \in P} \sum_{i \in SU_p} T_{ip,st}^{avg} = D_{st}^{U,avg} \quad \forall s \in S; \forall t \in T$$

Outlet pollutant concentration from wastewater central treatment unit

Maximum outlet pollutant concentration from any central treatment unit depends on maximum inlet pollutant concentration and associated minimum removal ratio of the central unit.

$$x_{c,st}^{T,max} = x_{c,st}^{in,max} (1 - RR_{c,st}^{min}) \quad \forall s \in S; \forall t \in T; \forall c \in C$$

The maximum pollutant concentration in the central treatment unit results from the maximum evaporation rate from the central unit over the year.

$$x_{c,st}^{in,max} = \frac{\sum_{p \in P} \sum_{i \in SU_p} T_{ip,st}^{max} x_{ip,st}^{source}}{\sum_{p \in P} \sum_{i \in SU_p} T_{ip,st}^{max} (1 - E_{st}^{max})}$$

$$T_{ip,st}^{max} = P_{ip,st}^{avg,max} \times T_{ip,st}^{avg}$$

Decentral desalination balance

Total average seawater flowrate into any decentral desalination unit is equal to the summation of average desalinated water used in other water sinks and average discharged brine from decentral desalination units.

$$\sum_{p \in P} T_{mp}^{Des,avg} = \sum_{p \in P} \sum_{j \in SN_p} T_{mp,jp}^{Des,avg} + D_{mp}^{Des,avg}, \quad \forall p \in P; \forall m \in M$$

Decentral desalination recovery

Total average brine discharges from any decentral desalination unit is calculated using the recovery ratio and average inlet seawater to decentral desalination unit.

$$(1 - R_{mp}) \sum_{p \in P} T_{mp}^{Des,avg} = D_{mp}^{Des,avg}, \quad \forall p \in P; \forall m \in M$$

Outlet pollutant concentration from decentral desalination unit

Maximum outlet pollutant concentration from any decentral desalination unit depends on inlet pollutant concentration and associated minimum removal ratio of the decentral unit.

$$x_{c,mp}^{T,max} = x_{c,mp}^{in} (1 - RR_{c,mp}^{min}), \quad \forall p \in P; \forall m \in M; \forall c \in C$$

Central desalination balance

Total average seawater flowrate into any central desalination unit is equal to the summation of average desalinated water used in other water sinks and average discharged brine from central desalination units.

$$T_{nk}^{Des,avg} = \sum_{p \in P} \sum_{j \in SN_p} T_{nk,jp}^{Des,avg} + D_{nk}^{Des,avg}, \quad \forall n \in N; \forall k \in K$$

Central desalination recovery

Total average brine discharges from any central desalination unit is calculated using the recovery ratio and average inlet seawater to central desalination unit.

$$(1 - R_{nk}) T_{nk}^{Des,avg} = D_{nk}^{Des,avg} , \forall n \in N ; \forall k \in K$$

Outlet pollutant concentration from central desalination unit

Maximum outlet pollutant concentration from any central desalination unit depends on inlet pollutant concentration and associated minimum removal ratio of the central unit.

$$x_{c,nk}^{T,max} = x_{c,nk}^{in} (1 - RR_{c,nk}^{min}) , \forall n \in N ; \forall k \in K ; \forall c \in C$$

Total wastewater discharge

Total average wastewater discharges equal the summation of average water source discharges and average treated water discharges from decentral/central treatment units.

$$WW^{total,avg} = \sum_{p \in P} \sum_{i \in SU_p} D_{ip}^{avg} + \sum_{p \in P} \sum_{r \in R} D_{rp}^{T,avg} + \sum_{s \in S} \sum_{t \in T} D_{st}^{T,avg}$$

Wastewater discharge load

Wastewater discharges load is calculated considering the worst case scenario which depends on source fixed pollutant concentration and maximum pollutant concentration from decentral/central treatment units.

$$WW^{total,avg} x_c^{WW,max} = \sum_{p \in P} \sum_{i \in SU_p} D_{ip}^{avg} x_{c,ip}^{Source} + \sum_{p \in P} \sum_{r \in R} D_{rp}^{T,avg} x_{c,rp}^{T,max} + \sum_{s \in S} \sum_{t \in T} D_{st}^{T,avg} x_{c,st}^{T,max}$$

To avoid any harmful acting to the environment and to abide by the environmental laws associated with the pollutants' discharge limits, the model considered designing the water-energy-network based on maximum contaminants' discharge concentrations. Calculating the discharge

load based on maximum pollutant concentration will help to avoid violations of the environmental regulations over different seasons. The maximum pollutant concentration is a result of the maximum evaporation from the open treatment unit.

The discharge concentration of each pollutant should be less than or equal to a maximum specific limit based on environmental restrictions.

$$x_c^{WW,max} \leq x_c^{Max} \quad \forall c \in C$$

Total brine discharge

Total average brine discharges equal the summation of average brine discharges from decentral/central treatment units and decentral/central desalination units.

$$B^{total,avg} = \sum_{p \in P} \sum_{r \in R} D_{rp}^{U,avg} + \sum_{s \in S} \sum_{t \in T} D_{st}^{U,avg} + \sum_{p \in P} \sum_{m \in M} D_{mp}^{Des,avg} + \sum_{n \in N} \sum_{k \in K} D_{nk}^{Des,avg}$$

Brine discharge load

Brine discharges load is calculated considering the worst case scenario of maximum concentration which depends on maximum pollutant concentration of decentral/central treatment unit and desalination unit brines.

$$\begin{aligned} B^{total,avg} x_c^{Brine,max} &= \sum_{p \in P} \sum_{r \in R} D_{rp}^{U,avg} x_{c,rp}^{U,max} \\ &+ \sum_{s \in S} \sum_{t \in T} D_{st}^{U,avg} x_{c,st}^{U,max} + \sum_{p \in P} \sum_{m \in M} D_{mp}^{Des,avg} x_{c,mp}^{U,max} + \sum_{n \in N} \sum_{k \in K} D_{nk}^{Des,avg} x_{c,nk}^{U,max} \\ &\forall p \in P ; \forall c \in C \end{aligned}$$

Energy balances and inequality constraints

In this analysis, the processes are assumed to be already fully heat integrated, and the minimum cooling requirement of each process was obtained using generated grand composite curves. Fouladi et al. proposed a nexus between water and energy through the minimum cooling requirement. The nexus basically depends on converting part of the minimum cooling requirement into power using a waste-heat-to-power unit where water is used as an energy carrier. The seasonal power demand of each element involved in the water-energy network was analyzed in this study. This includes the seasonal power demand of treatment units, desalination units, and cooling systems.

The power demands considering seasonal variations were compared to the basic power load to operate each plant. The average power generated from waste heat using the WHP unit can be utilized to satisfy the average power requirements of cooling systems, decentral and central interceptors (i.e. treatment units, desalination plants). The heat balance for the heat demand and supply within the water-energy network shows that minimum cooling requirement of any process is equal to the sum of average heat removed by waste-heat-to-power unit, and cooling systems. The waste heat converted into power via the WHP unit experiences a slight change over the seasons. The variation in the power generated from the WHP unit is due to changing cooling medium temperature. Accordingly, heat dissipated via any cooling system (i.e. air coolers, cooling towers, and once-through cooling seawater) experiences some seasonal changes as well.

$$\sum_{p \in P} Q_p^{D,AC,avg} + \sum_{p \in P} Q_p^{D,CT,avg} + \sum_{p \in P} Q_p^{D,OCSW,avg} + \sum_{p \in P} Q_p^{WHP,avg} = Q_p^{min,cooling}, \forall p \in P$$

In addition to the heat balance, the energy network requires some inequality constraints for energy sources and sinks including central/decentral interceptors (i.e. desalination plants, treatment units); as well as cooling systems.

Energy source inequality

The summation of all average energy transmitted to any sink is less than or equal to the average energy available in that source. This includes the average energy of source-to-air coolers, source-to-cooling towers, source-to-once through cooling seawater, in addition to source-to-central/decentral interceptors (treatment units, desalination plants).

$$\begin{aligned}
& \sum_{p \in P} \sum_{r \in R} PW_{ip,rp}^{T,avg} + \sum_{s \in S} \sum_{t \in T} PW_{ip,st}^{T,avg} + \sum_{p \in P} \sum_{m \in M} PW_{ip,mp}^{Des,avg} + \sum_{n \in N} \sum_{k \in K} PW_{ip,nk}^{Des,avg} \\
& + \sum_{p \in P} \sum_{j \in SN'_p} PW_{ip,j'p}^{CT,avg} + \sum_{p \in P} \sum_{j \in SN'_p} PW_{ip,j'p}^{OCsw,avg} + \sum_{p \in P} \sum_{j \in SN'_p} PW_{ip,j'p}^{AC,avg} \\
& \leq \sum_{p \in P} \sum_{i' \in SU'_p} PW_{i'p}^{avg} \\
& \forall p \in P ; \forall i' \in SU'_p
\end{aligned}$$

Energy sink inequality

The energy sink inequality illustrates that the average power rate transmitted from any power source to any power sink should be less than or equal to the average calculated power demand for that sink.

$$\begin{aligned}
& \sum_{p \in P} \sum_{r \in R} PW_{i'p,rp}^{T,avg} \leq \sum_{p \in P} \sum_{r \in R} PW_{rp}^{T,avg} , \forall p \in P ; \forall r \in R \\
& \sum_{s \in S} \sum_{t \in T} PW_{i'p,st}^{T,avg} \leq \sum_{s \in S} \sum_{t \in T} PW_{st}^{T,avg} , \forall s \in S ; \forall t \in T
\end{aligned}$$

$$\sum_{p \in P} \sum_{m \in M} PW_{i'p,mp}^{Des,avg} \leq \sum_{p \in P} \sum_{m \in M} PW_{mp}^{Des,avg}, \forall p \in P; \forall m \in M$$

$$\sum_{n \in N} \sum_{k \in K} PW_{i'p,nk}^{Des,avg} \leq \sum_{n \in N} \sum_{k \in K} PW_{nk}^{Des,avg}, \forall n \in N; \forall k \in K$$

$$\sum_{p \in P} \sum_{j' \in SN'_p} PW_{i'p,j'p}^{CT,avg} \leq \sum_{p \in P} \sum_{j' \in SN'_p} PW_{j'p}^{CT,avg}, \forall j' \in SN'_p$$

$$\sum_{p \in P} \sum_{j' \in SN'_p} PW_{i'p,j'p}^{OCSW,avg} \leq \sum_{p \in P} \sum_{j' \in SN'_p} PW_{j'p}^{OCSW,avg}, \forall j' \in SN'_p$$

$$\sum_{p \in P} \sum_{j' \in SN'_p} PW_{i'p,j'p}^{AC,avg} \leq \sum_{p \in P} \sum_{j' \in SN'_p} PW_{j'p}^{AC,avg}, \forall j' \in SN'_p$$

The average power generated using minimum cooling requirements is equal to the summation of the average power generated by the WHP unit and used in treatment units, desalination plants, and cooling systems. In the case of surplus power produced from waste heat, it can be exported. Power exports are calculated based on the following equation:

$$\sum_{p \in P} \sum_{i' \in SU'_p} PW_{i'p}^{Export,avg} = \sum_{p \in P} \sum_{i' \in SU'_p} PW_{i'p}^{avg} - \sum_{p \in P} \sum_{j' \in SN'_p} PW_{j'p}^{avg}$$

In the case of deficiency in the generated waste-heat-to-power, more power can be produced in the utility system. Average power required for the water-energy network and generated from the utility system is determined by the difference between average network power demand and power supplied by the WHP unit.

$$PW^{utility,avg} = \sum_{p \in P} \sum_{j' \in SN'_p} PW_{j'p}^{avg} - \sum_{p \in P} \sum_{i' \in SU'_p} PW_{i'p}^{avg}$$

The cost of the average power generated in the utility system can be calculated by accounting for the cost of fuel used to generate steam that is used across a steam turbine for power generation.

Steam Turbine model

Three main parameters have a significant effect on turbine efficiency, these are the steam turbine size, the steam load, and the pressure drop across the turbine. To take into account these aspects, Willan's line is used to determine the output power of the steam turbine [86]. The steam turbine model is shown below:

$$PW^{utility,avg} = C^{Turb} m^{steam,avg} - D^{Turb}$$

Where $PW^{Turbine}$ represents the power generated by the steam turbine, C^{Turb} is the slope of the Willan's line, and D^{Turb} is the intercept of Willan's equation. The slope and the intercept of Willan's equation can be calculated using the following equations:

$$D^{Turb} = \frac{L}{B} (\Delta h_{is} m_{max} - A)$$

$$C^{Turb} = \frac{L + 1}{B} \left(\Delta h_{is} - \frac{A}{m_{max}} \right)$$

Where L is the steam turbine intercept ratio, Δh_{is} represents the isentropic enthalpy change across the steam turbine, m_{max} is the maximum flowrate of steam in the turbine, A and B are regression parameters in the steam turbine model and they are calculated using the following equations:

$$A = b_0 + b_1 \Delta T_{sat}$$

$$B = b_2 + b_3 \Delta T_{sat}$$

The regression parameters (b_0, b_1, b_2, b_3) depend on the size and the type of the steam turbine. Two types of steam turbines are available which are the backpressure turbine and the condensing turbine. Backpressure turbine is used when there is a need for medium and low-

pressure steam, while in condensing turbine, the steam expands and exits the turbine below atmospheric pressure and condenses in a condenser. In this analysis, the condensing steam turbine ($W_{max} > 2$ MW) was used to produce the required power in the utility system as these turbines are capable of producing more electricity [87]. Regression coefficients of condensing steam turbines are represented in Table 31.

Table 31: Regression coefficients for condensing steam turbine with $W_{max} > 2$ MW

Regression Coefficient	Value
b_0 (MW)	-0.463
b_1 (MW/°C)	0.00353
b_2	1.220
b_3 (°C ⁻¹)	0.000148

Knowing the average power demand to be generated in the utility system, the steam turbine equation can be utilized to calculate the average required steam flowrate into the turbine. Determining the required steam flowrate is essential to calculate the average required fuel heat considering the steam turbine efficiency. The average heat demand from burning fuels is calculated using the following equation:

$$Q^{fuel,avg} = \frac{\Delta h^{gen} m^{steam,avg}}{\eta^{Turb}}$$

Where $Q^{fuel,avg}$ is the average required fuel heat to produce the average steam demand $m^{steam,avg}$ for power generation in the utility system, Δh^{gen} is the heat required to generate one unit of steam, and η^{Turb} is the efficiency of the steam turbine. The average cost of the fuel is

calculated by the following equation considering the required average heat and the fuel cost parameter per unit heat fuel.

$$C^{Fuel,avg} = Q^{fuel,avg} C^{fuel}$$

Where, $C^{Fuel,avg}$ is the average cost of total fuel needed to produce required heat, and C^{fuel} is the cost parameter of fuel per unit heat.

CHAPTER VI

ILLUSTRATIVE CASE STUDY

The proposed approach to deal with seasonality in industrial city water-energy integration network is illustrated via a case study which has been solved by implementing a stochastic method developed by Bishnu et al. [88]. Three scenarios are considered to investigate the impact of seasonality proposed approach on network total annual cost and explore some potential profitability options. Three processes are involved in this case study which are ammonia, methanol, and GTL plants. Process-related data including basic power load and minimum cooling requirement are shown in Table 17. Flowrates of different water sources and sinks; as well as pollutants concentrations are represented in Table 32 and Table 33 respectively. In total, the case study involves eight process water sources, and six process water sinks in addition to three irrigation sinks; one for each process. The data for four contaminants (TDS, ammonia, organics, and nitrogen) were obtained from earlier work done by Fouladi et al. [43].

Three cooling options are considered including air coolers, cooling towers, and once-through cooling seawater. Central and on-site decentral treatment units and desalination plants are involved in this study. Reverse osmosis is utilized as the desalination unit in this work. Four treatment interceptors are included which are dissolved air flotation, membrane bioreactor, nano-filtration, and wastewater reverse osmosis. One-stage and two-stage interceptor options were considered. Each interceptor is associated with a recovery ratio and minimum removal ratio obtained from earlier performed seasonality analysis. Values of interceptor minimum removal ratios are represented in Table 34. In addition, all required cost parameters including capital and operating cost are provided in Table 35 for all elements in the water-energy integration network.

The average power demand parameters for cooling systems and interceptors are provided in Table 36. The values of average-to-maximum parameters for water/power sources and sinks are demonstrated in Table 37. Also, piping cost and interceptor capital cost coefficients are represented in Table 38 and Table 39 respectively; while operating hours and annualizing factors are shown in Table 40. The environmental regulations on pollutant discharge concentration considered in this case study are illustrated in Table 41.

The formulated MINLP model was solved using simulated annealing which is a stochastic programming tool used for solving optimization problems. Simulated annealing models the physical annealing process which depends on heating the metal up to a certain temperature that allows recrystallization of the metal. At this temperature, defects are repaired and the metal is held at this temperature for a while and then it is allowed to cool down slowly and reach equilibrium at each temperature. Simulated annealing mimics the actual annealing process as the system is allowed to reach the maximum number of states and equilibrates at each temperature (i.e. complete Markov chain).

The first step towards determining the optimal network design is to provide an initial solution and perform transitions on this to generate a new solution. In other words, random moves for variables considering given mass/energy balances and constraints are performed to generate a new network structure. Then, the performance (i.e. TAC) of the new solution is evaluated. If it is better than the previous one, it is accepted as the current solution and further transitions are performed on this. On the other hand, if the solution was worse, it is not rejected outright but with a probability which depends on the difference in performance & temperature (which represents the stage of the search) [88]. Probability of the rejected solutions depends on Metropolis-Hastings criteria. The above-mentioned scheme is repeated and the search is terminated if conditions like

minimum temperature or number of transitions performed are met. These conditions are user specified. Implementation of this algorithm guarantees an exhaustive search with a near-global optimal solution. As the transitions performed have elements of randomness involved, it eliminates the chances for the solver to be stuck with a local minimum solution.

It is worth pointing out that the initial solution provided to the solver depends on a linear structure. This structure assumes that water from all sources is disposed to the environment, all water sink demands are satisfied by freshwater, and waste heat is discharged via cooling systems. The working mechanism of utilized simulated annealing tool is demonstrated using scenario 1. Figure 61 represents the algorithm of simulated annealing stochastic optimization method [88].

Table 32: Flowrates and multiple contaminant water source data

	FLOW	TDS	Organics	Ammonia	Nitrogen
SOURCE	ton/d	ppm	ppm	ppm	ppm
P1S1	45	50	4	1	50
P1S2	154	2500	20	3	25
P1S3	400	550	15	25	40
P2S1	281	500	100	1	5
P2S2	115	2500	20	3	25
P2S3	500	550	15	25	40
P3S1	16648	500	46	1	5
P3S2	147	550	15	25	40

Table 33: Flowrates and multiple contaminant water sink data

	FLOW	TDS	Organics	Ammonia	Nitrogen
SINK	ton/d	ppm	ppm	ppm	ppm
P1D1	2571	500	4	0.5	21
P1D2	840	200	4	0.5	5
P2D1	1912	500	4	0.5	21
P2D2	500	200	4	0.5	5
P3D1	7115	500	4	0.5	21
P3D2	163	200	4	0.5	5
P1I1	40	1750	150	5	75
P2I1	139	1750	150	5	75
P3I1	74	1750	150	5	75

Table 34: Interceptors minimum removal ratios for all contaminants

INTERCEPTOR	TDS	Organics	Ammonia	Nitrogen
DAF	0	76	83.6	79.4
MBR	0	89	98	93
NF	82.8	82.8	69.0	69.0
RO-WW	98.6	93.9	79.1	79.1
RO-SW	98.9	98.5	79.6	79.6

Table 35: Cost parameters for water-energy network elements [43] [86]

Freshwater cost from external utility $\left(\frac{\$}{m^3}\right)$	1.48
Electricity cost from external utility $C^E \left(\frac{\$}{kwh}\right)$	0.042
Electricity cost from external utility $C^E \left(\frac{\$}{kwyrr}\right)$	368
Decentral/central treatment unit capital cost parameter $C_{rp}^{CC}/C_{st}^{CC} \left(\frac{\$}{m^3}\right)$	DAF (0.046) MBR (0.109) NF (0.059) RO (0.088)
Decentral/central treatment unit operating cost parameter $C_{rp}^{OC}/C_{st}^{OC} \left(\frac{\$}{m^3}\right)$	DAF (0.176) MBR (0.47) NF (0.126) RO (0.189)
Decentral/central desalination unit (RO-SW) capital cost parameter $C_{mp}^{CC}/C_{nk}^{CC} \left(\frac{\$}{m^3}\right)$	0.181
Decentral/central desalination unit (RO-SW) operating cost parameter $C_{mp}^{OC}/C_{nk}^{OC} \left(\frac{\$}{m^3}\right)$	0.528
Air cooler capital cost parameter $C_{AC}^{CC} \left(\frac{\$}{kWyr}\right)$	12
Cooling tower capital cost parameter $C_{CT}^{CC} \left(\frac{\$}{kWyr}\right)$	5
Wastewater discharge cost parameter $C^{WW} \left(\frac{\$}{m^3}\right)$	0.3
Brine discharge cost parameter $C^B \left(\frac{\$}{m^3}\right)$	0.3
Waste-heat-to-power unit capital cost parameter $C_{WHP}^{CC} \left(\frac{\$}{kW}\right)$	2750
Waste-heat-to-power unit operating cost parameter $C_{WHP}^{OC} \left(\frac{\$}{kWh}\right)$	0.0125
Seawater cost $C^{SW} \left(\frac{\$}{m^3}\right)$	0.02
Natural gas cost $C^{NG} \left(\frac{\$}{GJ}\right)$	4.1

Table 36: Water/Power demand parameters for cooling systems and interceptors

Air cooler average power demand parameter $P_{AC}^{PW,avg} \left(\frac{kW}{MW} \right)$	35.33
Cooling tower average power demand parameter $P_{CT}^{PW,avg} \left(\frac{kW}{MW} \right)$	24.62
Cooling tower average makeup water demand parameter $P_{CT}^{MU,avg} \left(\frac{m^3}{h MW} \right)$	2
Once-through cooling seawater power demand parameter $P_{OCSW}^{PW} \left(\frac{kWh}{m^3} \right)$	0.0342
Once-through cooling seawater water use parameter $P_{OCSW}^{SW} \left(\frac{m^3}{h MW} \right)$	292
Desalination unit average power demand parameter $P_{Des}^{PW,avg} \left(\frac{kWh}{m^3} \right)$	4.493
Treatment unit average power demand parameter $P_{T,rp}^{PW,avg} / P_{T,st}^{PW,avg} \left(\frac{kWh}{m^3} \right)$	DAF (0.211) MBR (0.568) NF (0.583) RO (0.888)

Table 37: Average-to-maximum parameters for water/power sources and sinks

Average-to-maximum parameter for wastewater flowrate from all water sources to decentral/central treatment units $P_{ip,rp}^{avg,max} / P_{ip,st}^{avg,max}$	With cooling tower 1.03 Without cooling tower 1
Average-to-maximum parameter for seawater flowrate to decentral/central desalination $P_{mp}^{avg,max} / P_{nk}^{avg,max}$	1.02
Average-to-maximum power parameter for WHP unit $P_{WHP,p}^{avg,max}$	Ammonia (1.01), GTL (1.01) Methanol (1.07)
Average-to-maximum parameter for available sources water flowrate $P_{ip}^{avg,max}$	Process water sources/offices 1 Cooling tower blowdown 1.03
Average-to-maximum parameter for required sink water flowrate $P_{jp}^{avg,max}$	Process sinks/offices 1 Cooling tower makeup 1.03 Irrigation 1.47

Table 38: Piping cost coefficients [88]

Coefficient associated with piping cost calculations a	696
Coefficient associated with piping cost calculations b	1.24

Table 39: Interceptors capital cost coefficients

Treatment unit Capital cost coefficient α	1
Desalination unit Capital cost coefficient δ	1

Table 40: Operating hours and annualizing factors

Operating hours per year H_y ($\frac{hr}{year}$)	8760
Interceptor annualizing factor K_F (yr^{-1})	0.05
Piping cost annualizing factor γ (yr^{-1})	0.05

Table 41: Environmental regulations on discharged pollutants concentration [89]

	TDS	Organics	Ammonia	Nitrogen
Discharge pollutant concentration (ppm)	1500	46	3	100

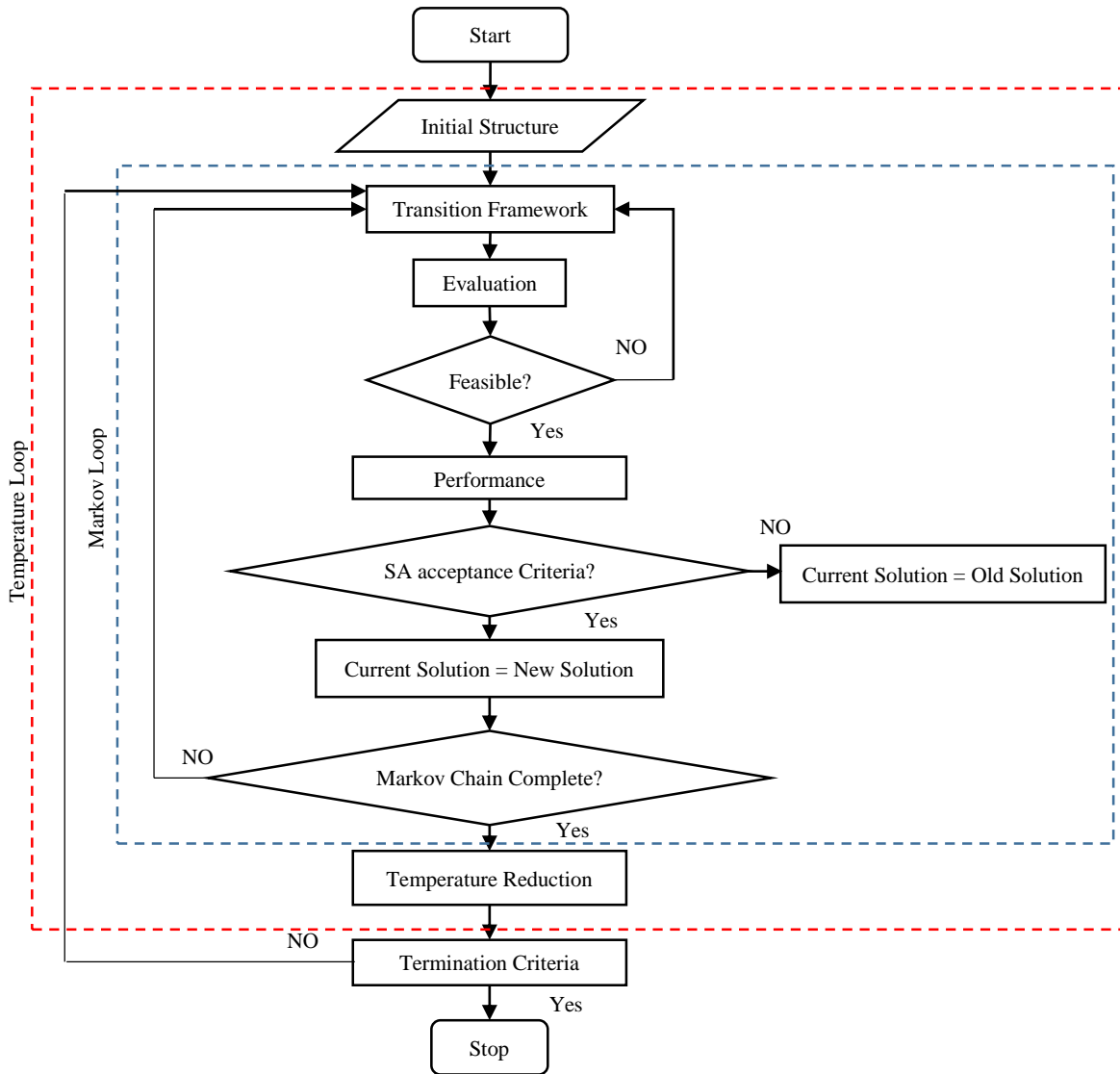


Figure 61: Flowchart of simulated annealing algorithm

Results and Discussion

Simulated annealing has been implemented using MATLAB software. A desktop PC with intel® core™ i7-2620M, 2.7 GHz, 16.00 GB RAM, and a 64-bit operating system was used to solve the case study. The optimal solution for each scenario was obtained after several runs until the solution converges asymptotically.

Base case: Without integration network

Without considering the use of water-energy integration network, all water demands are satisfied using freshwater, all wastewater (i.e. water supplies) are either discharged directly or after treatment. Also, this case involves discharging all waste heat via cooling systems, and all power demands need to be satisfied by power generation in the utility system. Total freshwater demands are about 13,353 tons/day; while total generated wastewater is about 18,290 tons/day. Total power demand from utility system is 112 MW and about 3075 MW of waste heat needs to be discharged via cooling systems. The total annual cost for satisfying process water and power demands, and discharging wastewater and waste heat without incorporating the water-energy integration network is approximately 97 MM \$/yr. The total annual cost is composed of 38 MM \$/yr as the capital cost, and 59 MM \$/yr as the operating costs. Capital cost includes the costs of the following units depreciated over project life; desalination units, treatment units, and cooling systems; while operating cost represents the costs required to operate desalination units, treatment units, and cooling systems.

Scenario 1: Without considering seasonality

This scenario demonstrates a typical case of designing the water-energy network based on annual average values without considering seasonal variations of water/energy elements. The scenario under investigation takes into account three cooling options (air cooler, cooling tower, once-through cooling seawater), four treatment units (DAF, MBR, NF, RO), one desalination option (RO); as well as a WHP unit. Table 42 illustrates source-to-sink, freshwater-to-sink, and source-to-discharge water allocation. Source-to-treatment unit water flowrates are represented in Table 43; while Table 44 provides information on treated water-to-sink and treated water-to-discharge allocation. It is worth mentioning that the symbols P1, P2, and P3 stand for ammonia,

methanol, and GTL plants respectively. Also, the symbols “S”, “D”, and “I” represent water supply/source, water demand/sink, and irrigation water demand respectively.

Table 42: Source-to-sink or discharge water allocation – Scenario 1

Sink	P1D1	P1D2	P2D1	P2D2	P3D1	P3D2	P1I1	P2I1	P3I1	Discharge
Source	ton/d	ton/d	ton/d	ton/d	ton/d	ton/d	ton/d	ton/d	ton/d	ton/d
P1S1	0	0	0	0	0	0	40	0	0	5
P1S2	0	0	0	0	0	0	0	0	0	0
P1S3	0	0	0	0	0	0	0	0	0	0
P2S1	0	0	0	0	0	0	0	139	0	0
P2S2	0	0	0	0	0	0	0	0	0	0
P2S3	0	0	0	0	0	0	0	0	0	0
P3S1	0	0	0	0	0	0	0	0	0	2477
P3S2	0	0	0	0	0	0	0	0	0	0
FW	0	840	0	500	0	163	0	0	0	0

Table 43: Source-to-treatment unit water allocation – Scenario 1

Treatment	1 Stage TR P1	2 stage TR P1	1 Stage TR P2	2 stage TR P2	1 Stage TR P3	2 stage TR P3
Source	ton/d	ton/d	ton/d	ton/d	ton/d	ton/d
P1S1	0	0	0	0	0	0
P1S2	154	0	0	0	0	0
P1S3	0	400	0	0	0	0
P2S1	0	0	142	0	0	0
P2S2	0	0	115	0	0	0
P2S3	0	0	0	500	0	0
P3S1	0	0	0	0	0	14171
P3S2	0	0	0	0	0	147

Table 44: Treated water-to-sink or discharge water allocation – Scenario 1

Sink	P1D1	P1D2	P2D1	P2D2	P3D1	P3D2	P1I1	P2I1	P3I1	Discharge
Treatment	ton/d	ton/d	ton/d	ton/d	ton/d	ton/d	ton/d	ton/d	ton/d	ton/d
1 Stage TR-P1	0	0	0	0	0	0	0	0	0	139
2 Stage TR-P1	0	0	0	0	0	0	0	0	0	324
1 Stage TR-P2	0	0	0	0	0	0	0	0	74	158
2 Stage TR-P2	0	0	0	0	0	0	0	0	0	405
1 Stage TR-P3	0	0	0	0	0	0	0	0	0	0
2 Stage TR-P3	2571	0	1912	0	7115	0	0	0	0	0

The results obtained using stochastic programming show that optimal water network design utilizes air coolers as the cheapest cooling option. Also, decentral one-stage and two-stage nano-filtration membrane units are selected for wastewater treatment as required. In addition, on-site decentral desalination plants were considered to satisfy freshwater demand of each process. This indicates that the cost required for central desalination and treatment units including piping systems outweighs the cost of decentral units and respective piping systems. These decisions were made based on minimizing the total annual cost (TAC) which is the objective function of the formulated problem. The total annual cost of the resultant network design considering the average required capacity of the desalination plant, treatment units, cooling system, and WHP unit is 75 MM \$/yr. Capital cost is the major contributor to this TAC which has a value of 58 MM \$/yr while operating cost represents only 17 MM \$/yr. A significant reduction is noticed in the operating cost of scenario 1 compared to the base case due to power production in the WHP unit which eliminates power generation fuel costs.

Table 45 demonstrates the allocation of power generated using waste heat via the WHP unit. It is worth pointing out that the search for power allocation is random assuming all plants are owned by the same authority. Accordingly, the power generated by the WHP unit is sent to a power grid and used for any plant within the industrial city. The overall benefits of utilizing the

power generated through the WHP unit and extra cost for power produced in the utility system will eventually be the same considering the whole industrial park. Extra 54 MW of power can be exported and used to satisfy the basic process power load. Power exports will help to save about 10 MM \$/yr considering power generation cost via WHP unit and utility system. Figure 62 provides an illustration for the designed water-energy network without considering seasonal variations. It is clearly shown that freshwater connections are only available for sinks that require freshwater supplies based on average demand and supply. Similarly, only water sources associated with environmental discharges are connected to discharge piping system. Both freshwater and discharge piping systems are designed based on average water flowrates. It is worth mentioning that the utility system is designed according to the required average power demand after utilizing power generated via the WHP unit.

Table 45: Allocation of power generated via WHP unit-scenario 1

Power (MW)			
Process	Ammonia	Methanol	GTL
Ammonia	37.28	0.00	4.35
Methanol	5.66	14.09	3.23
GTL	8.99	23.88	59.83

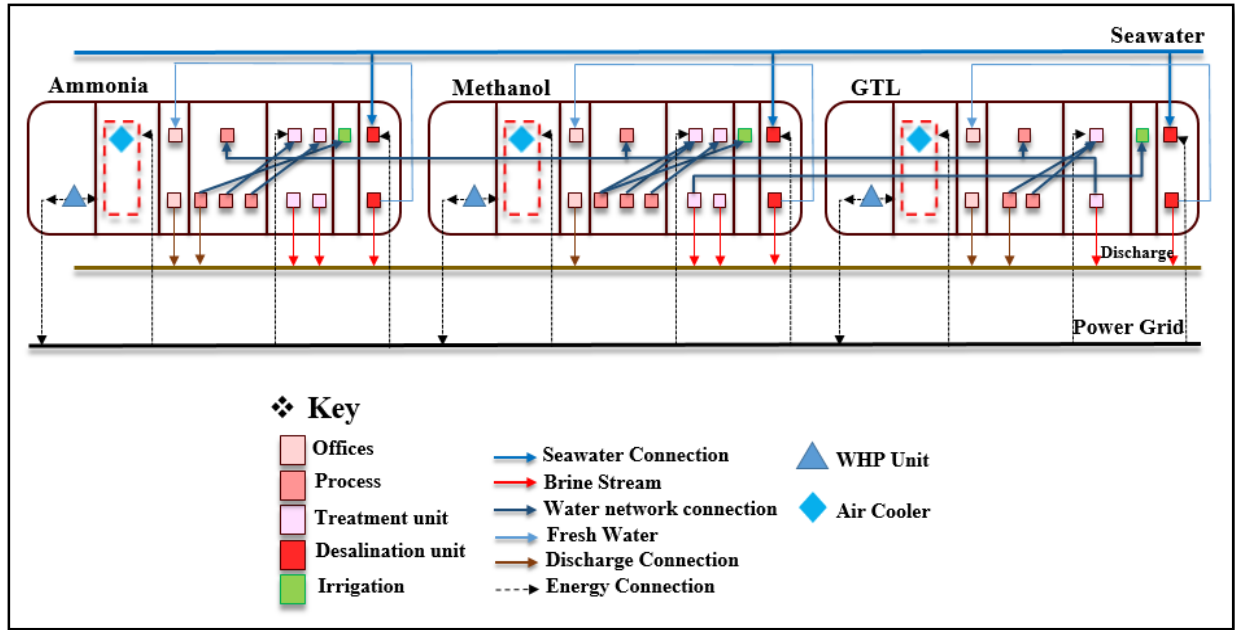


Figure 62: Water-energy network representation - scenario 1

Scenario 2: Considering seasonality

To handle seasonality of the water-energy network over the year, different elements of the network are designed based on maximum capacity including; desalination plants, treatment units, WHP unit, in addition to the utility system. This scenario considers the connectivity of all water sinks to freshwater based on maximum sink requirement to compensate for any extra water demand due to seasonality. To balance this out, it is taken into consideration to maximize the discharge connections to all water sources in this scenario based on maximum available flowrate in these sources. Results show that water network connections do not exhibit any changes due to seasonality. Also, the selected cooling option that requires the minimum cost for the designed water-energy network is air-cooled heat exchanger. Accordingly, waste heat will be rejected through air coolers.

Power is required to operate air coolers, treatment units, and desalination plants. Power requirements are satisfied primarily by power generation through the WHP unit. Any extra requirements are satisfied by power generation in the utility system. It is worth pointing out that the utility system is designed based on maximum power consumption over seasons. Maximizing utility system capacity helps to compensate for any seasonal changes in power demand throughout the year and to guarantee continuous operation in case of any WHP unit failure. Total annual cost (TAC) for the designed network is (78 MM \$/yr). Allocation of power generated by WHP unit for each plant based on a random search is represented in Table 46. Similar to scenario 1, exporting the extra power generated via the WHP unit (54 MW) saves around ten million dollars per year. A representation of the designed network is illustrated in Figure 63. Network representation indicates that all water sinks are connected to freshwater supply based on maximum sink demand while maximum discharge connections are made available for all water sources.

Table 46: Allocation of power generated via WHP unit - Scenario 2

Power (MW)			
Process	Ammonia	Methanol	GTL
Ammonia	34.55	0	7.08
Methanol	12.46	3.46	7.07
GTL	24.65	31.46	36.59

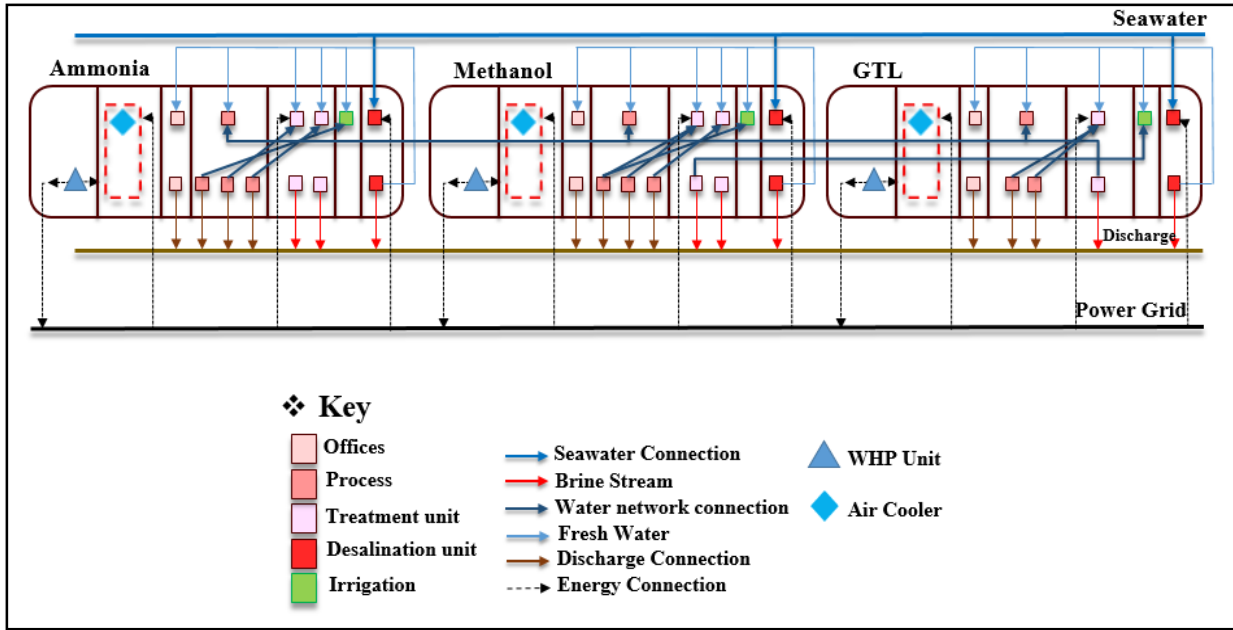


Figure 63: Water-energy network representation - scenario 2

It is noticed that water connectivity does not change after considering seasonal variations. Comparing the total annual costs of scenario 2 and scenario 1, an increase in the TAC is observed for scenario 2. This increase is due to taking into consideration the seasonal changes of water/power demand and supply as explained earlier. The percent of increase in TAC between the two scenarios is 4% which represents a total of (~3 MM \$/yr). Accordingly, a more reliable water-energy network design that handles seasonal variations and guarantees continuation of process operation in case of network failure can be achieved via increasing the TAC by three million dollars per year. The extra cost is mainly a result of increasing capital cost by maximizing network elements sizes. Figure 64 indicates the contribution of different cost elements to the increase in TAC. It shows that oversized cooling systems are the main contributor to the cost increase followed by maximizing the capacity of desalination units and the WHP unit. Oversized pipelines

and enforced freshwater and discharge connections represent a very small fraction of the TAC increase which is around 0.5%.

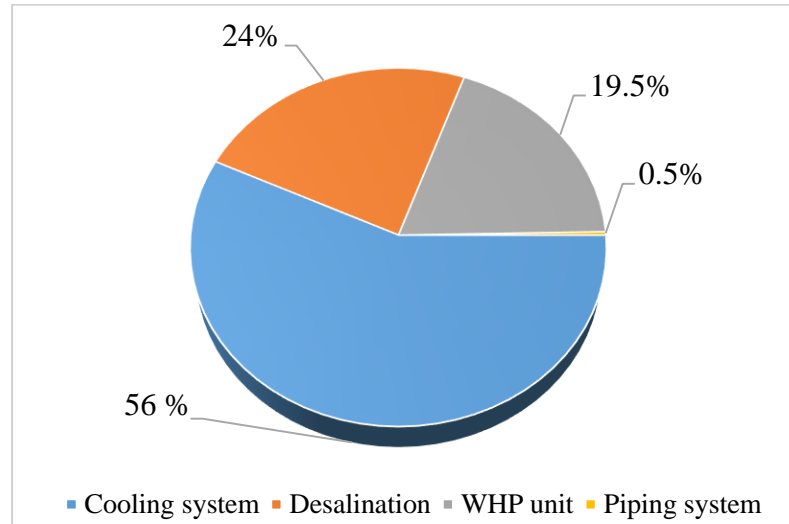


Figure 64: Elements' contribution to TAC increase of scenario 2

Scenario 3: Considering seasonality and allowing freshwater exports

The purpose of this scenario is to explore profitability options within the water-energy network by allowing freshwater exports while considering seasonal changes. The maximum amount of exported freshwater is determined to be twenty thousand tons per hour. Similar to earlier scenarios, some waste heat will be utilized to generate power through the WHP unit and the remaining heat will be discharged using cooling systems. The results show that water network connections will remain unchanged compared to scenario 1 and scenario 2. Also, the results of this scenario indicate that using a combination of once-through cooling seawater and air cooler will be the optimal option for cooling. It is worth noting that average seawater used for cooling purposes was allowed to be re-allocated into desalination plant to produce exported freshwater.

On average, about 38 MW of power needs to be generated via the utility system. The extra power demand is due to increasing desalination capacity for export purposes. Table 47 demonstrates the power allocation for scenario 3. The water-energy network structure of scenario 3 is illustrated in Figure 65.

Table 47: Allocation of power generated via WHP unit - Scenario 3

Power (MW)			
Process	Ammonia	Methanol	GTL
Ammonia	24.76	6.65	10.22
Methanol	9.67	8.19	5.12
GTL	15.88	9.21	67.60

The total annual cost (TAC) of the designed network is (-115 MM \$/yr). The overall cost of the network decreased compared to scenario 1 and scenario 2 due to the profit made by freshwater exports. In other words, the benefits of desalinating the re-allocated seawater and exporting freshwater outweighs the increase in RO power demand. The cost of the designed network considering seasonal variations and allowing freshwater exports is fully covered with a total net profit of 115 MM \$/yr. This TAC includes all proposed adjustments to take into account seasonal variations. This means that by modifying the policy and allowing freshwater exports, the TAC of the water-energy network considering seasonal changes is even less than the TAC of a similar network that does not consider seasonality.

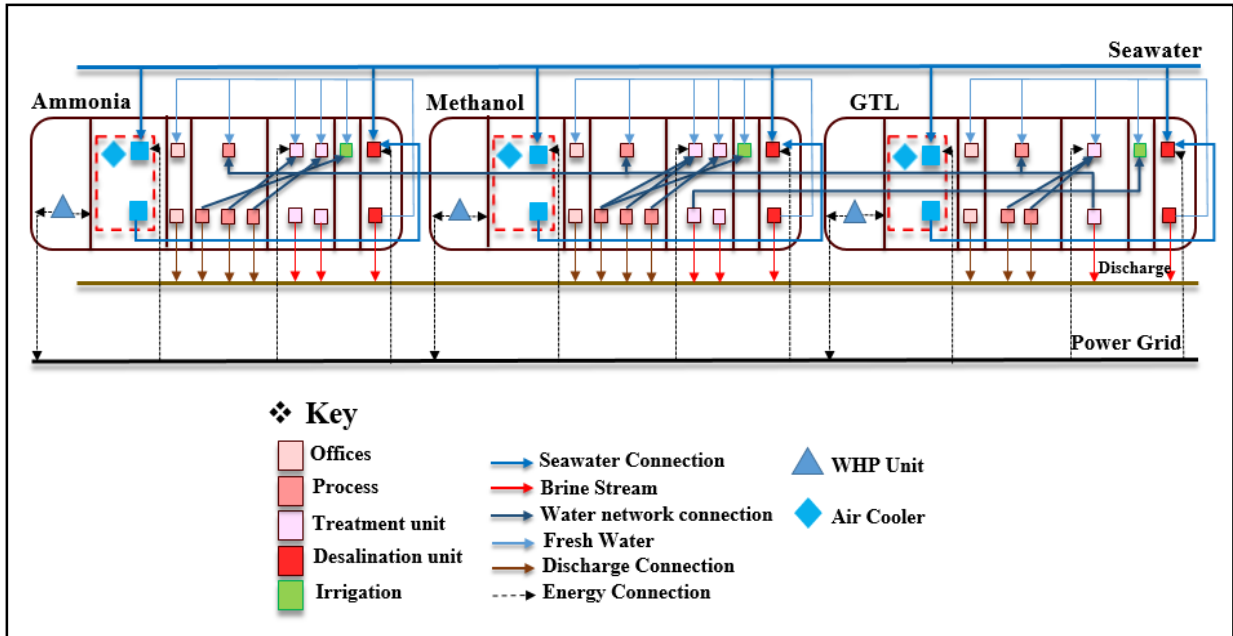


Figure 65: Water-energy network representation - scenario 3

Comparing all three scenarios, it is noticed that scenario 2 requires a higher total annual cost (TAC) compared to scenario 1. This is due to seasonality considerations based on the proposed approach which includes maximizing the capacity of desalination units, treatment units, and WHP unit, based on maximum requirements over the seasons. In addition, the observed cost increase is due to maximizing freshwater and discharge connections for all water sinks and sources respectively. Furthermore, a reduction in the total annual cost is observed in scenario 3 compared to scenario 1 and scenario 2. This indicates that allowing re-allocation of seawater used for cooling and exporting freshwater will decrease the network total annual cost even when seasonal variations are considered. This is due to the profit made by exporting freshwater which emphasizes the point of studying and exploiting the benefits of water-energy nexus and policy modifications.

Figure 66 illustrates how the optimal solution of scenario 1 was obtained over the number of evaluation states to elucidate the working mechanism of simulated annealing. It is clearly shown that 10,634 states were evaluated to reach the optimal solution with (75 MM \$/yr) as the minimum total annual cost of the designed water-energy network. In order to demonstrate the performance of the utilized simulated annealing solving method, several runs have been implemented for solving scenario 1. Table 48 represents the results of the ten runs. The average minimum total annual cost is about (75.27 MM \$/yr). The average convergence time for the represented runs is 1 hour, 23 minutes, and 29 seconds which required evaluating 10,999 states on average. The standard deviation of the total annual cost of the same runs is about 0.62 MM \$/yr and the percent standard deviation is around 0.82% as indicated in Table 49. Almost 70% of the TAC of the ten runs fall within one standard deviation. This statistical analysis shows that utilized simulated annealing method provides precise results.

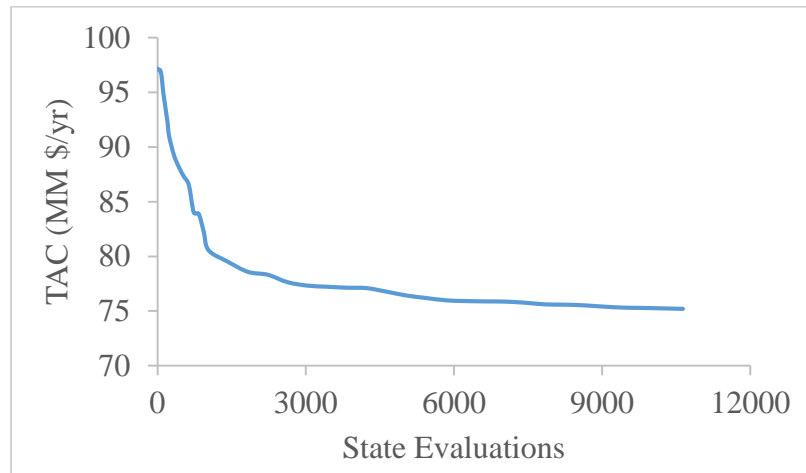


Figure 66: Simulated annealing convergence for scenario 1

Table 48: Scenario 3 results considering ten runs

Number of States	Objective Value TAC (MM \$/yr)	Time (hr:min:s)
10782	75.11	1:13:52
11385	74.98	1:24:43
10634	75.21	1:08:01
10342	76.34	1:05:03
11834	74.41	1:49:52
10092	76.53	1:13:12
11175	74.97	1:28:15
11256	75.07	1:31:54
10743	75.18	1:22:23
11743	74.92	1:38:34

Table 49: Standard deviation, average, and percent SD for scenario 1 results

Standard Deviation (MM \$/yr)	0.62
Average (MM \$/yr)	75.27
% Standard deviation/Average	0.82

The total annual cost elements including; capital and operating costs were calculated considering cost parameters obtained from either earlier case studies or the literature especially when actual cost parameters were not readily available. Any inaccuracy in the performed cost predictions shall not affect the observations of the case study as the same calculations techniques were performed for all scenarios. In other words, any overestimation or underestimation of the cost would result in a systematic error that would be carried out throughout all scenarios and would not affect the outcomes of the case study. Also, the approach capabilities were demonstrated for a representation of the water-energy integration network however, it is believed that this approach will help to enhance the sustainability and tolerance of other integration networks considering seasonal variations.

CHAPTER VII

CONCLUSION AND FUTURE WORK

Conclusion

Seasonal changes of the water-energy network elements have been analyzed. The significance of the observed seasonal variations has been assessed considering three processes; ammonia, methanol, and GTL. According to the assessment results, a novel approach has been proposed to design a tolerant water-energy network that can handle seasonality efficiently. A mixed-integer nonlinear mathematical model has been modified to optimize the design of the water-energy network considering seasonal changes. A case study which consists of three scenarios has been considered to illustrate the impact of taking into account all potential seasonal changes on the total annual cost of the network. Simulated annealing solving method has been implemented to solve the considered scenarios. Scenario 1 and scenario 2 results have proved that a more reliable water-energy network can be designed by a slight increase in the total annual cost. Moreover, scenario 3 results have shown that exploiting the water-energy nexus while considering seasonal variations is economically profitable. These results open the door for allowing some policy changes within the industrial city due to the observed benefits of designing the integration network across the water-energy nexus considering seasonal variations.

Future work

Several recommendations may be considered in the future to improve the design of the water-energy integration network such as:

- Expanding the seasonality problem to include analysis and assessment of the impact of the seasonal variations on the carbon integration network.

- Incorporate a multi-objective model to capture different design aspects of integration network including the economic aspect (TAC), and the environmental aspects (minimum discharge and emissions). This could be done by incorporating the use of renewable fuels.
- Consider utility system in the seasonality problem which allows utilizing waste heat directly as a source of thermal energy (if needed), and converting some of the waste heat into different steam grades.
- Take into consideration the spatial constraints for water transport within the industrial city.
- Perform the seasonality analysis for other promising treatment technologies such as membrane distillation which is a thermally driven separation technique.
- Develop a software package with a well-developed database for analyzing seasonal variations of different elements of the water-energy network. This tool would facilitate the design of reliable and tolerant integration networks by understanding seasonality impact on network elements.

REFERENCES

- [1] A. Hoekstra and A. K. Chapagain, “Water footprints of nations. Water use by people as a function of their consumption pattern,” *Water Resour. Manag.*, vol. 21, no. 1, pp. 35–48, 2007.
- [2] M. M. El-halwagi, “Pollution Prevention through Process Integration: Systematic Design Tools,” *Acad. Press. San Diego*, 1997.
- [3] B. A. Phillips, “When do the seasons begin and end ?,” 2018.
- [4] G. Gloz, “Why does the Earth have different seasons ?” .
- [5] R. H. Linnhoff, B. Townsend, D. W., Boland, D., Hewitt, G. F., Thomas, B. E. A., Guy, A. R. and Marsland, *Linnhoff, B. Townsend, D. W., Boland, D., Hewitt, G. F., Thomas, B. E. A., Guy, A. R. and Marsland, R. H. (1982). A User Guide on Process Integration for the Efficient Use of Energy, 1st edition. IChemE, Rugby. 1982.*
- [6] J. R. Flower and B. Linnhoff, “Thermodynamic analysis in the design of process networks,” *Comput. Chem. Eng.*, vol. 3, no. 1–4, pp. 283–291, 1979.
- [7] B. Linnhoff and E. Hindmarsh, “the Pinch Design Method for Networks,” *Chem. Eng. Sci.*, vol. 38, pp. 745–763, 1983.
- [8] S. G. Hall and B. Linnhoff, “Targeting for Furnace Systems Using Pinch Analysis,” *Ind. Eng. Chem. Res.*, vol. 33, no. 12, pp. 3187–3195, 1994.
- [9] J. J. Klemeš and Z. Kravanja, “Forty years of Heat Integration: Pinch Analysis (PA) and Mathematical Programming (MP),” *Curr. Opin. Chem. Eng.*, vol. 2, no. 4, pp. 461–474, 2013.

- [10] S. a. Papoulias and I. E. Grossmann, "A structural optimization approach in process synthesis—I," *Comput. Chem. Eng.*, vol. 7, no. 6, pp. 695–706, 1983.
- [11] S. A. Papoulias and I. E. Grossmann, "A structural optimization approach in process synthesis - {III: Total processing systems}," *Comput. Chem. Eng.*, vol. 7, no. 6, pp. 723–734, 1983.
- [12] S. A. Papoulias and I. E. Grossmann, "A structural optimization approach in process synthesis—II: Heat recovery networks," *Comput. Chem. Eng.*, vol. 7, no. 6, pp. 707–721, 1983.
- [13] C. A. Floudas and I. E. Grossmann, "Synthesis of flexible heat exchanger networks for multiperiod operation," *Comput. Chem. Eng.*, vol. 10, no. 2, pp. 153–168, 1986.
- [14] A. Saboo and M. Morari, "RESHEX—an interactive software package for the synthesis and analysis of resilient heat exchangers networks. 2. Discussion of area targeting and network synthesis algorithms.," vol. I, no. 6, pp. 591–599, 1986.
- [15] C. A. Floudas and I. E. Grossmann, "Automatic generation of multiperiod heat exchanger network configurations," *Comput. Chem. Eng.*, vol. 11, no. 2, pp. 123–142, 1987.
- [16] T. F. Yee and I. E. Grossmann, "Simultaneous optimization models for heat integration♦II. Heat exchanger network synthesis," *Comput. Chem. Eng.*, vol. 14, no. 10, pp. 1165–1184, 1990.
- [17] T. F. Yee, I. E. Grossmann, and Z. Kravanja, "Simultaneous optimization models for heat integration-I. Area and energy targeting and modeling of multi-stream exchangers," *Comput. Chem. Eng.*, vol. 14, no. 10, pp. 1151–1164, 1990.
- [18] R. D. Colberg, M. Morari, and D. W. Townsend, "Resilience target for heat exchanger network synthesis," *Comput. Chem. Eng.*, vol. 13; Jg. 19, no. 7, p. 821, 1989.

- [19] X. Feng and X. X. Zhu, "Combining pinch and exergy analysis for process modifications," *Appl. Therm. Eng.*, vol. 17, no. 3, pp. 249–261, 1997.
- [20] J. Klemes, V. R. Dhole, K. Raissi, and S. J. Perry, "TARGETING AND DESIGN METHODOLOGY FOR REDUCTION OF FUEL , POWER AND CO , ON TOTAL," vol. 17, pp. 993–1003, 1997.
- [21] K. P. Papalexandri and E. N. Pistikopoulos, "A Multiperiod MINLP Model for Improving the Flexibility of Heat Exchanger Networks," *Comput. Chem. Eng.*, vol. 17, pp. S111–S116, 1993.
- [22] K. P. Papalexandri, "A Multiperiod MINLP For The Synthesis of Flexible Heat and Mass Exchange Networks," *Science (80-.)*, vol. 18, no. 11112, pp. 1125–1139, 1994.
- [23] J. H. Kim and C. Han, "Short-Term Multiperiod Optimal Planning of Utility Systems Using Heuristics and Dynamic Programming," *Ind. Eng. Chem. Res.*, vol. 40, no. 8, pp. 1928–1938, 2001.
- [24] S. Bungener, R. Hackl, G. Van Eetvelde, S. Harvey, and F. Marechal, "Multi-period analysis of heat integration measures in industrial clusters," *Energy*, vol. 93, pp. 220–234, 2015.
- [25] A. J. Isafiade, M. Short, M. Bogataj, and Z. Kravanja, "Integrating renewables into multi-period heat exchanger network synthesis considering economics and environmental impact," *Comput. Chem. Eng.*, vol. 99, pp. 51–65, 2017.
- [26] P. Y. Liew, S. R. Wan Alwi, W. S. Ho, Z. Abdul Manan, P. S. Varbanov, and J. J. Klemeš, "Multi-period energy targeting for Total Site and Locally Integrated Energy Sectors with cascade Pinch Analysis," *Energy*, vol. 155, pp. 370–380, 2018.
- [27] N. Takama, T. Kuriyama, K. Shiroko, T. Umeda, and C. C. Engineering, "Optimal water

- allocation in a petroleum refinery,” vol. 4, 1980.
- [28] M. M. El-Halwagi and V. Manousiouthakis, “Automatic synthesis of mass-exchange networks with single-component targets,” *Chem. Eng. Sci.*, vol. 45, no. 9, pp. 2813–2831, 1990.
- [29] Y. Wang and R. Smith, “Design of Distributed Effluent Treatment Systems,” 1994.
- [30] V. Dhole, N. Ramchandani, R. Tanish, and M. Wasilewski, “Make your process water pay for itself,” 1996.
- [31] S. G. Olesen and G. T. Polley, “A SIMPLE METHODOLOGY FOR THE DESIGN OF WATER NETWORKS HANDLING SINGLE CONTAMINANTS,” no. Figure 1, pp. 420–426, 1997.
- [32] S. J. Doyle and R. S. Fellow, “TARGETING WATER REUSE WITH MULTIPLE CONTAMINANTS,” 1997.
- [33] B. Galan and I. E. Grossmann, “Optimal Design of Distributed Wastewater Treatment Networks,” vol. 5885, no. 1996, pp. 4036–4048, 1998.
- [34] D. L. C. X.S. Zheng, X. Feng, “Design water allocation network with minimum freshwater and energy consumption,” 2003.
- [35] L. Savulescu, J. Kim, and R. Smith, “Studies on simultaneous energy and water minimisation — Part I : Systems with no water re-use,” vol. 60, pp. 3279–3290, 2005.
- [36] L. Savulescu, J. Kim, and R. Smith, “Studies on simultaneous energy and water minimisation — Part II : Systems with maximum re-use of water,” vol. 60, pp. 3291–3308, 2005.
- [37] Z. A. Manan, S. Y. Tea, S. Rafidah, and W. Alwi, “A new technique for simultaneous water and energy minimisation in process plant,” vol. 7, no. April, pp. 1509–1519, 2009.

- [38] R. Zhou, L. Li, H. Dong, and I. E. Grossmann, “Synthesis of Interplant Water-Allocation and Heat-Exchange Networks . Part 1 : Fixed Flow Rate Processes,” 2012.
- [39] R. Zhou, L. Li, H. Dong, and I. E. Grossmann, “Synthesis of Interplant Water-Allocation and Heat-Exchange Networks. Part 2: Integrations between Fixed Flow Rate and Fixed Contaminant-Load Processes,” 2012.
- [40] S. Y. Alnouri, P. Linke, and M. El-halwagi, “Water integration in industrial zones : a spatial representation with direct recycle applications,” pp. 1637–1659, 2014.
- [41] S. Y. Alnouri, P. Linke, and M. El-halwagi, “Optimal Interplant Water Networks for Industrial Zones : Addressing Interconnectivity Options Through Pipeline Merging,” vol. 60, no. 8, 2014.
- [42] S. Y. Alnouri, P. Linke, and M. El-halwagi, “A synthesis approach for industrial city water reuse networks considering central and distributed treatment systems,” *J. Clean. Prod.*, vol. 89, pp. 231–250, 2015.
- [43] J. Fouladi, P. Linke, M. M. El-Halwagi, and H. R. Parsaei, “A Systematic Approach For Designing Industrail Park Integration Networks Across The Water-Energy Nexus.” Texas A&M university at Qatar, Doha, 2017.
- [44] O. Burgara-Montero, J. M. Ponce-Ortega, M. Serna-González, and M. M. El-Halwagi, “Incorporation of the seasonal variations in the optimal treatment of industrial effluents discharged to watersheds,” *Ind. Eng. Chem. Res.*, vol. 52, no. 14, pp. 5145–5160, 2013.
- [45] S. K. Bishnu, P. Linke, S. Y. Alnouri, and M. El-Halwagi, “Multiperiod planning of optimal industrial city direct water reuse networks,” *Ind. Eng. Chem. Res.*, vol. 53, no. 21, pp. 8844–8865, 2014.
- [46] K. Arredondo-Ramírez, E. Rubio-Castro, F. Nápoles-Rivera, J. M. Ponce-Ortega, M.

- Serna-González, and M. M. El-Halwagi, “Optimal design of agricultural water systems with multiperiod collection, storage, and distribution,” *Agric. Water Manag.*, vol. 152, pp. 161–172, 2015.
- [47] S. Bishnu, P. Linke, S. Alnouri, and M. El-Halwagi, “Multi-Period Water Network Synthesis for Eco Industrial Parks considering Regeneration and Reuse,” *Chem. Prod. Process Model.*, vol. 12, no. 3, 2017.
- [48] L. Gaudard, F. Avanzi, and C. De Michele, “Seasonal aspects of the energy-water nexus: The case of a run-of-the-river hydropower plant,” *Appl. Energy*, vol. 210, pp. 604–612, 2018.
- [49] D. M. Al-Mohannadi, S. Y. Alnouri, S. K. Bishnu, and P. Linke, “Multi-period carbon integration,” *J. Clean. Prod.*, vol. 136, pp. 150–158, 2016.
- [50] K. Takemoto, S. Kanamaru, and W. Feng, “Climatic seasonality may affect ecological network structure : Food webs and mutualistic networks,” vol. 121, pp. 29–37, 2014.
- [51] C. Bakker *et al.*, “Shocks , seasonality , and disaggregation : Modelling food security through the integration of agricultural , transportation , and economic systems,” vol. 164, no. April, pp. 165–184, 2018.
- [52] P. O. Lolika, S. Mushayabasa, C. P. Bhunu, C. Modnak, and J. Wang, “Modeling and analyzing the effects of seasonality on brucellosis infection,” vol. 104, pp. 338–349, 2017.
- [53] SPX COOLING PRODUCTS, “Air Cooled Heat Exchangers.” [Online]. Available: <https://spxcooling.com/products/detail/air-cooled-heat-exchangers>. [Accessed: 01-May-2017].
- [54] “Integrated Pollution Prevention and Control (IPPC) Reference Document on the application of Best Available Techniques to Industrial Cooling Systems November 2000,”

- 2000.
- [55] P. Smith, "Summer Is Heating Up - Top 5 Ways To Save On Cooling Tower Bleed," 2018. [Online]. Available: <https://eldonwater.com/summer-heating-up-top-5-ways-save-cooling-tower-bleed/>. [Accessed: 03-Jun-2017].
- [56] D. Ludovisi and L. Llc, "WATER CONSUMPTION OF COOLING TOWERS IN DIFFERENT CLIMATIC ZONES OF THE U.S.," 2015, pp. 1–5.
- [57] J. C. Kloppers and D. G. Kröger, "Loss coefficient correlation for wet-cooling tower fills," *Appl. Therm. Eng.*, vol. 23, no. 17, pp. 2201–2211, 2003.
- [58] "What Is Cooling Tower Bleed-O / Blowdown ?" [Online]. Available: <http://www.terlyn.com/what-is-cooling-tower-bleed-off-blowdown-2/> .
- [59] P. N. Cheremisinoff, N.P.; Cheremisinoff, *Cooling Towers: Selection, Design and Practice*. .
- [60] Qatar Petroleum, "Ras Lafa Industrial City - From Qatar To The World," Doha, Qatar, 2011.
- [61] Office of Water, U. S. E. P. Agency, and D. Washington, "2018 Edition of the Drinking Water Standards and Health Advisories Tables," 2018.
- [62] A. Parker, "FACTORS THAT AFFECT REVERSE OSMOSIS MEMBRANE FLOW RATE: AN OVERVIEW."
- [63] N. Dhungle, "Waste heat to power systems," 2012.
- [64] O. Al-Ani and P. Linke, "Power Generation Targets from Hot Composite Curves," 2018.
- [65] "Carnot Cycle." [Online]. Available: <http://hyperphysics.phy-astr.gsu.edu/hbase/thermo/carnot.html>. [Accessed: 09-Mar-2018].
- [66] R. Allen, "Crop Coefficients," 2003.

- [67] “The Fundamental Questions of Irrigation.” [Online]. Available:
[http://www.thematrix.it/irrigationit/lessons/lesson 6/0601 CropWat.pdf](http://www.thematrix.it/irrigationit/lessons/lesson%206/0601%20CropWat.pdf). [Accessed: 06-Mar-2018].
- [68] M. Smith and P. Steduto, “Yield response to water: the original FAO water production function,” *Yield response to water*, pp. 1–10, 2012.
- [69] N. Muhammad, N. Al-Kaabi, and Y. Al-Khulaifi, “Qatar Agriculture and Food Security.” 2012.
- [70] “Doha Monthly Climate Averages.” [Online]. Available:
<https://www.worldweatheronline.com/doha-weather-averages/ad-dawhah/qa.aspx>.
[Accessed: 04-Mar-2018].
- [71] J. Nyvall, “Soil Water Storage Capacity and Available Soil Moisture,” 2002.
- [72] R. Restuccia, “Beginners Guide : How Much Water Does My Landscape Need,” 2016.
[Online]. Available: <https://www.jainsusa.com/blog/beginners-guide-how-much-water-does-my-landscape-need>. [Accessed: 02-Jul-2017].
- [73] C. Ross, “Dissolved air flotation (daf) systems.” [Online]. Available:
<http://www.evoqua.com/en/brands/Environmental-Treatment-Systems/Pages/dissolved-air-flotation.aspx>. [Accessed: 10-Mar-2018].
- [74] J. K. Edzwald, “Developments of High Rate Dissolved Air Flotation for Drinking Water Treatment.”
- [75] J. Guillermo and C. Torrealba, “Determination of Air Flotation Parameters to Perform Solid Liquid Separation Treatment in an Activated Sludge Treating Grease Waste by Promoting Filamentous Bacteria,” 2007.
- [76] P. Palaniandy, H. A. Aziz, and M. F. Murshed, *5 Dissolved Air Flotation (DAF) for*

Wastewater Treatment, no. August. 2017.

- [77] S.K.D. Consultancy & Services, “Dissolved Air flotation (DAF).” [Online]. Available: <http://www.skdwater.com/daf.php>. [Accessed: 06-Aug-2018].
- [78] P. Li, Q. Wu, H. Wu, S. Wen, L. Wang, and S. Li, “Flocculation - Air Flotation Treatment of Wastewater from Paper-making Reconstituted Tobacco Sheet Flocculation - Air Flotation Treatment of Wastewater from Paper-making Reconstituted Tobacco Sheet,” 2018.
- [79] S. Liers, J. Baeyens, and I. Mochtar, “Modeling dissolved air flotation,” 1996.
- [80] A. Amta, E. Calendars, and C. Amta, “Membrane Bioreactors for Wastewater Treatment.” [Online]. Available: https://www.amtaorg.com/Membrane_Bioreactors_for_Wastewater_Treatment.html. [Accessed: 01-May-2018].
- [81] J. Ma, D. Song, P. Wang, and G. Wen, “Membrane Bioreactor Application in Water Treatment 4 . 5 Membrane Bioreactor Application in Water Treatment,” *Compr. Membr. Sci. Eng. II*, no. 2012, pp. 104–117, 2018.
- [82] Y. Zeng *et al.*, “MBR Book - Principles and Applications of Membrane Bioreactors for Water and Wastewater Treatment (2nd Edition),” 2011.
- [83] H. H. Bengtson, “Biological Wastewater Treatment Processes III : MBR Processes,” Stony Point, New York.
- [84] Y. Liu *et al.*, “Performance of a Sequential Anaerobic Baffled Reactor (ABR)/ Membrane Bioreactor (MBR) System Treating Caffeine Wastewater,” *2011 Int. Symp. Water Resour. Environ. Prot.*, vol. 2, no. 50879029, pp. 1406–1409.
- [85] STS Canada, “Nanofiltration.” [Online]. Available:

- <https://www.stscanadainc.com/nanofiltration.html>. [Accessed: 03-May-2018].
- [86] R. J. Hassiba and P. Linke, “On the simultaneous integration of heat and carbon dioxide in industrial parks,” vol. 127, pp. 81–94, 2017.
- [87] “Types of Steam Turbines,” 2011. [Online]. Available:
<https://www.turbinesinfo.com/types-of-steam-turbines/> . [Accessed: 01-May-2018].
- [88] S. Bishnua, J. Fouladi, P. Linke, and M. El - Halwagi, “Stochastic Optimization Tools for Water-Heat Nexus Problems.” Elsevier, Texas, USA, 2018.
- [89] “Executive By-Law for The Environment Protection Law,” Doha, Qatar, 2002.